

***Completely Water-based Emulsions as
Compartmentalized Systems via Pickering
Stabilization***

Dissertation

zur Erlangung des akademischen Grades
Doktor der Naturwissenschaften (Dr. rer. nat.)
in der Wissenschaftsdisziplin „Kolloidchemie“

eingereicht an der
Mathematisch-Naturwissenschaftlichen Fakultät
der Universität Potsdam
von
Jianrui Zhang

Potsdam-Golm, im Mai 2020

This work is licensed under a Creative Commons License:
Attribution – Non Commercial – Share Alike 4.0 International.
This does not apply to quoted content from other authors.
To view a copy of this license visit
<https://creativecommons.org/licenses/by-nc-sa/4.0/>

Published online on the
Publication Server of the University of Potsdam:
<https://doi.org/10.25932/publishup-47654>
<https://nbn-resolving.org/urn:nbn:de:kobv:517-opus4-476542>

Table of Contents

1. Introduction	1
2. Background and Motivation	4
2.1. <i>Aqueous Two-Phase System (ATPS)</i>	4
2.1.1. The types of ATPS	4
2.1.2. The dynamics mechanism of ATPS	6
2.1.3. Factors influencing partitioning of biomolecules in ATPS	8
2.1.3.1. Molar mass (MW) and concentration of polymer	8
2.1.3.2. Hydrophobicity	9
2.1.3.3. pH	9
2.1.3.4. Temperature	10
2.1.4. The applications of ATPS for separation and extraction	10
2.1.4.1. Cells and organelles	10
2.1.4.2. Low molecular weight compounds	11
2.1.4.3. Drug residues in food and water	12
2.1.4.4. Environmental remediation	13
2.2. <i>Water-in-water emulsions</i>	14
2.2.1. Emulsion formation and stabilization	15
2.2.2. Control of droplet size and morphology	19
2.3. <i>Basic knowledge of Pickering emulsions</i>	22
2.3.1. The stabilization mechanism of Pickering emulsions	23
2.3.2. Control properties of Pickering emulsions	25
2.3.2.1. Stabilization of emulsions by adsorbed particles	25
2.3.2.2. Control of emulsion droplet size by formulation and process parameters	26
2.3.2.3. Emulsion type and emulsion inversion	28
3. Outline	29
4. Water-in-water Pickering emulsion stabilized by polydopamine particles and crosslinking	31
4.1. <i>Overview</i>	31
4.2. <i>Results and Discussion</i>	32
4.3. <i>Conclusion</i>	43
5. Supramolecular Compartmentalized Hydrogels via Polydopamine Particle Stabilized Water-in-Water Emulsions	45
5.1. <i>Overview</i>	45

5.2. <i>Results and Discussion</i>	46
5.3. <i>Conclusions</i>	57
6. Water-in-Water Pickering Emulsion stabilized by Carbon Nitride	58
6.1. <i>Overview</i>	58
6.2. <i>Results and Discussion</i>	59
6.3. <i>Conclusions</i>	66
7. Conclusion and Outlook.....	67
8. Appendix	70
8.1. <i>Materials</i>	70
8.2. <i>Synthesis Procedures</i>	72
8.2.1. Synthesis of materials described in Chapter 4.....	72
8.2.2. Synthesis of materials described in Chapter 5.....	73
8.2.3. Synthesis of materials described in Chapter 6.....	74
8.3. <i>Characterization</i>	76
8.4. <i>Appendix Figures</i>	81
8.5. <i>Abbreviations</i>	103
8.6. <i>Publication List</i>	105
8.7. <i>Declaration</i>	107
9. References	108
10. Acknowledgements	117

1. Introduction

Human history is inevitably connected to materials. Everything could be materials, and a material is a substance or mixture of substances that constitutes an object. Materials can be pure or impure, living or non-living matter. As human beings constantly shaped materials to serve their needs, it is significant for the improvement of civilization and to make a contribution to innovation. A beginning of a new era always is accompanied by the evolution of materials. Throughout history, human tried to gain more knowledge to develop their way to fictionalize materials. And the self-assembly process is a very important step. When compared with the previous time, materials themselves should be built from one to another part, at the moment all these isolated parts can be assigned in such a way that are assembled by themselves. Applying this approach makes it clear why the self-assembly process attracted scientists all over the world, as it represents the foundation of life. A tunable process is inevitable for the aim to approach the nanoscale level in material design.

Products based on self-assembly mechanisms are indispensable in our everyday life; they all utilize small molecules, e.g. surface-active agents, like surfactants in soap and daily shampoo for shower. Surfactants are usually organic compounds that are amphiphilic, meaning they contain both hydrophobic groups (their tails) and hydrophilic groups.¹ These amphiphilic molecules have been widely used, while the design of small molecules is limited due to the available size of the molecule and few applications in different liquid phases. On one hand, macromolecules can offer a sheer infinite possibility of opportunities for tailored design. Here, the toolbox of polymer architecture can be applied containing modification in composition, topology and even the introduction of certain functionalities. As a result, the approach of self-assembly via block copolymers spread out to diverse research fields, such as (nano)electronics,²⁻³ (nano)lithography,⁴⁻⁵ and catalysis,⁶⁻⁷ appeared to realize demands. One

Chapter 1

prominent area that is gathering more and more attention is the biomedical field. On the other hand, a water-based polymer system, which is named as the aqueous two-phase system (ATPS), allows application in pure water systems.⁸ ATPS mixes two aqueous solutions of water-soluble polymers, which turn biphasic when exceeding a critical polymer concentration. It has shown significance recently to water-in-water (w/w) emulsions due to their potential applications.⁸⁻¹⁰ W/w emulsions cannot be stabilized by ordinary surfactants, as they miss the scale of the phase boundary.¹¹⁻¹⁷ On the contrary, solid particles adsorbed at the interfaces can be exceptionally efficient stabilizers forming so-called Pickering emulsions.¹⁸⁻¹⁹ Nanoparticles can bridge the correlation length of polymer solutions and are thereby the best option for w/w emulsions. The presence of the solid particles at the interface inhibits coalescence of droplets, leading to efficient stabilization. Here, chemists use various nanoparticles^{14, 16, 20} in order to achieve the desired function while economical questions gain less concern, in contrast to industrial related applications. As a consequence, the boundaries of knowledge in many areas of cosmetics or food, possibly as an alternative to deliver ingredients²¹⁻²² with preferred solubility in the dispersed phase could be pushed further.

All the mentioned applications above benefit from the inherent property of aqueous systems. Moreover, there are other applications in permeability and thus the compartmentalized structure is desired. In addition the system was further developed towards colloidosome formation via crosslinking and supramolecular hydrogels. Usually, colloidal shell synthesis can be conducted via the self-assembly of appropriate nanoparticles between liquid interfaces and subsequent crosslinking.²³⁻²⁶ Moreover, formation of a supramolecular hydrogel network within ATPS emulsions should allow capturing their fine structure, resulting in micro-compartmentalized, fully aqueous hydrogel materials.²⁷ However, functionality and processability of aqueous multi-phase systems still need to be enhanced for the utilization of ideal encapsulation devices in the future.

Chapter 1

In addition to the basis of human demands, also researchers are denoted to current healthcare. W/w emulsions, compartmentalized hydrogels and crosslinked hydrophilic polymer networks, are promising as synthetic materials for tissue engineering as high water content of hydrogels are similar to biological tissues. Therefore, new approaches are applied in order to fabricate aqueous-based structure with diverse mechanical features and advanced healthcare materials.

In the present thesis, particle stabilized water-in-water emulsions as well as compartmentalized hydrogels are investigated that show promising properties for future application in the biomedical field.

2. Background and Motivation

2.1. Aqueous Two-Phase System (ATPS)

Aqueous two-phase systems (ATPSs), also known as all-aqueous systems, are formed by phase separation of an aqueous mixture containing two incompatible additives, such as two polymers or polymer and salts, above critical concentrations.²⁸⁻²⁹ In 1896, Martinus Beijerinck recognized this phenomenon for the first time when he found the formation of two immiscible phases after dissolving concentrated starch and gelatine in water.³⁰ ATPSs were rediscovered by Per Ake Albertsson in the 1950s for utilizing them to concentrate and isolate different types of biological materials.³¹ Since then, these systems have gained tremendous attention in a variety of areas, such as food industry, chemical synthesis, and biomedical engineering.³²⁻³³ In particular, the simultaneous possession of different affinities, i.e., partitioning of (bio)molecules towards the two immiscible phases, has established ATPSs in various conventional applications,³⁴⁻³⁶ such as extraction,^{34, 37} separation,³⁸⁻³⁹ purification,⁴⁰⁻⁴¹ and enrichment of cell organelles,⁴²⁻⁴⁵ proteins,^{31, 46} carbon nanotubes,⁴⁷⁻⁴⁸ and metal ions.⁴⁹

Therefore, the unique ability of aqueous two-phase systems (ATPSs) to create aqueous–aqueous interfaces through phase separation and the characteristics of these interfaces has created new opportunities in biomedical applications.

2.1.1. The types of ATPS

The most common biphasic systems are formed by two polymers (usually poly(ethylene glycol) (PEG) and dextran) or a polymer and a salt (e.g., phosphate, sulfate or citrate). Other types include ionic liquids and short-chain alcohols.^{32, 34, 37, 50-51} In addition to this, ionic and/or cationic surfactant mixtures are used for the formation of ATPSs, which are usually named as aqueous surfactant two-phase systems (ASTP systems).^{50, 52} Polymer-polymer/salt systems have been studied for more than five decades. Polymer-polymer systems are preferably used

Chapter 2

for the separation, recovery and purification solutes sensitive to the ionic environment as these systems pose low ionic strength. High ionic strength is the main disadvantage of polymer-salts system.⁵³ Alcohol-salt ATPS are inexpensive as compared to polymers and copolymers based ATPS. These systems are also characterized by low viscosity, easy constituent recovery, and reduced settling times, but a major drawback of using this type of ATPS is that many proteins are not compatible with alcohol rich phase.⁵⁴⁻⁵⁵

The aqueous micellar two-phase system was first introduced by Bordier for the separation of integral membrane proteins.⁵⁶ These systems are also useful for ionic environment sensitive solutes as nonionic surfactants can be used for the formation. Mixed micellar systems are becoming popular for showing selectivity features.⁵⁷ Most recently, ionic liquids (ILs) based ATPSs were developed.⁵⁸ Poly-phase systems (three or four polymer phases) also have been constructed for the separation of biomolecules.³² Single-polymer ATPSs have also been reported, which utilize only one polymer for the formation of ATPS in water.⁵⁹ PEGs of different molar mass are widely used as polymers in ATPS due to their low toxicity, low price and low volatile nature.³⁸ Table 2.1 shows different types of ATPS with representative examples.

Chapter 2

Table 2.1. Types of ATPS with representative examples

Types of ATPS	Representative examples		
	Composition of ATPS	Product	Results
Polymer-polymer	PEG-dextran ⁶⁰	Chitinase	Successful partitioning of chitinase towards bottom phase
Polymer-salt	PEG-K ₂ HPO ₄ ⁶¹	B-phycoerythri	Recovery yield = 90 % Purification factor = 4
Alcohol-salt	Ethanol- K ₂ HPO ₄ ⁵⁵	2,3-butanediol	Recovery yield > 98 %
Micellar/reverse micellar ATPS	n-Decyltetra(ethylene oxide) ⁶²	Bacteriophages	Bacteriophages partitioning towards micelle poor phase
Ionic liquids (ILs) - based ATPS	Imidazolium-K ₂ HPO ₄ ⁶³	Curcuminoids	Extraction yield= 96 % Purity= >51 %

2.1.2. The dynamics mechanism of ATPS

Just as oil and water that are immiscible with each other, two immiscible aqueous phases from the phase-separated ATPS also have an inherent interfacial tension, γ . However, in contrast to the o/w systems, the interfacial tension of the w/w system is typically very low, sometimes less than $1 \mu\text{N m}^{-1}$. The low interfacial tension associated with w/w interfaces favors the formation of all-aqueous jets, rather than droplets due to the slow growth of the Rayleigh-Plateau (RP) instability. Theoretically, the effective growth rate (ω_r) of the RP instability on a liquid jet (radius: r_0 , viscosity: μ_1) surrounded by an immiscible outer fluid (viscosity: μ_0) can be predicted by linear stability analysis, in the form of⁶⁴⁻⁶⁵

$$\omega_r = \frac{\gamma}{16\mu_0 R} \frac{F(x,\lambda)}{x^9(1-\lambda^{-1})-x^5} \quad (2.1)$$

where γ , R , k , x , and λ indicate the interfacial tension of two phases, size of the channel, dimensionless wavenumber, dimensionless radius of the jet (defined as r_0/R), and the viscosity ratio (defined as μ_1/μ_0), respectively. The function $F(x, \lambda)$ is expressed as

Chapter 2

$$F(x, \lambda) = x^4(4 - \lambda^{-1} + 4 \ln x) + x^6(-8 + 4 \lambda^{-1}) + x^8[4 - 3 \lambda^{-1} - (4 - 4 \lambda^{-1}) \ln x] \quad (2.2)$$

To simplify, the growth rate can be roughly estimated as $\omega_r \sim \gamma/(r_0\mu_0)$.⁶⁶

Compared to o/w systems with high interfacial tensions, the growth rate of the linear instability in w/w jets is much smaller, resulting in a significantly slower breakup into droplets and thus providing a possibility to achieve a long and stable liquid jet. Stable w/w jets have been achieved by combining ATPSs with microfluidic techniques, as demonstrated in glass capillary-based and polydimethylsiloxane (PDMS)-based microfluidic channels, respectively (Figure 2.1a and 2.1b).⁶⁷⁻⁶⁸ For instance, when two immiscible phases with an interfacial tension of 0.3 mN m^{-1} , extracted from aqueous mixtures of 7 wt% PEG (molecular weight $M_w = 10 \text{ kDa}$) and 10 wt% DEX ($M_w = 500 \text{ kDa}$), are injected into the microfluidic channels, the generated jet can be as long as 160 mm (Figure 2.1b). On the contrary, in conventional o/w systems, even with addition of sufficient surfactants,⁶⁹⁻⁷⁰ such long jets are still very difficult to achieve. The ability to form long and stable all-aqueous jets in microchannels also provides a very promising approach to fabricate surfactant-free microfibers.⁷¹ In addition, the perturbation growth rate measured in experiments is found to be one order of magnitude smaller than that predicted from linear stability analysis, suggesting a different mechanism might account for the breakup of liquid jets with low interfacial tensions.^{68, 72}

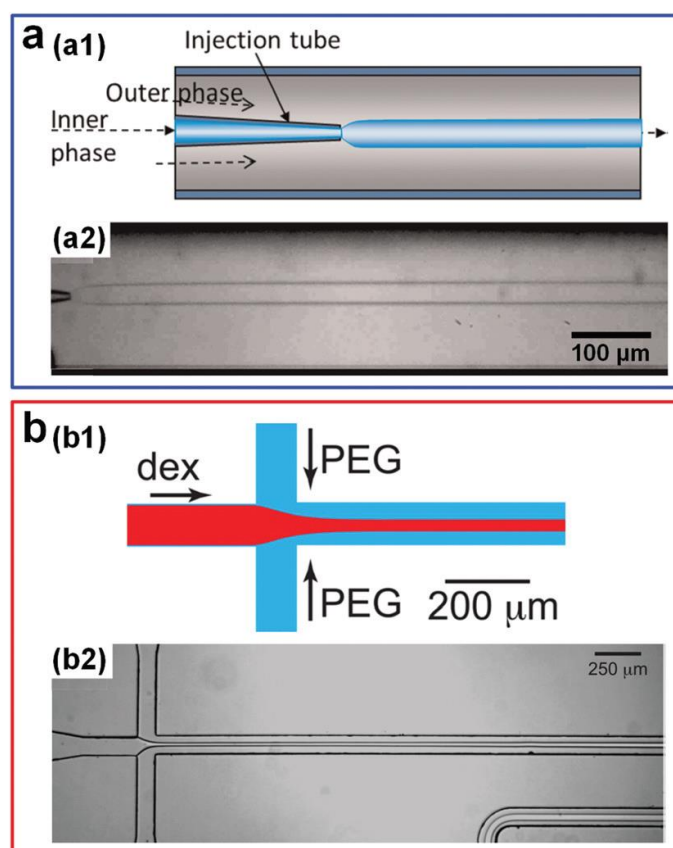


Figure 2.1. Stable w/w jets formed in microfluidic channels. (a) Schematic showing formation of w/w jets via a glass-capillary-based microfluidic device with a co-flow geometry (a1), and a typical image of the resulting stable jet (a2).⁶⁷ (b) Schematic showing formation of w/w jets in a PDMS-based microfluidic device with a flow-focusing geometry (b1), and a typical image of the resulting stable jet (b2).⁶⁸

2.1.3. Factors influencing partitioning of biomolecules in ATPS

Most of the ATPSs are optimized according to the physicochemical properties of solutes of biomolecules. Main factors influencing partition behavior in ATPS are collected in the following sections.

2.1.3.1. Molar mass (MW) and concentration of polymer

As most of the ATPSs are composed of polymer-polymer/salt. MW of polymers greatly influence the partition. Generally,

Chapter 2

- \uparrow MW of polymer \rightarrow \downarrow concentration of polymer required for phase formation
- \uparrow Differences between the MW of polymers \rightarrow \uparrow asymmetrical curve of the phase diagram
- \uparrow MW of PEG \rightarrow \downarrow value of K

In a polymer-salt system, partition towards polymer rich phase decreases upon increasing the concentration of polymer while in a polymer- polymer system partition decreases towards phase having high MW polymer. The main reason behind this phenomenon is the increase in the steric exclusion of biomolecule from the high MW polymer-containing phase or because of changes in the hydrophobicity of phases.^{34, 73} For example, as increase in the MW of polymer increases hydrophobicity by reducing the hydrophilic groups/hydrophobic area.⁷³

2.1.3.2. Hydrophobicity

Hydrophobicity plays an important role in the partitioning of proteins. Two main effects, i.e., phase hydrophobicity effect and salting out effect, are involved in hydrophobic interactions.⁷³⁻
⁷⁴ In polymer – salt systems, hydrophobicity may be manipulated by varying the value tie line length (TLL), MW of polymer and by adding a salt (e.g., NaCl). The low NaCl concentrations (<1 M) do not affect ATPS, however, high salt concentrations (>1 M) changes the phase diagram.⁷⁵ Thus, the addition of salt in ATPSs has a significant effect on the partition coefficient.⁷⁶ These salts contain ions of different hydrophobicities and the hydrophobic ions force the partitioning of counter ions to phase with higher hydrophobicity and vice versa. The salting-out effect moves the biomolecule from salt-rich phase to polymer-rich phase.⁷⁷

2.1.3.3. pH

The pH of ATPS may alter the charge and surface properties of the solute, which affects the partitioning of biomolecule. The net charge of the biomolecule turns negative in case of higher pH than the isoelectric point (pI) and positive if lesser than pI. If the pH is equal to pI, the net

charge will be zero.⁷⁷ It has been reported that the partitioning of negatively charged biomolecule in a system at higher pH increases the partition coefficient and target biomolecule prefers DEX-rich phase. Higher pH values than pI of biomolecule induce an affinity towards PEG-rich phase because of the positive dipole moment.^{74, 78}

2.1.3.4. Temperature

Temperature greatly affects the composition of two phases in an ATPS, and the phase diagram. The changes in temperature also affect partition through viscosity and density. Therefore, it is always recommended by the researchers to have a strict control of temperatures in ATPS related experiments. In general, phase separation is obtained at lower temperature in a polymer-polymer ATPS with lower concentrations of polymer,⁷⁹ however, an opposite effect is seen in polymer- salt system.⁸⁰

2.1.4. The applications of ATPS for separation and extraction

2.1.4.1. Cells and organelles

Purification of whole cells and their organelles using ATPS have been investigated by several authors. There are many reasons behind the purification of these cells and their organelles. For example, platelets contain various growth factors (e.g., platelet derived growth factor, transforming growth factor β and vascular endothelial growth factor). Thus, platelets are used as healing stimuli in different medical conditions. Sumida and co-workers reported the separation of platelets from whole blood using 16 types of polymers in a polymer-based ATPS. They concluded that poly (2- methylacryloxyethyl phosphorylcholine-co-*n*-butyl methacrylate) based separations were suitable for therapeutic purposes.⁸¹ Separation of cells in ATPS depends on numerous intrinsic properties like, electrochemical charge, size, hydrophobic and hydrophilic surface properties or in other words, interaction between the cell/organelle and polymer used in ATPS draw the separation pattern.⁸²

Chapter 2

Nowadays microfluidic devices are used for the separation of blood cells. Toner and Irimia excellently reviewed the use of such devices for blood cell separations.⁸³ For the first time a microfluidic separation method was applied to blood based on ATPS by SooHoo and coworkers. Whole blood was exposed to PEG-dextran ATPS and the results showed a different ratio between leukocytes and erythrocytes.⁸⁴

ATPS has also been used for several decades in plant related research. Numerous studies have been reported for the separation of whole-cell from cell lysates, e.g., isolation of plasma membrane vesicles from maize,⁴² purification of symbiosomes from pea and selection of high yielding cells from cultured strawberry cells.⁴³

Extracellular vesicles such as exosomes and microvesicles are used as biomarkers for blood based diagnostic purposes. But there is a lack of effective purification strategies. Recently, Shin et al., demonstrated an ATPS based method for the purification of such extracellular vesicles. A polymer-polymer (PEG-dextran) ATPS was used which resulted in almost 70 % recovery just in a time span of 15 min.⁸⁵

2.1.4.2. Low molecular weight compounds

Low molecular weight biomolecules (e.g., phytochemicals and secondary metabolites) are considered as high value products due to their broad applications in food or pharmaceutical industry. In traditional extraction and separation techniques, organic solvents are widely used, which are toxic and inflammable. This problem can be solved by the help of ATPS. However, there are only few studies regarding the application of ATPS for the processing these kind of biomolecules.⁸⁶

Chethana et al., investigated the extraction and purification of betalains (derivatives of betalamic acids) from *Beta vulgaris*.⁴¹ As a natural food colorant, the demand of betalains is increasing, mainly because of its antimicrobial and antiviral activities. The differential

Chapter 2

partitioning resulted in the 70-75 % of betalains in PEG-rich phase and sugars in salt-rich phase. Wu et al., showed the extraction of anthocyanins from mulberry (*Morus atropurpurea* Roxb.) Moreover, they stated that the ATPS did not alter the composition of these natural pigments and the antioxidant activity of the extract was relatively high as compared to conventional extraction techniques.⁸⁷ Other reported studies include the recovery of crocins from *Crocus sativas* using an ethanol-potassium phosphate ATPS⁸⁸ and the extraction of anthocyanins from *Brassica oleracea* L.⁸⁹

Recently, Zhang and co-workers used aqueous two-phase extraction (ATPE) for the enrichment of genistein and apigenin from pigeon pea roots (*Cajanus cajan* (L.) Millsp.). They employed an ATPS composed of 28 % ethanol and 22 % K_2HPO_4 , and the recoveries were 93.8 % and 94 % for genistein and apigenin, respectively.⁸⁶ The extraction of natural products from plant matrix by ATPE is getting more importance due to increase in the demand in the nutraceutical industry.

2.1.4.3. Drug residues in food and water

ATPS is also a novel technology for the separation and enrichment of drug residues in the water,⁹⁰ food from animal origin⁹¹ and herbs.⁹² ATPS has several advantages over traditional organic solvent extraction, or solid phase extraction (SPE) methods. It is regarded as an environmental friendly extraction procedure as both phases of ATPS contains water and no toxic volatile organic solvent is consumed in the process.⁹⁰ Moreover, a demulsification step is necessary in common extraction methods (e.g., SPE, disperse SPE). However, in ATPS it is possible to directly extract analytes in one single step.⁹³

Detection of residues at lower concentration is also possible with these biphasic systems. Han et al., showed the determination of chloramphenicol residues at concentrations lower than $1.5 \mu\text{g kg}^{-1}$, which was not possible in previously reported, dispersive liquid-liquid micro-extraction and matrix solid-phase dispersion methods.⁹¹ Pesticides and herbicide residues may

Chapter 2

also accumulate in the animal derived foods (e.g., milk). Recently, Yang and co-workers investigated five triazine herbicides in milk using ATPE. The simple ATPS was composed of acetonitrile and K_2HPO_4 . The limits of detection (LOD) were 2.1, 2.6, 2.3, 2.8 and 2.5 $\mu g L^{-1}$ for atraton, desmetryn, atrazine, terbumeton and terbuthylazine, respectively. The lowest average recovery of analytes was as high as 86.3%.⁹³

Roxithromycin (ROX) is a semi-synthetic antibiotic used frequently in human and veterinary medicine. Li et al. reported the extraction of ROX residues in aqueous environment and proved that IL-based ATPS was more efficient than traditional solvent extraction for ROX and other hydrophobic antibiotics.⁹⁰

2.1.4.4. Environmental remediation

The applications of ATPS are not only limited to biotechnology, but also being extended to environmental remediation in various ways.³²

Textile industry is responsible for the discharge of 10-15 % of annually produced 1 million tons of biodegradation resistant dyes. These dyes and their metabolites are toxic and carcinogenic in nature, thus posing a high potential danger to aquatic biota and human health.⁹⁴ Different physical and chemical methods have been studied for the removal of dyes from wastewaters. However, most of these methods are expensive, low efficient and laborious.⁹⁵ But these drawbacks could be overcome by ATPS which is an economic and eco-friendly method for the removal of textile dyes.⁹⁶ Recently, Ferreira and coworkers studied the IL-based ATPS for the extraction of a set of dyes in textile effluents⁹⁴ and Ivetic et al. investigated a PEG-salt ATPS model for Acid blue 9.⁹⁷ Results showed ATPS as an excellent alternative dye removal method with high yield.

ATPS can be also applied for large scale removal of microorganisms from cutting fluids and demonstrated to be more effective than biocide treatment and irradiation. Other examples

include the removal of metal ions,⁹⁸ food coloring dyes aromatics from industrial and environmental settings.⁹⁹

2.2. *Water-in-water emulsions*

Water-in-water (w/w) emulsions are colloidal dispersions of an aqueous phase in another aqueous phase. Such dispersions can be formed in mixtures of at least two hydrophilic macromolecules, which are thermodynamically incompatible in solution, generating two immiscible aqueous phases.³⁰ W/w emulsions are much less known than conventional oil-in-water or water-in-oil emulsions, despite the fact that phase separation in aqueous mixtures is highly common. However, the kinetic stability of water-in-water emulsions is generally difficult to control, as amphiphilic molecules do not adsorb on water-water interfaces. The colloidal stability of droplets in such systems is poor because of the lack of significant inter-droplet repulsion forces, and therefore emulsions in many aqueous biphasic systems are highly unstable. Consequently, surfactants are not good stabilizers for w/w emulsions, however, colloidal stability is enabled by the addition of particles, and the formation of water-in-water emulsions is feasible.

Repulsive interactions between polymer molecules produce segregative phase separations (at high macromolecule concentrations) or cosolubilization (at low concentrations). This behavior is a general phenomenon commonly observed in mixtures of hydrophilic polymers.¹⁰⁰ As an illustration, a comprehensive review listed around 100 different combinations of proteins and polysaccharides that resulted in segregative phase separation.¹⁰¹ Moreover, the same phase separation can also be found in many other combinations of macromolecules, and therefore, there is an almost unlimited number of systems that can be used to form w/w emulsions.

Water-in-water emulsions have a wide range of applications, which greatly expanded over the years, taking advantage of their all-aqueous nature, in absence of both oil and surfactant.

Chapter 2

Interestingly, w/w emulsions can be obtained in completely biocompatible systems, using mixtures of edible biopolymers, such as proteins and polysaccharides. Consequently, w/w emulsions might have many potential applications in food formulations. Moreover, they can be used to encapsulate hydrophilic active components for drug delivery.

2.2.1. Emulsion formation and stabilization

These emulsions can be prepared by applying mechanical agitation in ATPS. The phase with smaller volume fraction becomes the internal phase, and phase inversion occurs approximately at compositions in which the volume fraction of the two phases is approximately equal. Bicontinuous emulsions can be formed at compositions near to the inversion point at 1:1 volume ratio. This is illustrated in Figure 2.2, which shows examples of various w/w emulsions prepared in the water/gelatin/maltodextrin system.¹⁰² The two phase region appears at high concentrations, where gelatin-in-maltodextrin, maltodextrin-in-gelatin, and even bicontinuous emulsions can be formed, depending on compositions.

At the boundary line, denoted as binodal line, the chemical potentials of the two polymers are the same in both phases. The pairs of phases in thermodynamic equilibrium are indicated by tie-lines. It is interesting to remark that phase inversion occurs at approximately 1/1 volume ratio, in the center of the tie-lines in Figure 2.2, because the phase with larger volume fraction tends to be the external continuous phase. The tie-lines converge at the critical point, in which the composition difference between phases disappears. Beyond the critical point, the two immiscible phases vanish, forming one single phase. The tie-lines can be accurately determined by a simple method, based on measurements of volume ratio and densities, as reported by Atefi et al. .¹⁰³

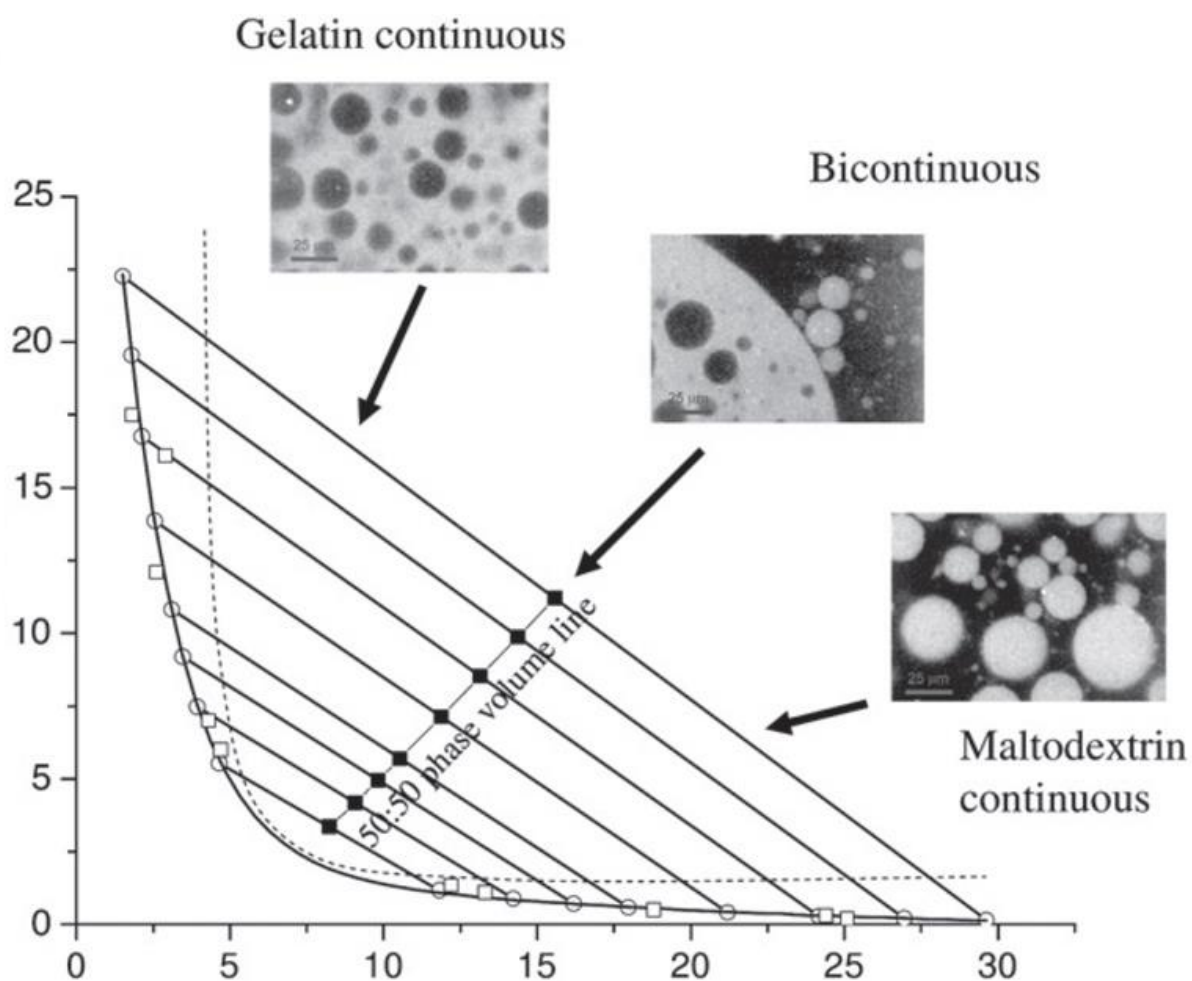


Figure 2.2. Scheme of w/w emulsion formation in the gelatin/malto dextrin system.¹⁰²

It is well-known that interfacial tensions at water-water interfaces are very low, often below the below the 10^{-2} mN/m range.^{17, 20, 104-105} For example, in the system composed of H₂O/dextran/PEG,^{17, 106-107} interfacial tension is only 0.07 mN/m at 8 wt% dextran and 6 wt% PEG,¹⁷ and it is even lower near the critical point. For comparison, one should consider that the typical values of tension in oil/water interfaces, in absence of surfactant, are in the range of 30 mN/m.

Ultralow values around 10^{-3} mN/m have been measured in gelatin/dextran and gelatin/arabic gum systems, using the spinning drop technique.^{20, 104} Antonov and coworkers have been able to measure interfacial tensions as low as 10^{-5} mN/m by a rheo-optical technique,¹⁰⁵ near to the critical point of the sodium caseinate/sodium alginate aqueous system. These values of

Chapter 2

interfacial tension are so low that spinning drop technique cannot be used any more. Furthermore, it has been demonstrated that interfacial tension depends on the difference in composition between the two aqueous phases, along the binodal line. Interfacial tension reaches extremely low values near the critical point,¹⁰⁵ where tension becomes virtually zero.

Moreover, it has been described that electrostatic charges at the w/w interface, originating from mixtures of polyelectrolytes and neutral polymers, even more reduce the already extremely low interfacial tension.¹⁰⁸⁻¹⁰⁹ The results suggested that an electrostatic potential difference spontaneously appears at the interface, producing a reduction in interfacial tension, which can be explained by the Poisson-Boltzmann theory.

The main disadvantage of water-in-water emulsions is their usual lack of stability, especially in compositions near the critical point. Fast coalescence or flocculation tend to occur, leading to rapid and irreversible phase separation, despite the fact that w/w emulsions do not undergo Ostwald Ripening. In w/w emulsions, the interfaces between the two phases are ill-defined, and are usually thicker in comparison to oil-water interfaces. Hence, water-water interfaces have length scales larger than the correlation length of the polymer solutions.¹¹⁰ Therefore, small hydrophilic molecules do not encounter an interface when they move from one polymer phase to the other. As a consequence, small molecules do not adsorb on water-water interfaces, and thus, poor stability is the main disadvantage for using w/w emulsions in practical applications. In conclusion, the stabilization of w/w emulsions is of utmost technological importance, and finding new methods for the effective stabilization of emulsions is an important challenge for chemists. Consequently, much scientific effort is currently devoted to deal with this issue.

Poortinga reported the first results that describe w/w emulsions stabilized by adsorption of particles at the water-water interface.¹⁶ Later, Firoozmand, Murray and Dickinson reported that addition of particles was able to stop spinodal phase separation by adsorption of particles at the

Chapter 2

interface.¹¹¹ It was clearly demonstrated that Pickering emulsions can be prepared in water/water systems. As such, a new approach for achieving colloidal stability of w/w systems was achieved.

W/w emulsions by mixing immiscible solutions of dextran and PEG were prepared in the presence of either latex particles or globular proteins. They observed that particles were able to adsorb on the interface, despite of the very low interfacial tension. Adsorption was weak in the case of latex particles, but better results were obtained when using a globular whey protein (β -lactoglobulin), which adsorbed stronger on the interface. Good interface coverage was achieved, as shown in Figure 2.3a. The presence of protein particles on the droplet surface did not inhibit macroscopic phase separation, but nevertheless stability was certainly increased, with a much slower phase separation.¹¹

The protein solutions were treated by heat at 85 °C, inducing aggregation of protein molecules, and obtaining stable suspensions of soft hydrogels based on proteins. These hydrogel particles were able to adsorb on the interface much stronger than native untreated protein. As a result, remarkable stable w/w emulsions could be obtained, because of the Pickering mechanism.⁹ This experimental result can be easily understood, considering that the energy of adsorption of a particle strongly depends on particle size,¹¹² as:

$$\Delta G = \pi R^2 \gamma (1 - \cos \theta)^2 \quad (2.3)$$

Where ΔG is the energy of adsorption, R is the radius of particles, γ is the interfacial tension and θ is the contact angle of adsorbed particles on the interface. Considering that the interfacial tension is very low in w/w emulsions, the energy of adsorption remains low except for large particles. Native proteins were not able to stabilize the emulsions because they were too small, and partial aggregation resulted in larger particles able to successfully adsorb and stabilize.

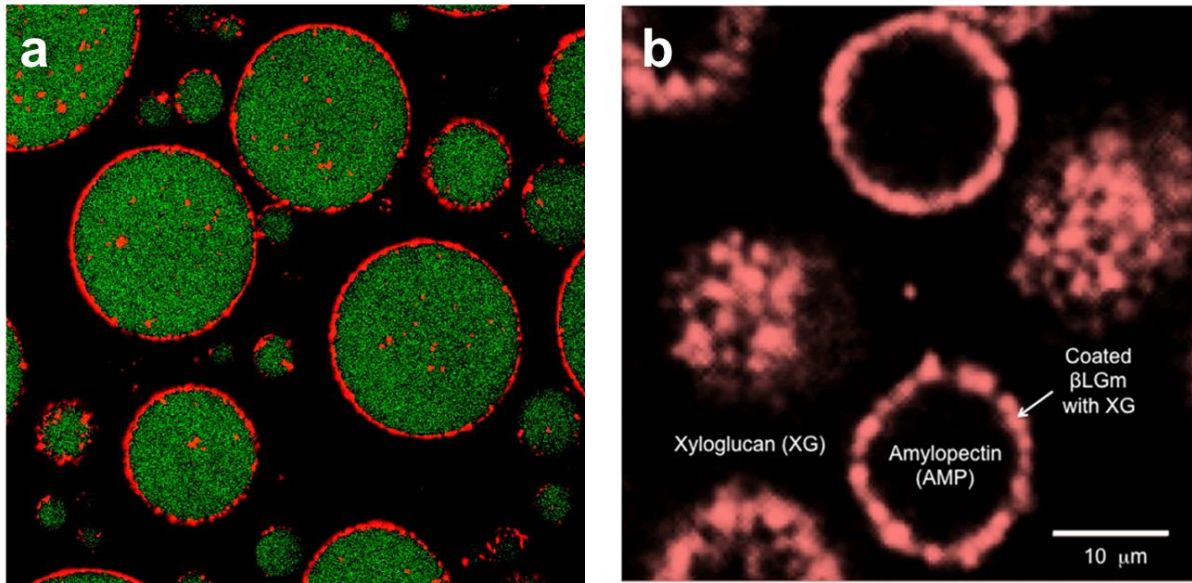


Figure 2.3. Examples of w/w emulsions stabilized by particles. (a) Image observed by confocal laser scanning microscopy with fluorescent labeling of droplets that contain dextran, dispersed into a solution of PEG. Protein particles adsorbed on the interface appear as orange. (b) Amylopectin-in-xyloglucan emulsions, stabilized by β -lactoglobulin microgels surface-coated with xyloglucan.^{11, 113}

The adsorption contact angle of spherical latex particles was measured by Balakrishnan et al., observing fluorescently labeled particles at the interface of labeled dextran, in the PEG/dextran system.^{11, 114} In this system, the contact angle is 145° . Therefore, the energy of adsorption, calculated according Equation (2.3), is approximately $7kT$.¹¹ This is not a very large energy of adsorption, nevertheless, it is high enough to anchor the particles at the interface, against thermal motion. In any case, the energy of particle adsorption greatly depends on particle size, increasing with R^2 . Balakrishnan used latex particles with sizes around $1 \mu\text{m}$, and it could be presumed that this is an appropriate size for achieving good stabilization.

2.2.2. Control of droplet size and morphology

As a consequence of the low values of interfacial tension in w/w emulsions, it is possible to control the droplet size of the emulsions by modulating the shear rate. For example,

Chapter 2

maltodextrin-rich droplets, dispersed into a continuous phase enriched in gelatin, can be obtained with a droplet size of around 7 μm , achieved by applying a shear rate of 100 s^{-1} in a 100 μm gap between two parallel plates.¹¹⁵ The droplet size is increased to around 30 μm by slowing shear rate down to 10 s^{-1} and increasing the gap to 500 μm . In any case, as mentioned before, these emulsions are quite unstable in absence of a stabilizing agent, unless shear is continuously applied, or gelification and/or crosslinking takes place either in the internal or the external phase.

Norton and coworkers have dealt with the issue of controlling morphology by applying shear to gelifying systems.¹¹⁶⁻¹¹⁷ An interesting work showed that anisotropic elongated microgel particles with controlled shape ratio could be obtained by applying shear simultaneously to gelation.¹¹⁷ Viscosity of some biopolymer solutions in water such as gelatin, significantly depends on temperature, and careful tuning of this parameter during controlled shear, allows obtaining non-spherical particles in a kinetically trapped state.

Structures in two-aqueous phase mixtures decrease their interfacial area by minimizing the free energy of the system, with the final morphology dependent on temperature, molecular ordering and the relative phase volume of the equilibrium phases.¹¹⁸⁻¹¹⁹ As a consequence, many different transient structures, which are inherently unstable, can be observed. For example, bicontinuous structures can be formed during fast decrease of temperature that induces spinodal decomposition.¹¹⁹ Interestingly, non-spherical structures can be kinetically arrested, and thus preserved, by crosslinking in the dispersed phase.¹¹⁸ It should be remarked that non-spherical shapes are not unfavorable, given that interfacial energy is very low, thus allowing a large interfacial area. In conclusion, a very wide variety of different shapes can be obtained (spheres, ellipsoids, rods, fibrils, etc.). There is an almost unlimited number of different morphologies, and authors are investigating different methods for controlling size and shape, which are usually based on shearing and arresting phase separation.^{117, 120-121}

Chapter 2

A high degree of control in the droplet size of w/w emulsions can be achieved by microfluidic techniques.^{67, 118, 122-124} Various authors have studied the application of microfluidic techniques for the formation of w/w emulsions with controlled morphologies in detail.⁶⁷ As an illustrative example, the formation of monodisperse droplets is displayed in Figure 2.4. The main differences with respect to previous microfluidic methods for production of monodisperse o/w or w/o emulsions, are that the interfacial tension is very low and the Rayleigh-Plateau (RP) instability grows slowly. For this reason, the droplets are generated by applying a quite small hydrostatic pressure that induces flowing at relatively low speeds.

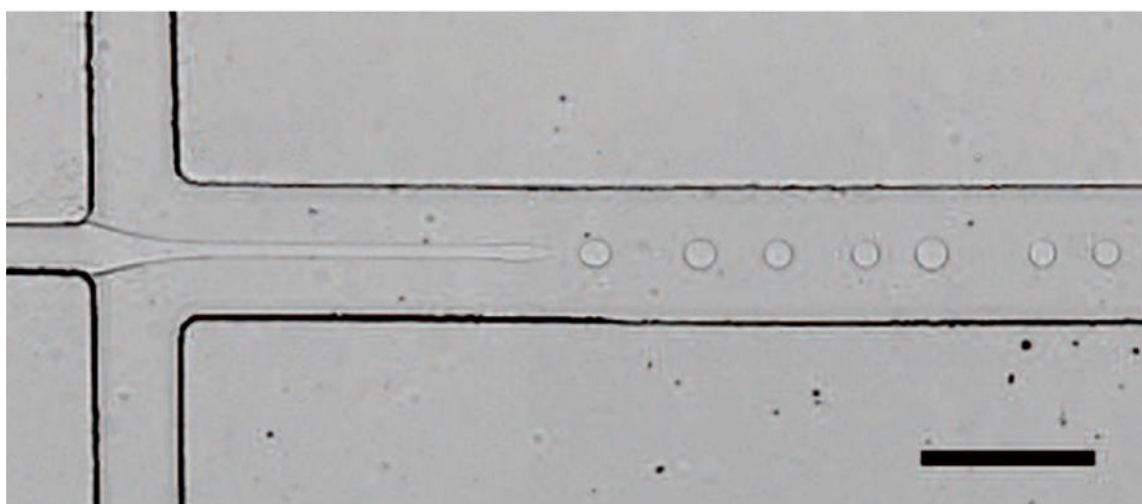


Figure 2.4. Example of a microfluidic device that produces rather monodisperse water-in-water droplets. A small hydrostatic pressure required, because of the ultralow interfacial tension in w/w aqueous two-phase systems.¹²⁴

2.3. Basic knowledge of Pickering emulsions

Pickering emulsions are emulsions of any type, either oil-in-water (o/w), water-in-oil (w/o), or even multiple emulsions, stabilized by solid particles instead of surfactants (Figure 2.5).^{112, 125-127} Moreover, they are generally used for water-in-water emulsion preparation. Pickering emulsions are named after S.U. Pickering whose publication¹²⁸ is considered as the first report of o/w emulsions stabilized by solid particles adsorbed at the surface of oil droplets. Pickering emulsions retain the basic properties of classical emulsions stabilized by surfactants (emulsifiers), so that a Pickering emulsion can be substituted for a classical emulsion in most applications. The high resistance to coalescence is a major benefit of the stabilization by solid particles. The ‘surfactant-free’ character makes them attractive to several fields, in particular cosmetic and pharmaceutical applications where surfactants often show adverse effects, e.g. irritant or hemolytic behavior.¹¹² Solid stabilizing particles are necessarily smaller than emulsion droplets. Thus, solid particles of nanometric size (or sub-micron, ~100 nm) allow the stabilization of droplets as small as few micrometers diameter; but stabilization of larger droplets is possible as well.^{112, 125} Micron-sized solid particles can stabilize larger droplets, the diameter of which possibly reaching few millimeters. The availability of stable millimeter-sized emulsions is a supplementary benefit of Pickering emulsions with respect to classical emulsions; this possibility comes from their high stability against coalescence.¹²⁹

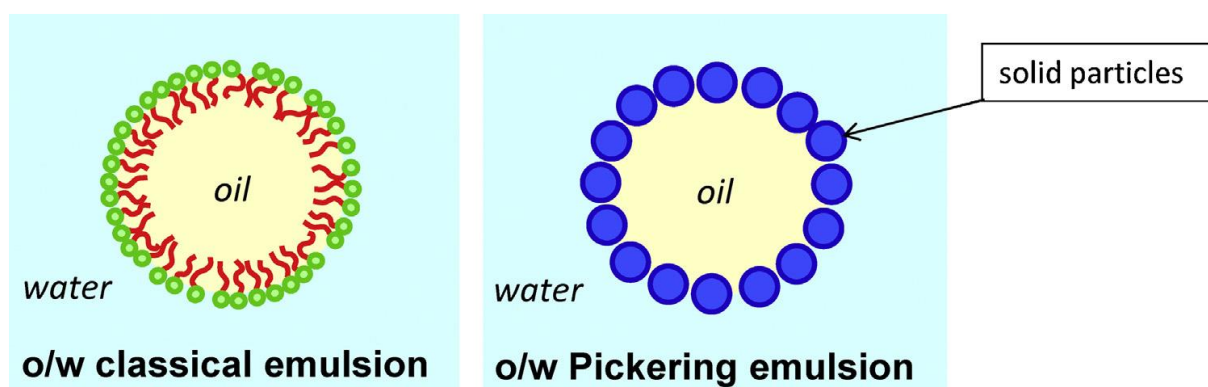


Figure 2.5. Sketch of a classical (surfactant-based) emulsion and a Pickering emulsion. The solid particles adsorbed at the oil-water interface stabilize the droplets in place of the surfactant molecules.

As in the case of surfactants, stabilization of emulsion droplets takes place by means of adsorption of solid particles at the surface of emulsion droplets. The mechanism of adsorption is very different to surfactants, as the solid particles are not amphiphilic. Partial wetting of the surface of the solid particles by water and oil is the origin of the strong anchoring of solid particles at the oil-water interface.

2.3.1. The stabilization mechanism of Pickering emulsions

Successful preparation of stable emulsions requires fulfillment of two main criteria: The emulsions are stable for a long time against any destabilization phenomena (coagulation, coalescence, Ostwald ripening), and the emulsification process is possible. The long-term stability mainly depends on the formulation but the process also matters as the droplet size is often governed by the shear rate of the emulsification process, in the same way as for any emulsifier based emulsion. The fabrication of emulsions is not only a matter of the process, the stabilizing agents also contribute a lot. The physical chemistry of Pickering emulsions, encompasses the phenomena of adsorption of particles, droplet stabilization by adsorbed particles, kinetics of adsorption that influence the emulsification process, and rheological properties that control creaming and sedimentation.

Chapter 2

Adsorption of solid particles at the oil–water interface requires the partial wetting of the solid by water and oil. This is a matter of interfacial energies of the three interfaces: solid–water, solid–oil, and oil–water, respectively γ_{s-w} , γ_{s-o} , and γ_{o-w} . Partial wetting of the solid by water inside an oil medium requires that the adhesion energy of water, $E_{Adh}(w/o)$, is positive and the spreading coefficient of water, $S(w/o)$, is negative:

$$E_{Adh}(w/o) = \gamma_{s-o} + \gamma_{o-w} > 0 \quad (2.4)$$

$$S(w/o) = \gamma_{s-o} - \gamma_{o-w} - \gamma_{s-w} < 0 \quad (2.5)$$

An equivalent point is to consider the wetting of the solid by oil inside a water medium where the positive adhesion energy, $E_{Adh}(o/w)$, and the negative spreading coefficient, $S(o/w)$, of oil read:

$$E_{Adh}(o/w) = -S(w/o) = \gamma_{s-w} + \gamma_{o-w} - \gamma_{s-o} > 0 \quad (2.6)$$

$$S(o/w) = -E_{Adh}(w/o) = \gamma_{s-w} - \gamma_{o-w} - \gamma_{s-o} < 0 \quad (2.7)$$

A very hydrophilic surface of the solid particles would be totally wet by water, so that the solid particles do not adsorb because they remain dispersed in the aqueous phase of the emulsion. On the same footing, too hydrophobic particles are totally wet by the oil. Under partial wetting conditions, the contact angles in water, θ_w , and in oil, θ_o , are given by Young's law ($\theta_o = \pi - \theta_w$):

$$\cos \theta_w = \frac{\gamma_{s-o} - \gamma_{s-w}}{\gamma_{w-o}} \quad \cos \theta_o = \frac{\gamma_{s-w} - \gamma_{s-o}}{\gamma_{w-o}} \quad (2.8)$$

Adsorption of solid particles under partial wetting conditions is very strong. The free energy of adsorption (the free energy input required for desorption of one particle, either into the aqueous or the oil phase) is related to the interfacial tensions and the size of the solid particles. For spherical particles of radius R , it reads¹³⁰⁻¹³¹

$$\Delta_{ads}F = -\pi R^2 \gamma_{o-w} (1 - \cos(\theta_w)) \text{ for } \theta_w < 90^\circ \quad (2.9)$$

$$\Delta_{ads}F = -\pi R^2 \gamma_{o-w} (1 + \cos(\theta_w)) \text{ for } \theta_w > 90^\circ \quad (2.10)$$

Adsorption is the strongest when the contact angle is 90° , which indeed corresponds to a maximum stability of emulsions in most instances.¹³² Obviously, large particles having a larger contact area of oil and water show up a larger adsorption free energy. Nanoparticles strongly adsorb to oil–water interface as well; there is no lower limit of particle size according to the wetting-based theory (Equation (2.9) and (2.10)). Indeed, the adsorption free energy is mostly much larger than the thermal energy, even when the solid particles are very small.

2.3.2. Control properties of Pickering emulsions

2.3.2.1. Stabilization of emulsions by adsorbed particles

Many types of particles, either inorganic or organic, fulfill the partial wetting condition for most common oils. Examples are calcium carbonate and barium sulfate,¹³³ clays (montmorillonite¹³³⁻¹³⁴ and laponite¹³⁵), carbon black,¹³⁶⁻¹³⁸ latex,¹³⁹⁻¹⁴² magnetic particles,¹⁴³⁻¹⁴⁴ carbon nanotubes¹⁴⁵ or block copolymer micelles.¹⁴⁶ Odd particles such as catanionic nanocrystals,¹⁴⁷ spores¹⁴⁸ or bacteria¹⁴⁹⁻¹⁵⁰ proved to be efficient stabilizers of Pickering emulsions as well. Functional particles feature supplementary properties; for example, thermosensitive poly(*N*-isopropylacrylamide) particles give temperature-sensitivity to the emulsions¹⁵¹⁻¹⁵⁴ and pH-sensitive emulsions have been prepared with the help of pH-responsive particles.¹⁵⁵⁻¹⁵⁶ Finally, stabilization of Pickering emulsions by proteins as solid particles have been claimed.¹⁵⁷⁻¹⁵⁸

Destabilization of emulsions occurs in two successive steps: coagulation and coalescence. The surface coating by solid particles mainly acts against coalescence. The adsorbed layer of solid particles forms a rigid coating around the liquid droplets that has been compared to an egg shell.¹²⁵ Reorganization of surface materials required for liquid droplets to merge is prevented by the mechanical barrier that prevents coalescence. The mechanical strength of the particles layer comes from aggregation of solid particles at the droplet surface. Solid particles are held

together at the oil–water interface by means of attractive interactions which are required for building up the rigid layer of solid particles. In particular capillary forces are specific to particles adsorbed at the liquid-liquid interface. All types of interactions between adsorbed particles influence the stability of Pickering emulsions: dispersion, electrostatic... Even for interactions that are not specifically interfacial, the presence of the oil-water interface influences their contribution to the overall interactions. For instance, electrostatic repulsions between charged particles operate at a dielectric discontinuity between oil and water, which introduces peculiar behavior that may not follow intuitive expectations relying on well-known behavior in a homogeneous dielectric medium.¹⁵⁹⁻¹⁶⁰

2.3.2.2. Control of emulsion droplet size by formulation and process parameters

In case where the solid particles adsorb as a dense monolayer, the total oil–water interfacial area is set by the amount of solid particles. Under such conditions, simple geometrical considerations give a relationship between the droplet diameter and the mass ratio of dispersed phase to the solid particles. For an o/w emulsion this reads.¹⁶¹⁻¹⁶³

$$d = \frac{6}{\rho_{oil}\alpha_{solid}} \frac{M(oil)}{M(solid)} \quad (2.11)$$

where d is the droplet diameter, ρ_{oil} is the density of oil and α_{solid} is the interfacial area covered per mass of solid particles. Such a relationship has often been observed in experiments.¹⁶⁴⁻¹⁶⁵

The underlying assumption may not be satisfied in every case however. Indeed, there are several reports showing microscopy pictures of stable Pickering emulsion droplets with incomplete coverage of the droplets by solid particles.¹⁶⁵⁻¹⁶⁷ Solid particles may also aggregate at the droplet surface; Frelichowska et al. gave a geometrical relationship relating α_{solid} to the fractal dimension of solid particles aggregates. Departure from the linear relationship (Equation (2.11)) has been observed in case of high ratio $M(oil)/M(solid)$.^{163, 168-169}

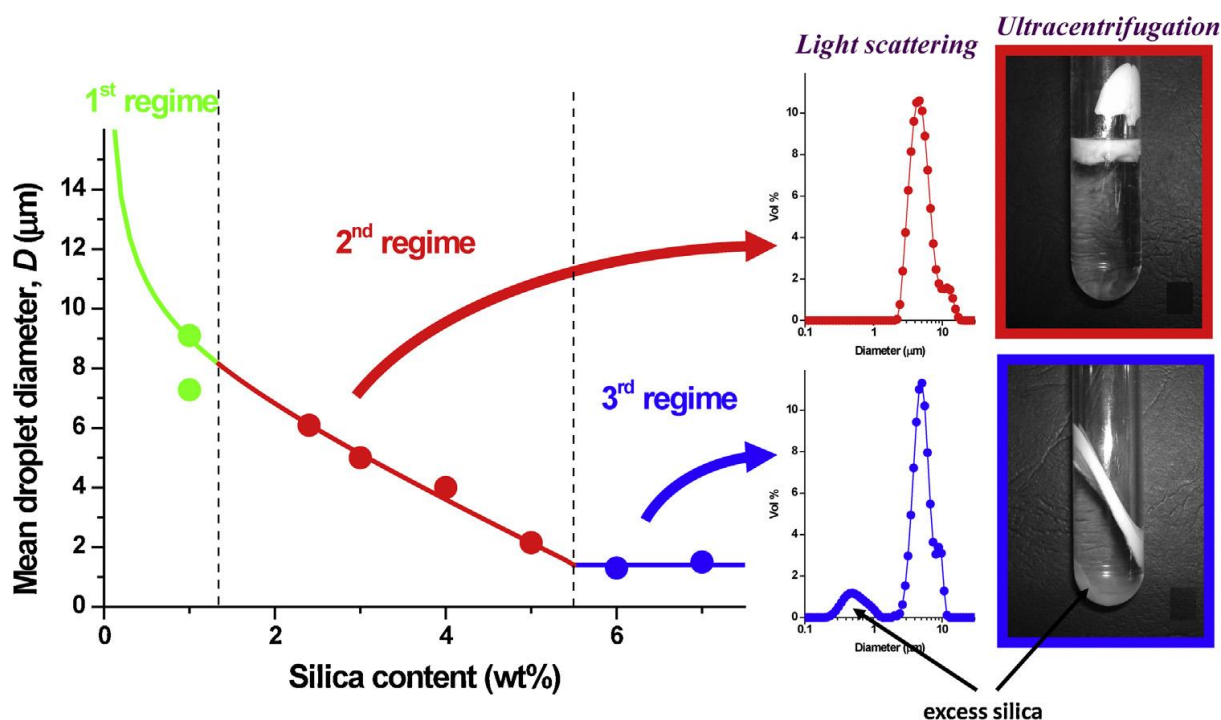


Figure 2.6. Mean droplet diameter of o/w Pickering emulsions of 2-ethylhexyl stearate oil (Stéarinerie Dubois) stabilized by HDK® H30 hydrophobic silica (Wacker): three regimes are encountered according to the concentration of silica at constant oil content (20 wt%). In the third regime, excess silica particles are detected as a supplementary population of submicron particles by light scattering measurements, and as sediment in ultracentrifugation experiments. None of these features is observed in the second regime.¹⁶³

The emulsification of o/w Pickering emulsions takes place under three distinct regimes depending on the solid particle to oil mass ratio, $M(\text{particles})/M(\text{oil})$ (Figure 2.6). Emulsification fails in the first regime at low solid content. In the second regime, the droplet size is controlled by $M(\text{particles})/M(\text{oil})$ according to Equation (2.11); α_{solid} may not be constant however. Finally a third regime is reached at high $M(\text{particles})/M(\text{oil})$ where the droplet size is controlled by the emulsification process.

2.3.2.3. Emulsion type and emulsion inversion

The emulsion type is controlled by the wettability of the solid particles.^{112, 132} In the same way as a water-soluble hydrophilic emulsifier (high HLB) orients the emulsification process towards an o/w emulsion type (and a hydrophobic emulsifier gives a w/o emulsion), hydrophilic particles favor o/w Pickering emulsions. More specifically, o/w emulsions are favored when the contact angle in water, θ_w , is smaller than 90° . Conversely, $\theta_w > 90^\circ$ favors w/o emulsions. This is strongly reminiscent of the Bancroft rule of emulsifiers. Kruglyakov assigned a HLB value to particles on this basis.¹⁷⁰⁻¹⁷¹ A major difference between particles and emulsifiers stands in the range of emulsion stability with respect to surface hydrophilic character of the particles. Thus, optimum stability of surfactant-based emulsions is reached when the surfactant hydrophilic character (HLB value) is significantly shifted off the HLB of a balanced surfactant. In between the ranges for optimum stability of w/o emulsions ($3 < \text{HLB} < 7$) and o/w emulsions ($9 < \text{HLB} < 15$), there is a gap (around $\text{HLB} = 8$) where none of these emulsions is stable. Conversely, optimum stability of Pickering emulsions is ensured when the contact angle is close to 90° , that is, for solid particles that are balanced regarding their wetting properties. These solid particles are well-suited for the stabilization of either o/w or w/o emulsion type. As a consequence, phase inversion can be triggered by changes of the wetting behavior,¹³² but also by means of several parameters such as the relative water and oil contents^{132, 172-173} or the medium where the solid particles have been initially dispersed.¹⁷²⁻¹⁷⁴ There is a strong hysteresis in the phase inversion phenomena that cannot occur with surfactant based emulsions.¹⁷⁴

3. Outline

In order to investigate the general potential of ATPSs for biomaterials and compartmentalized systems, various solid particles were applied to stabilize all-aqueous emulsion droplets. The target ATPS to be investigated should fulfill the following criteria: The system should be prepared via mixing of two aqueous solutions of water-soluble polymers, which turn biphasic when exceeding a critical polymer concentration. For ATPS, the interface between the two phases is rather undefined and spans a region larger than the characteristic correlation length of the polymer solutions. Hydrophilic polymers with a wide range of molar mass such as dextran/poly(ethylene glycol) (PEG) can therefore be applied. Solid particles adsorbed at the interfaces can be exceptionally efficient stabilizers forming so-called Pickering emulsions,¹⁸⁻¹⁹ and nanoparticles can bridge the correlation length of polymer solutions and are thereby the best option for w/w emulsions.

The first approach towards the investigation of ATPS was conducted with all aqueous dextran-PEG emulsions in the presence of PDP in Chapter 4. The water-in-water emulsions were formed via a PEG/dextran system via utilizing PDP as stabilizers. Studies of the formed emulsions were performed via LSCM, OM, cryo-SEM and tensiometry. Furthermore, crosslinker functionality in terms of the crosslinkable the solid PDP is incorporated in order to inhibit demulsification of the Pickering emulsion. TEM, SEM and FTIR were used to visualize the morphology of PDP before and after crosslinking. Further application of PDP stabilized water-in-water emulsions is to form supramolecular compartmentalized hydrogels as demonstrated in Chapter 5. Here, hydrogels are prepared in pre-formed water-in-water emulsions and gelation via α -CD. Studies of the formed complexes are performed via XRD and the mechanical properties of the hydrogels were measured with oscillatory shear rheology. The hydrogels and emulsions are assessed via OM, SEM and CLSM as well. The last chapter broadens the investigations from the previous two systems by utilizing various CN as different stabilizers in ATPS. The CN extends the

Chapter 3

generality of aqueous two-phase Pickering emulsions as verified by SEM, TEM and DLS. Furthermore, emulsification and demulsification are probed. The various all aqueous phase systems will provide model for future fabrication of biocompatible materials, cell micropatterning as well as separation of compartmentalized systems.

4. Water-in-water Pickering emulsion stabilized by polydopamine particles and crosslinking ¹

4.1. Overview

As introduction in the theoretical part, aqueous multi-phase systems have attracted significant attention recently, in particular water-in-water Pickering emulsions. In here, dextran and poly(ethylene glycol) (PEG)-based aqueous emulsions are stabilized by polydopamine nanoparticles (PDP). Remarkably, stable emulsions are obtained from the biocompatible material that can be broken either via dilution or surfactant addition. Further crosslinking of PDP via poly(acrylic acid) and carbodiimide strengthens the stability of emulsion droplets in a colloidosomes-like structure. After this crosslinking, demulsification via dilution or surfactant addition was largely hindered as shown in schematic overview (Figure4.1).

¹ Terms of use: This chapter was adapted with permission from Jianrui Zhang, Jongkook Hwang, Markus Antonietti, Bernhard V. K. J. Schmidt, “Water-in-water Pickering emulsion stabilized by polydopamine particles and crosslinking”; *Biomacromolecules*, **2019**, *20(1)*, 204-211. Copyright 2019 American Chemical Society.

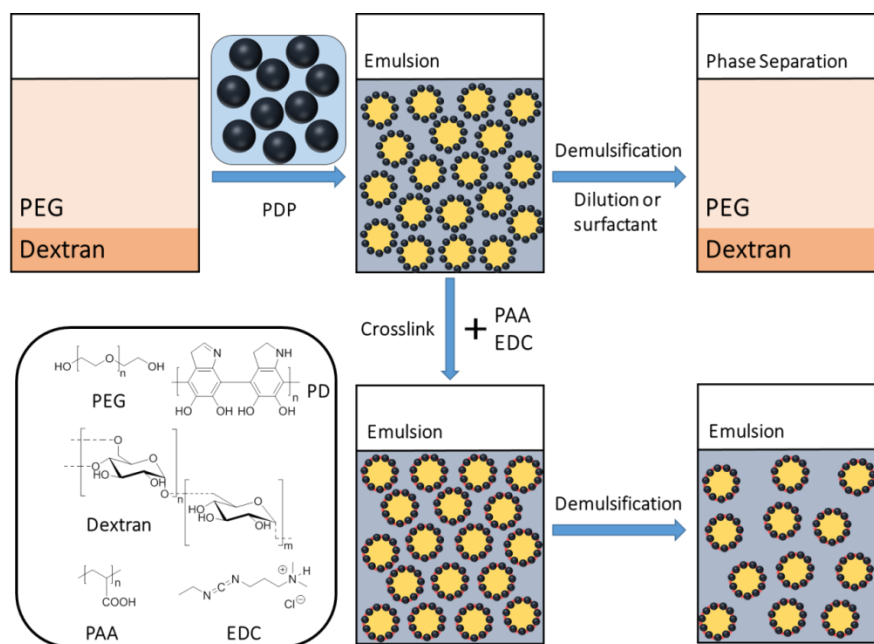


Figure 4.1. Overview of the dextran/PEG water-in-water emulsion formation employing polydopamine particles (PDP) and crosslinking with poly(acrylic acid) (PAA) / 1-ethyl-3-(3-dimethylaminopropyl)carbodiimide (EDC). Insets: Structures of dextran (idealized), PEG, PD (idealized), PAA and EDC.

4.2. Results and Discussion

PDP stabilized water-in-water Pickering emulsions

The PDP to stabilize aqueous two-phase system (ATPS) emulsions was easily obtained by air-promoted oxidative condensation of dopamine at basic pH. In a typical synthesis, PDP with an average size of around 400 nm was obtained and characterized via SEM and TEM (Figure A1). As a common ATPS, dextran and poly(ethylene glycol) (PEG) were employed, and the two phase system was emulsified by addition of 0.2 g/L PDP (Figure 4.2). The optical microscopy images indicate droplet formation, which corresponds to a water-in-water emulsion system as known from literature.^{11, 175} The formed droplets show a broad dispersity of droplet sizes that

is in the range of 1 to 20 μm in a stable emulsion with a number average of around 15.21 μm (Figure 4.2d). Clearly, a bimodal distribution of droplet sizes can be observed in the optical microscopy image, which is only marginally reflected in the number average of the droplet sizes. The dispersity might be due to the emulsion formation method that was based on hand shaking at first. A more in-depth investigation of the formed droplets was performed via cryo-SEM imaging that reveals droplet formation as well (Figure 4.2f and 4.2g) in contrast to reference samples without PDP addition (Figure A2). The observed droplets show partly additional roughness, which might be due to the freeze fracture process, hydration of the droplet surface as well as polymers in the surrounding. PDP based emulsions show a long-term stability for at least 16 weeks (Figure 4.2e).

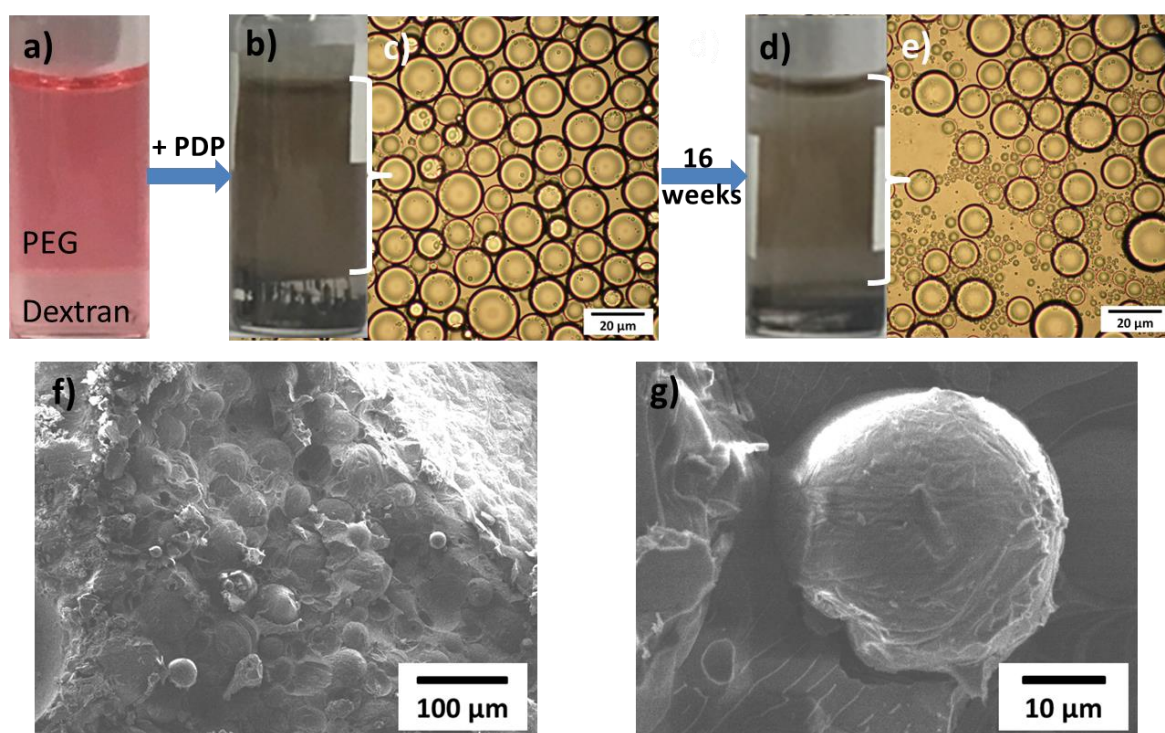


Figure 4.2. Images of the PEG_{35k} (7 wt%)/dextran_{40k} (3 wt%) water-in-water system formed via shaking by hand: Optical images of (a) an aqueous two-phase system (stained with red dye for visualization), (b) PDP (0.2 g/L) stabilized emulsion and (d) a long-term stable emulsion after 16 weeks; optical microscopy images of (c) emulsion droplets and (e) long-term stable

emulsion droplets; cryo-SEM images (f) emulsion droplets and (g) magnification of a single emulsion droplet.

To further verify the formation of a w/w emulsion stabilized by PDP, FITC-labelled PEG was introduced into a dextran-in-PEG emulsion and imaged via CLSM (Figure 4.3b). The visible dark liquid droplets and clear bright continuous phase region shows the presence of fluorescently labelled PEG continuous phase outside the emulsion droplets, which indicates the near complete separation of PEG and dextran, as expected. CLSM images show larger droplets than observed in optical microscopy, which can be explained via addition of FITC-labelled PEG solution (0.5 mL) causing 12.5% dilution of the entire emulsion.

Once stable emulsions were prepared, in addition to the emulsion phase on top, another phase on the bottom was observed as well. To verify the nature of the bottom phase, optical microscopy and CLSM were performed (Figure A4). No droplets could be observed, which clarifies that the lower phase is not the emulsion phase.

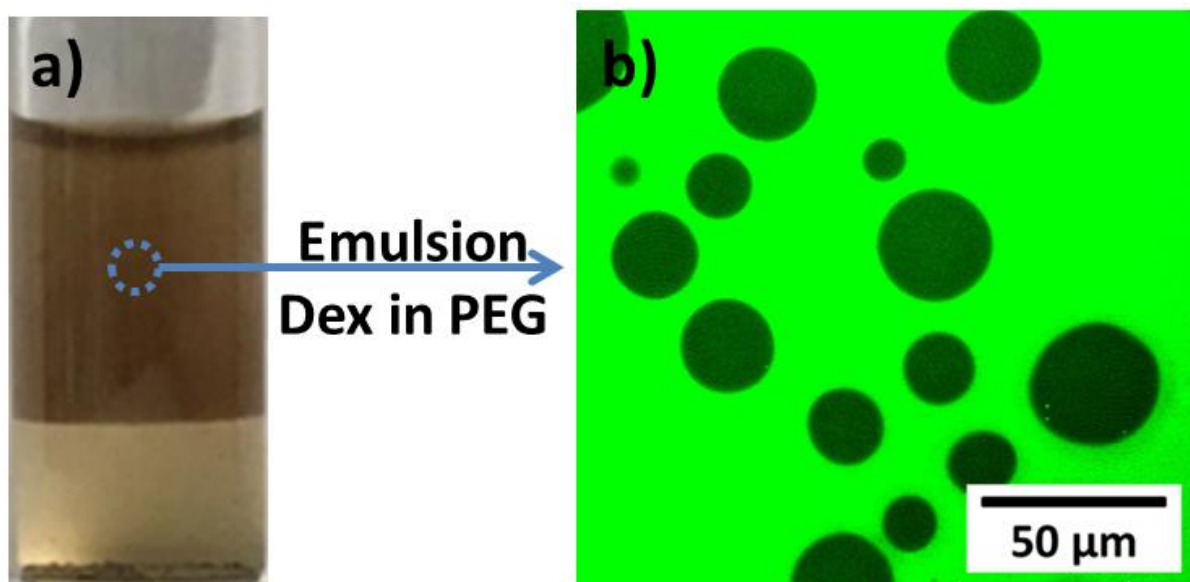


Figure 4.3. Emulsion images of the system PEG_{35k} (5 wt%)/dextran_{40k} (5 wt%) formed via shaking by hand; dextrans-in-PEG: Photograph of (a) two phase system and (b) CLSM image of emulsion droplets via utilization of FITC-labelled PEG.

Chapter 4

Further studies of Pickering emulsion formation

As mentioned before, emulsions with considerable dispersity were formed with hand shaking. In order to decrease dispersity of droplet sizes, the procedure was evaluated further. Vortex treatment for 30 s led to decreased dispersity of emulsion droplets and generally smaller droplet sizes (Table A1), also shown in an exemplary droplet size histogram (Figure A5). For further analysis of the ATPS Pickering emulsion formation via PDP, various ATPS were investigated regarding their droplet sizes employing different PEG and dextran molar masses and different ratios (Table A2). Total weight percentage of (PEG + dextran) was kept at 10 wt% in all cases. In most cases, stable emulsions are formed as expected from the literature.^{11, 22} For the combination of low molar mass PEG_{20k} and dextran_{40k}, with addition of 0.2 g/L PDP (final concentration) at a concentration of PEG from 4 wt% to 2 wt% and a concentration of dextran from 6 wt% to 8 wt%, stable emulsions could not be obtained. The molar mass of PEG_{20k} is too low to obtain emulsions at low PEG concentrations, which is due to the well-known effect of molar masses on ATPS formation. At concentrations of PEG_{20k} above 4 wt%, emulsions were obtained. Accordingly, once other conditions are employed (PEG_{20k}/dextran_{100k} and PEG_{35k}/dextran_{40k}) for water-in-water emulsions with 0.2 g/L PDP, stable emulsions could be formed in the range of 8 wt% to 2 wt% and 2 wt% to 8 wt% for PEG and dextran respectively (Table A2). Moreover, these water-in-water emulsions were stable for more than 16 weeks. Overall, a variation of droplet sizes was observed for the emulsions with different composition, parts of them even have differences in the number average diameter of up to 14 μm (Table 4.1 and A2).

Indeed, PDP plays an effective role in stabilizing ATPSs in all cases as well. Even when changing the concentrations of PDP from 0.2 g/L to 0.4 g/L and 0.6 g/L, a PDP-stabilized Pickering emulsion could be obtained (Table 4.1 and Table A3). As expected, the droplet sizes decrease when the concentration of PDP suspension is increased. Nevertheless, droplet sizes depend significantly on PEG and dextran concentrations as well. While increasing the

Chapter 4

concentration of PDP from 0.2 g/L to 0.6 g/L, the average size of droplets reduces by 10 μm in the case of PEG_{35k} (3 wt%)/dextran_{40k} (7 wt%). For PEG_{35k} (5 wt%)/dextran_{40k} (5 wt%) the droplet sizes decreased around 5 μm , when the PDP concentration was increased from 0.2 g/L to 0.6 g/L. Contrary, in the case of emulsions based on PEG_{35k} (7 wt%)/dextran_{40k} (3 wt%) no significant changes in droplet size were observed, when the PDP concentration was changed.

Previous studies show that the average droplet size of solid-stabilized emulsions decreases with increasing particle concentration as more particles are available to stabilize the higher interface of smaller droplets.^{137, 176-177} It seems reasonable to assume that, for given homogenization conditions, the phase being broken down into droplets is fragmented initially to the same extent, irrespective of the particle concentration. Depending on the amount of particles adsorbed on the droplet surfaces, the droplets will coalesce, reducing the total droplet surface area, until the particle coverage is sufficient to stabilize the droplets against further coalescence.¹⁶⁹ The coverage with particles can be estimated via the total volume of the emulsion, average droplet sizes and concentration of particles assuming complete accumulation of PDP on droplet surfaces. The amount of PDP that actually takes part in emulsion stabilization differs from the initially added amount as some PDP is left at the bottom after emulsification. Thus, the concentration of PDP has to be corrected according to the amount of precipitate. By the volume of emulsion and the average droplet size, the interface can be obtained. Finally, via the corrected amount of particles that take part in stabilization, the surface coverage is calculated (refer to the Supporting Information for details on the calculation, eq A1-A4). For emulsion PEG_{35k} (7 wt%)/dextran_{40k} (3 wt%) with 0.2 g/L PDP, the surface coverage of the interface layer is $1.168 \times 10^{-6} \text{ g/cm}^2$.

Chapter 4

Table 4.1. Dependence of PEG_{35k}/dextran_{40k} water-in-water emulsion droplet size on PDP suspension concentration with standard deviation. Emulsions obtained via vortex for 30 s.

PDP concentration (g/L)	$C_{\text{PEG}} = 3 \text{ wt}\%$ $C_{\text{Dex}} = 7 \text{ wt}\%$	$C_{\text{PEG}} = 5 \text{ wt}\%$ $C_{\text{Dex}} = 5 \text{ wt}\%$	$C_{\text{PEG}} = 7 \text{ wt}\%$ $C_{\text{Dex}} = 3 \text{ wt}\%$
0.2	16.01±0.88 μm	10.72±0.91 μm	4.62±1.03 μm
0.4	12.3±1.06 μm	10.01±1.01 μm	4.96±0.83 μm
0.6	5.81±0.93 μm	6.02±0.94 μm	5.01±0.86 μm

PDP was synthesized under alkaline conditions and contains basic amine groups. Hence, it is important to analyze the applicability of PDP at different pH values for emulsifying Pickering emulsions. A regular tendency of droplet sizes with respect to pH change is observed for three various ratios of PEG and dextran (Figure 4.4). As the pH value is increased, especially approaching alkaline condition, the size of emulsified droplets decreases by 20%. To elucidate the effect of pH on emulsion droplet size, zeta potential and hydrodynamic diameter of pristine PDP were investigated at first. Under alkaline condition, PDP has negative zeta potential, but with decreasing pH, the zeta potential value first turns less negative, then a positive zeta potential is reached below pH 6 (Figure A6). In addition, we found that pH dependent dynamic aggregation behavior of PDP can greatly affect the emulsification capability of PDP. Acidic conditions lead to insignificant aggregation of PDP in water, which is confirmed by the decreased hydrodynamic diameter of PDP. The observed particle sizes increase gradually with increasing pH from 2 to 11 (Figure A6). Particle sizes between 500 nm and 1.0 μm for different pH indicate that PDP tends to form aggregates in suspension, considering the size of as-made PDP \sim 400 nm observed from SEM.

In order to obtain further information about the observed multiphase system, interfacial tensions of the individual aqueous phases were measured via the pendant drop method (Figure A8).

Chapter 4

Influence of pH on the interfacial tension were measured between PEG_{35k} (3 wt%) and dextran_{40k} (7 wt%) solution in the presence of PDP. A minor decrease in interfacial tension from 70 mN/m to 60 mN/m moving from pH 2 to pH 11 was observed (Figure A7). A more significant change can be observed in the case of contact angles of PDP between PEG_{35k} and dextran_{40k} solution (Figure A8). The contact angle is approaching 90° with increasing pH value, which is in line with the interfacial tension of PDP suspension (0.2 g/L) that gradually decreases at increased pH. Compared to aqueous solution with the absence of PDP, the presence of PDP in aqueous solution reduces interfacial tension only marginally at the same pH value, for example, at the pH value of 7, the interfacial tension between PEG_{35k} and dextran_{40k} solution is 70.41 mN/m and 66.60 mN/m without and with PDP respectively. Also the reduction of interfacial tension is increasing when raising the pH value (Figure A7). The approximately 90° of contact angle and decreasing interfacial tension both contribute to the observed stable emulsions with droplets of smaller size.

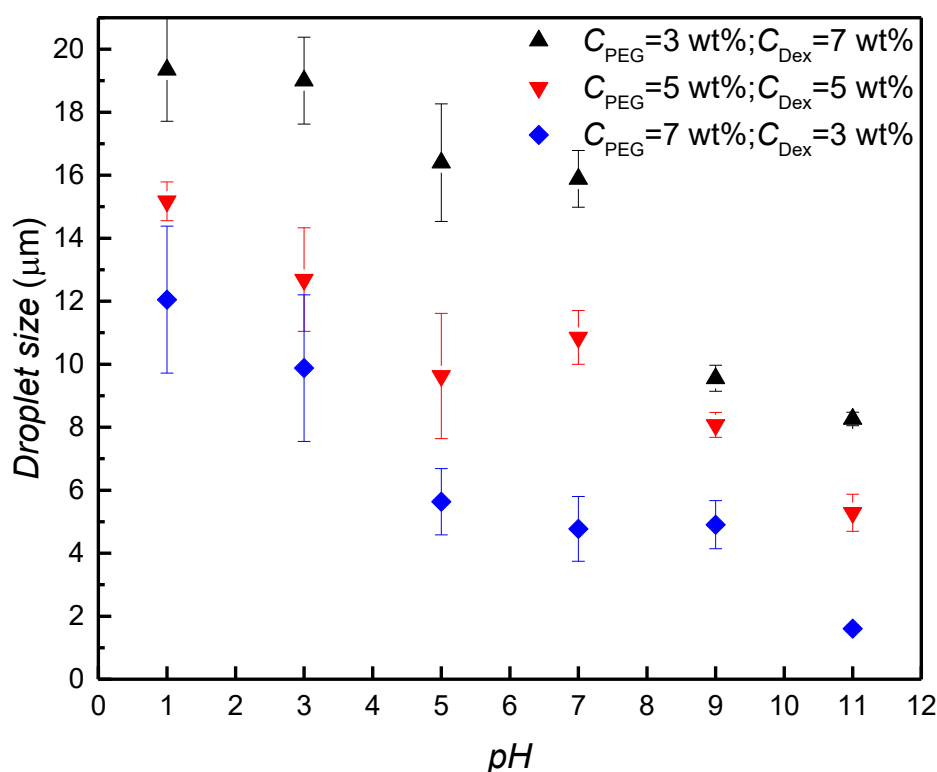


Figure 4.4. pH dependence on emulsion droplet size for different ratios of PEG_{35k} and dextran_{40k} via vortex for 30 s (3 wt% of PEG_{35k}; 7 wt% of dextran_{40k}, 5 wt% of PEG_{35k}; 5 wt% of dextran_{40k}, 7 wt% of PEG_{35k}; 3 wt% of dextran_{40k}).

Demulsification studies

The effective emulsification process occurs without addition of other external compounds. However, the long-term stability of dextran-PEG emulsions, as for all colloidal systems, is limited. Several studies have reported the demulsification of stable two-phase systems, and the disassembly of particles at the phase interface. Nevertheless, triggered demulsification is of particular interest as well. Therefore, a number of methods to demulsify PDP-stabilized emulsions were studied in here.¹⁷⁸⁻¹⁷⁹ First, a dextran_{40k}-in-PEG_{35k} emulsion (3 wt%, 7 wt%, respectively) was prepared with 0.2 g/L PDP as the stabilizer. These emulsions were very stable and no obvious phase separation was observed over 16 weeks as mentioned before (Figure 4.2e). One option to demulsify the emulsion is dilution (Figure 4.5a, b, c and d) as the phase diagram of dextran/PEG ATPS features only a two-phase region at high polymer concentrations. When the as-formed emulsion phase on top was diluted by 50%, the emulsion breaks which the absent of droplets can be observed via optical microscopy anymore. Moreover, phase separation occurs yielding two phases again as initially observed without stabilizer addition. Further dilution by 200% leads to the formation of a one-phase system, which matches the expectations from the phase diagram. As dilution below the binodal line leads to a remixing of the polymer phases, i.e. the water-in-water interface resolves pulling the PDP particles to it. Demulsification can be also obtained by applying charged surfactants (Figure 4.5/A9). Therefore, 4 mM of sodium dodecyl sulfate (SDS) was introduced into the PDP-stabilized dextran-in-PEG emulsions. Then, the mixture was vortexed for 30 s. Optical microscopy images of separated two phases confirm the successful demulsification of water-in-water emulsions. The introduction of negatively charged SDS has a profound effect on PDP.

The hydrophobic part of surfactant interacts with the PDP surface, which leads to electrostatic repulsion between individual PDPs and thus droplet coalescence is initiated as the solid-stabilizer is expelled from the droplet surface. A similar result was obtained with the cationic surfactant (cetyltrimethylammonium bromide) CTAB (Figure A9). Thus, it is indicated that demulsification via surfactant addition is possible regardless of the sign of surfactant charge.

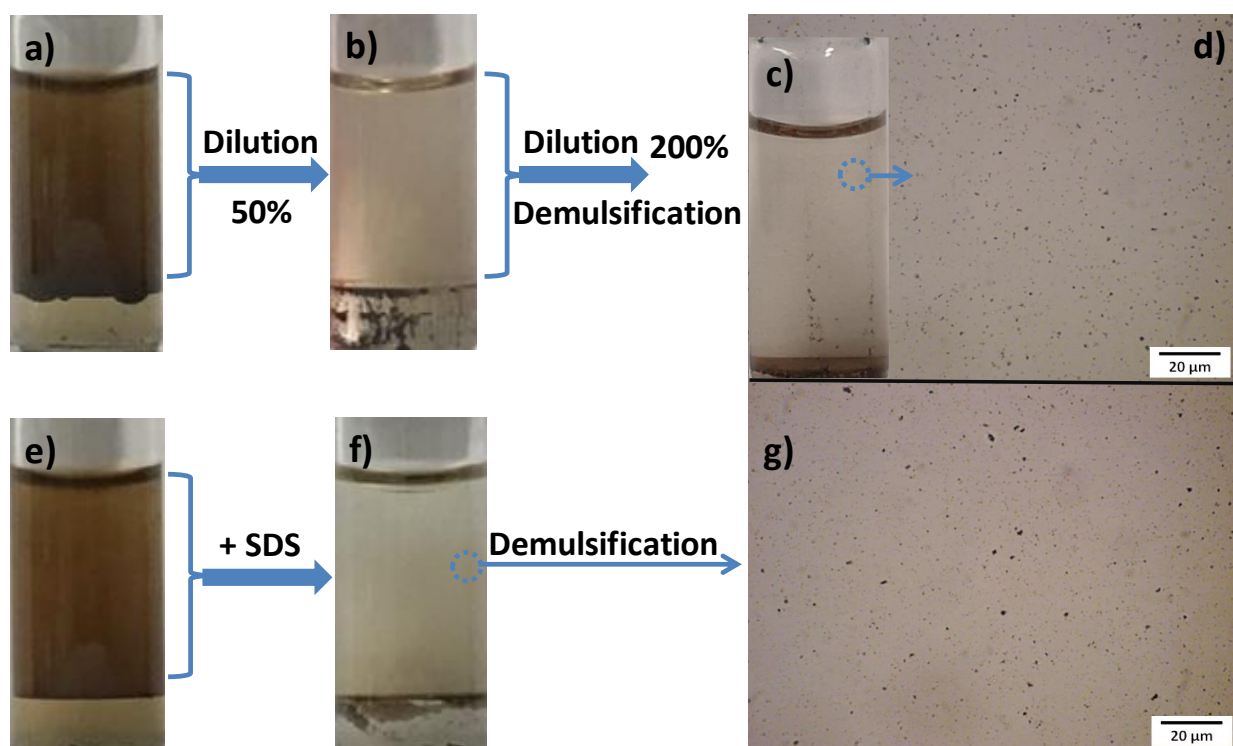


Figure 4.5. Demulsification of a PEG_{35k} (7 wt%)/dextran_{40k} (3 wt%) emulsion via vortex for 30 s: Optical images of (a) and (e) dextran-in-PEG emulsions, (b),(c) and (f) phase separation after dilution by 50%, 200% and SDS addition respectively; optical microscope images of (d) and (g) of demulsified suspensions.

Crosslinking of PDP stabilized emulsions

To prevent demulsification of the Pickering emulsion, stabilization of the interface layer towards colloidosomes can be considered. Therefore, interparticle crosslinking of the PDP at

Chapter 4

the boundary layer was attempted by using PAA and water-soluble carbodiimide EDC to strengthen the surface structure of emulsion droplets. As a test reaction crosslinking of PDP only was performed, which resulted in the formation of crosslinked structures via amide formation (Figure A10). Moreover, amide formation was observed in FT-IR spectroscopy via the appearance of the carbonyl stretching band around 1640 cm^{-1} (Figure A11).

Subsequently, emulsion droplets were crosslinked with PAA_{450k} to form a colloidosome-like structure. Therefore, to a dextran-in-PEG emulsion, PAA_{450k} (100 mM) and EDC (PAA: EDC, 1:1.2) were added. Afterwards, the crosslinked emulsion droplets are stable enough to be depicted via cryo-SEM (Figure 4.6a/A12). The rough surface of the colloidosome and a protuberant thorn-like structure reaching from the surface indicate the crosslinked structure of PDP. The structures look crystal-like. Therefore, XRD measurements of crosslinked PDP were performed after water removal (Figure A13). In XRD no signals indicating incorporation of crystalline structures were found. Furthermore, cryo SEM investigations of crosslinked PDP without polymer addition did not show any crystalline structures (Figure A10). It can be assumed that the sharp structures in the cryo SEM image of crosslinked emulsion droplets originate from crystals formed in the cryo process or are related to the added polymers – most likely to semi-crystalline PEG. Furthermore, for different molar mass of PAA_{1250k} and dextran/PEG ratios (Figure A14), crosslinked emulsion droplets could be obtained as well. Again, FITC labelled PEG was applied to locate the PEG phase in CLSM (Figure 4.6b). The bright continuous phase region shows the presence of fluorescently labelled PEG outside of crosslinked emulsion droplets.

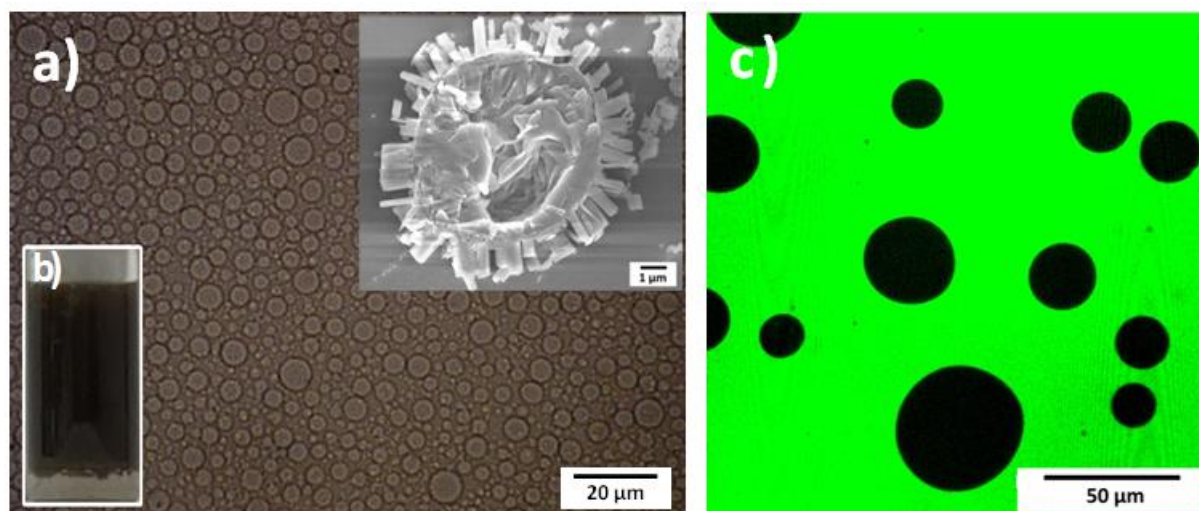


Figure 4.6. Emulsion images after crosslinking with PAA_{450k}/EDC of the system PEG_{35k} (7 wt%)/dextran_{40k} (3 wt%) with 0.2 g/L PDP as stabilizer formed via shaking by hand: Optical microscopy images of (a) dextran-in-PEG emulsion droplets (insert cryo-SEM images of crosslinked emulsion droplets); optical images of (b) dextran-in-PEG emulsion (7 wt% of PEG_{35k}; 3 wt% of dextran_{40k}) and CLSM images of (c) emulsion droplets dextran-in-PEG emulsion droplets with FITC-labelled PEG.

After crosslinking, the same demulsification methods as before were applied to study the stability. For dilution, in contrast to the previous non-crosslinked Pickering emulsion, the droplets remained intact upon dilution with water but exhibited increased size, which is another indication for successful crosslinking. Nevertheless, partial coalescence was observed as well (Figure 4.7c), leading to swelling of droplets to sizes around 20 μm. Besides, after addition of SDS or CTAB no change in emulsion stability was observed (Figure 4.7f/A15) indicating the formation of crosslinked emulsion droplets.

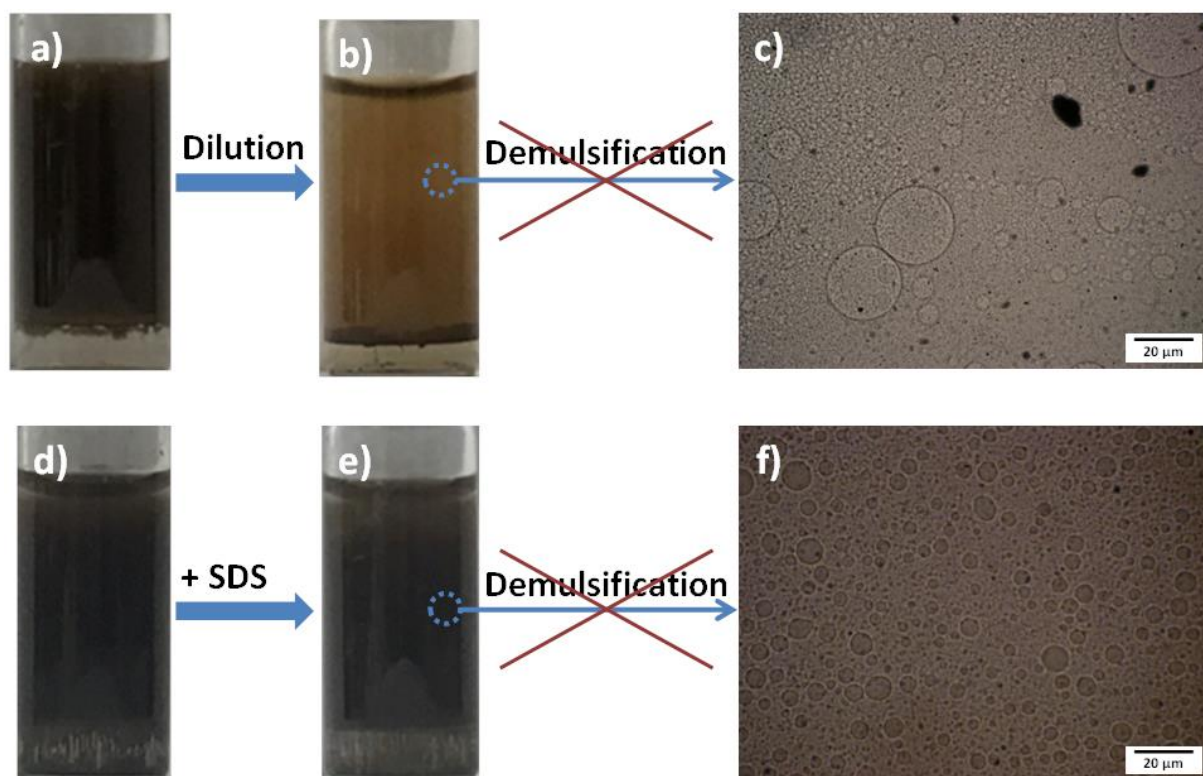


Figure 4.7. Demulsification trials of PEG_{35k} (7 wt%)/dextran_{40k} (3 wt%) system via vortex for 30 s after crosslinking with PAA/EDC: Optical images of (a) and (d) emulsions before attempted demulsification, (b) and (e) the mixture after attempted demulsification emulsions; optical microscopy images of (c) and (f) after attempted demulsification.

4.3. Conclusion

Overall, stable all-aqueous dextran–PEG Pickering emulsions were obtained via the utilization of PDP as well as colloidosomes-like structures after crosslinking of the particles. Pickering emulsions were formed with various polymer contents, at different pH and various PDP contents that were used to tailor droplet sizes. As expected, dilution of this emulsion with water below the level required for formation of the ATPS resulted in disassembly of the emulsion droplets. To prevent demulsification of the Pickering emulsion, crosslinking of the solid PDP by PAA and water-soluble carbodiimide EDC was performed strengthening the outer surface structure of emulsion droplets. After crosslinking, in contrast to the previous Pickering

Chapter 4

emulsion, the capsules remained intact after surfactant addition and upon dilution with water although minor swelling of the droplets was observed. These results demonstrate the enhanced stability of emulsion. After crosslinking, such types of aqueous emulsions could potentially provide new opportunities for a wide variety of emerging applications, e.g., in cosmetics or food products, possibly as an alternative to deliver ingredients with preferred solubility in the dispersed phase. The PDP-mediated formation of all aqueous emulsions is expected to be generalized to different types of water-in-water emulsions with other polymers and offer new opportunities in surface modification and microencapsulation.

5. Supramolecular Compartmentalized Hydrogels via Polydopamine Particle Stabilized Water-in-Water Emulsions ²

5.1. Overview

PDP show a significant role in stabilization of water-in-water emulsions in chapter 4 and has promising perspectives for ATPS. Moreover, compartmentalized hydrogels constitute a significant research area for example for catalytic and biomedical applications. As presented here, a generic method is used for compartmentalization of supramolecular hydrogels by using water-in-water emulsions based on aqueous two-phase systems. By forming the supramolecular hydrogel throughout the continuous phase of all-aqueous emulsions, distinct, micro-compartmentalized materials were created. The basis for the presented compartmentalized water-in-water hydrogels are polydopamine particle-stabilized water-in-water emulsions from dextran and poly(ethylene glycol) (PEG). Addition of α -cyclodextrin (α -CD) led to supramolecular complexation with PEG and subsequent hydrogel formation. Due to the supramolecular nature of the compartmentalized hydrogels, selective network cleavage could be induced via competing guest addition, while the emulsion sub-structure was kept intact as shown in Figure 5.1.

² Terms of use: This chapter was adapted with permission from Jianrui Zhang, Baris Kumru, Bernhard V. K. J. Schmidt, "Supramolecular Compartmentalized Hydrogels via Polydopamine Particle Stabilized Water-in-Water Emulsions"; *Langmuir* **2019**, 35(34), 11141-11149. Copyright 2019 American Chemical Society.

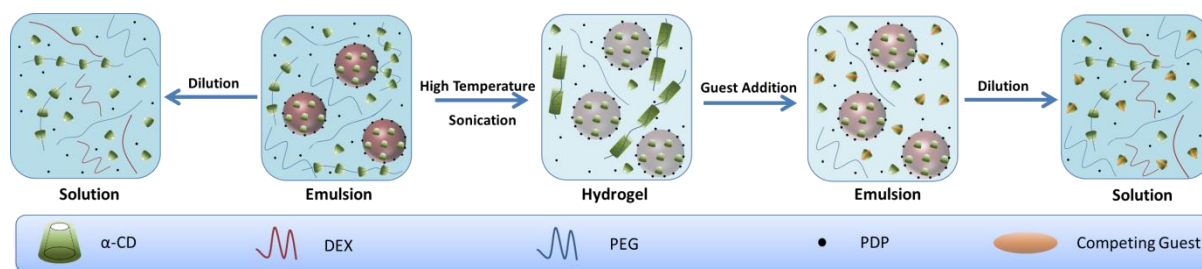


Figure 5.1. Schematic overview of compartmentalized hydrogel formation via water-in-water emulsions.

5.2. Results and Discussion

Compartmentalized Hydrogels via PDP Stabilized Water-In-Water Emulsions

The PDP was prepared in a facile method under alkaline condition, in order to produce compartmentalized hydrogels. In a typical experiment, PDP was fabricated to achieve uniform particles with a size of 400 nm as previously reported in chapter 4. Compartmentalized hydrogels were prepared via gelation of w/w emulsions stabilized by PDP (0.2 g/L) containing various weight ratios of PEG and dextran as well as different molar masses of PEG and different concentrations of α -CD. At first, a PDP suspension was prepared in an α -CD solution. Solutions of dextran and PEG were prepared by dissolving the solid in Milli-Q water at neutral pH with stirring. Finally, the polymer solution was added to the PDP/ α -CD mixture (final concentration, 0.2 g/L of PDP) for emulsification via ultrasonication to obtain a hydrogel (Figure 5.2d). In this way, a compartmentalized hydrogel with well-dispersed compartments could be achieved. A color difference between emulsions and hydrogels was observed, which was due to slight differences in imaging conditions of optical microscopy as the compartmentalized hydrogel (Figure 5.2a) is less transparent compared to the emulsion (Figure 5.2d).

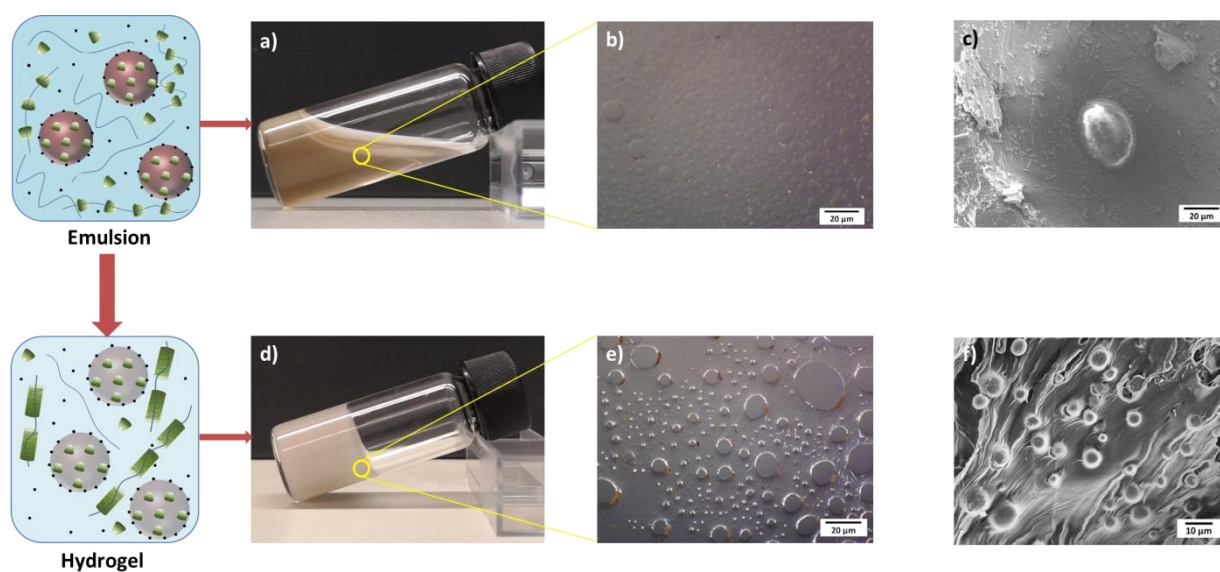


Figure 5.2. Images of the PDP (0.2 g/L) stabilized PEG_{35k} (7 wt%)/dextran_{40k} (3 wt%) water-in-water system (140 mg/mL of α -CD): Optical images of (a) PDP stabilized emulsion and (d) compartmentalized hydrogel after heating to 65 °C and cooling to the ambient temperature, respectively; optical microscopy images of (b) emulsion droplets at ambient temperature and (e) emulsion droplets within a compartmentalized hydrogel; cryo-SEM image (c) emulsion droplets; SEM image (f) emulsion droplets within a compartmentalized hydrogel.

Previously, it has been indicated that PDP based emulsions show a long-term stability for at least 16 weeks referring to chapter 4. After ultrasonication, the emulsions were heated to 65 °C and then cooled down to the ambient temperature to obtain compartmentalized hydrogels. Investigation via optical microscopy indicates droplet formation inside of the hydrogel, which corresponds to a w/w emulsion system as known from previous studies in chapter 4. However, before cooling down to ambient temperature, the mixture was observed under optical microscope (OM) and also frozen for cryo-SEM (Figure 5.2b and 5.2c) to prove the stability of the emulsion inside the hydrogels as the droplets exist during hydrogel formation. Hence,

compartmentalized hydrogels were formed as observed via OM showing w/w droplets in the hydrogels (Figure 5.2e), which shows that the w/w emulsion was stable through the hydrogel formation process, i.e. at higher temperature. The droplet size inside the hydrogel shows dispersity from 1 to 25 μm and the average droplet size is $25\pm 1.2 \mu\text{m}$ (Figure 5.2e), which matches the observed droplet sizes in corresponding emulsions (the average droplet size $\sim 22\pm 0.9 \mu\text{m}$ in Figure 5.2b), showing there is no obvious change during the hydrogel formation even if the temperature varies. To gain further insight on the formed droplets inside the hydrogels and their stability, SEM imaging after freeze drying of the hydrogel was applied (Figure 5.2f). Spherical compartments with sizes in the range of 1 to 25 μm were observed, which shows the stability of the compartmentalized architecture even in the dry state.

To further verify the existence of a w/w emulsion stabilized by PDP inside of the compartmentalized hydrogels, FITC labelled PEG (2K) was introduced into a dextran-in-PEG emulsion-based hydrogel and imaged via CLSM (Figure 5.3). The visible dark liquid droplets and clear bright continuous phase region shows the presence of fluorescently labelled PEG continuous phase outside the emulsion droplets, which indicates the separation of PEG and dextran in the hydrogel state, as expected. Confocal microscopy offered a dependable trend for the phase separation contained within the emulsion droplets of different polymer phase. However, without PDP addition, the droplet structure cannot be observed in the compartmentalized hydrogels (Figure A16), which also confirms the role of PDP as a stabilizer in the w/w emulsion. Different characterization methods were applied to show the structure of emulsion droplets and compartmentalized hydrogel, in this way, we can investigate the stability of the compartmentalized hydrogel and give a broader insight into the structure of the fabricated materials.

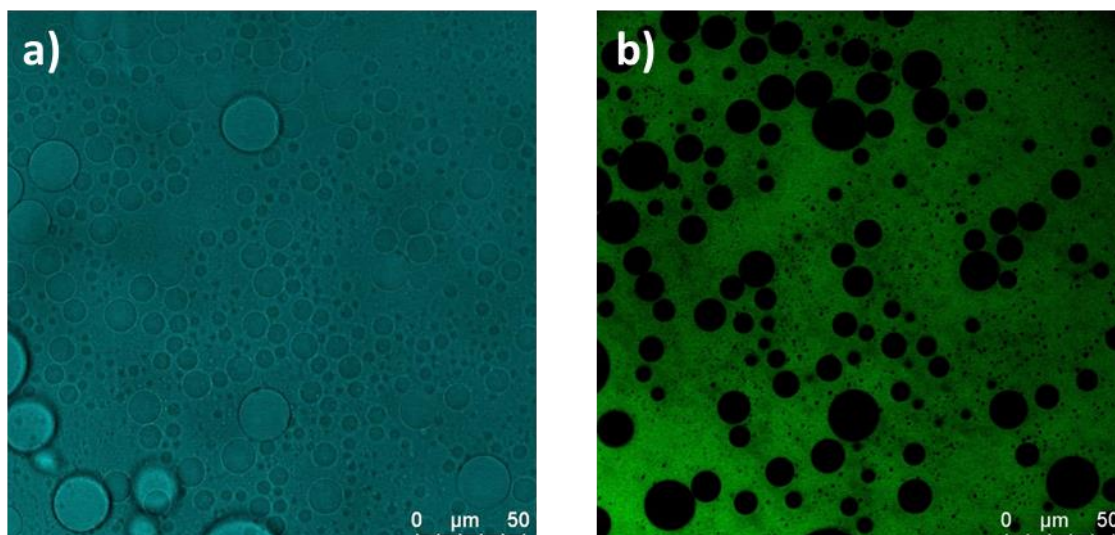


Figure 5.3. Emulsion droplet images within a compartmentalized hydrogel of the system PEG_{35k} (7 wt%)/dextran_{40k} (3 wt%); dextran-in-PEG: Bright field images of (a) emulsion droplets within a compartmentalized hydrogel and (b) CLSM image of emulsion droplets within a compartmentalized hydrogel via utilization of FITC-labelled PEG (2k).

To gain additional insights into the crosslinking mechanism, XRD measurements of compartmentalized hydrogels were performed after water removal (Figure 5.4a).¹⁸⁰ To characterize the crystalline structure of aggregations in the hydrogels, we measured the XRD patterns of a compartmentalized hydrogel in the freeze-dried state and compared them with those from well-dried emulsions without addition of α -CD. In contrast, no signals indicating incorporation of crystalline structures were found for the normal emulsions after freeze drying (Figure 5.4a), however, the diffraction pattern of the hydrogel exhibits a number of sharp reflections including strong ones at $2\theta = 20.0^\circ$ ($d = 4.44 \text{ \AA}$) and 22.7° ($d = 3.96 \text{ \AA}$). These are assigned to the 210 and 300 reflections from the hexagonal lattice with $a = 13.6 \text{ \AA}$. The strong reflection is a typical peak observed for PICs with α -CD,¹⁸¹⁻¹⁸² according to the electron density distribution of the core of the α -CD molecules with a radius of $\sim 5 \text{ \AA}$. It is a well-known fact that PEG/ α -CD PICs have a channel type crystalline structure due to the long-chain nature of

the guest molecules. These characteristic reflections which appeared in the profiles from the freeze-dried hydrogels indicate that the compartmentalized hydrogels are formed via supramolecular crosslinking. Thus, such crystalline aggregations induced by inclusion complexation formation can be considered to play the major role in the gelation.

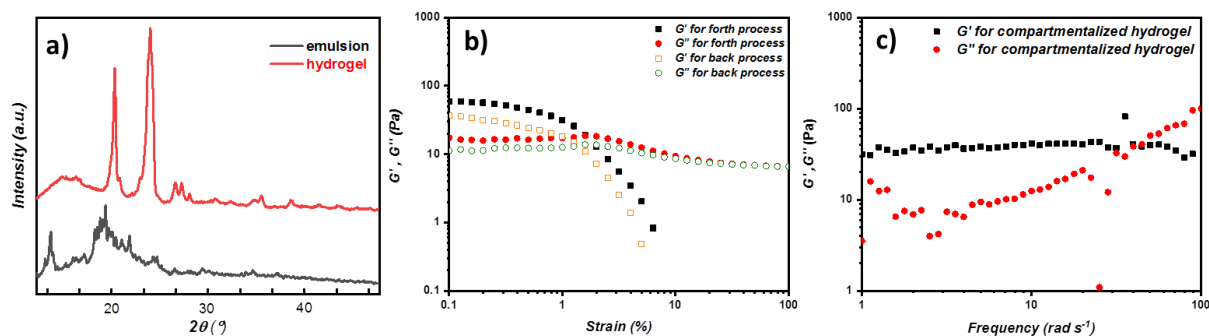


Figure 5.4. Characterization of compartmentalized hydrogels via PDP (0.2 g/L) stabilized PEG_{35k} (7 wt%)/dextran_{40k} (3 wt%) water-in-water system (140 mg/mL of α -CD): (a) X-ray diffraction (XRD) patterns of compartmentalized hydrogels and emulsions; (b) strain dependency after heating to 65 $^\circ\text{C}$ and cooling to the ambient temperature; and (c) G' and G'' values of hydrogel against frequency with constant strain (0.1%).

Moreover, oscillatory shear rheology was used to investigate the network formation between α -CD and PEG. In the case of PDP w/w emulsion-based hydrogel G' exceeds G'' in the range of 0.1 to 100% of strain, which is a strong indication of hydrogel formation. Albeit the absolute values of G' (59.5 Pa at 0.1% strain) show that rather soft hydrogels are obtained (Figure 5.4b). The formed hydrogels show significant shear-thinning behavior which is another feature of the supramolecular soft hydrogels. Frequency dependent rheology measurements in the presence of hydrogel network did not show significant change in the region between 0–20 rad/s for both G' and G'' , however, in the range from 40 rad/s for G'' , the loss modulus increases remarkably (Figure 5.4c). Thus, at this point the supramolecular network breaks and a sol-like behavior is

observed. Besides, viscosity only changed at shear rates between 0 and 10/s, and then no obvious variation was observed for higher shear rates because the gel phase turned into a sol (Figure A17a). However, in the case of emulsions without addition of α -CD, there was no hydrogel formation, which was confirmed by G'' exceeding G' in the range of 0.1 to 100% of strain (Figure A17b). Compared with the compartmentalized hydrogels, solely PEG-based hydrogels (Figure A17c) without dextran addition are stable as well. In fact, PEG-based hydrogels were stronger than compartmentalized hydrogel with dextran. Apparently, dextran addition weakened the strength of the hydrogel network, but not to an extent to break the network.

Further Studies of Compartmentalized Hydrogel Formation

In order to investigate the formation of compartmentalized hydrogels further, the parameters of polymer molar masses were investigated as well as α -CD concentration. For the case of PEG with molar mass less or equal than 3000 g/mol, no stable hydrogels with α -CD were observed (Figure A18a),¹⁸³ which was confirmed by rheology results (Figure A18a) as G'' exceeds G' in the range of strain from 0% to 10%. Nevertheless, precipitate formation at the bottom of glass vessels was observed. The low molar mass of PEG is probably not sufficient to support enough α -CD for hydrogel formation. Therefore, formation of hydrogels via inclusion complexes with highly ordered secondary structures should be related to the structural length of PEG in the present system.

In previous works, it was shown that in order to form a α -CD and PEG network a minimal concentration of α -CD about 50 mg/mL is required to obtain a hydrogel with sufficient stiffness to form a self-standing gel.¹⁸³ At lower concentrations (Figure A18b), the emulsion-based α -CD network formed with PEG (40K, 7wt %) is not strong enough and does not reach a sufficiently high density to resist gravity. The creaming mixture flow at the α -CD concentration of 50 mg/mL, which indicates that no strong hydrogel network is formed at a concentration

Chapter 5

below $c_{\alpha\text{-CD}} \leq 50$ mg/mL. In the case of the emulsions, the stability of the w/w emulsion droplets is enhanced with PDP as stabilizers that attaches to the droplets for emulsification. Therefore, creaming was observed instead of sedimentation. On the other hand, when the concentration of $\alpha\text{-CD}$ is increased, increased amounts of $\alpha\text{-CD/PEG}$ aggregates are formed. The increased aggregate accumulation results from an increase in the amount of inclusion complex formation between the PEG chains and $\alpha\text{-CD}$ molecules. Therefore, the density of the network at steady state increases with increasing $\alpha\text{-CD}$ concentration. If in addition this complexation between $\alpha\text{-CD}$ and PEG is sufficiently strong to resist the buoyancy, creaming no longer takes place. Moreover, it appears from the present observations that the network with the embedded emulsion droplets was not sufficiently strong to resist the buoyancy of the droplets for $c_{\alpha\text{-CD}} \geq 200$ mg/mL. The collapsed precipitate forms a layer at the bottom of the glass vessels (Figure A18b). Also, no hydrogel formation could be observed in rheology (Figure A20) for $c_{\alpha\text{-CD}} \geq 200$ mg/mL. Thus, multicompartement hydrogel formation is observed in the range of $50 \text{ mg/mL} \leq c_{\alpha\text{-CD}} \leq 200 \text{ mg/mL}$, with no network formation at low concentration and demixing at high concentrations.

Furthermore, PEG-dextran aqueous system containing $\alpha\text{-CD}$ (140 mg/mL) and PDP (0.2 g/L) were prepared with different ratios of PEG and dextran and hydrogels formed with $\alpha\text{-CD}$ (Figure A18c). At these compositions, the systems were fully phase-separated with two water phases.¹⁸⁴ Nevertheless, the polymers are not fully separated but enriched in one or the other phase.¹⁸⁵ Figure A18c shows how the compartmentalized hydrogels in $\alpha\text{-CD-PDP}$ aqueous system evolved visually with changing PEG/dextran weight ratios. At all weight ratios with dextran in the dispersed phase and PEG in the continuous phase compartmentalized hydrogels are formed, which is consistent with rheology results (Figure A21). Unexpectedly, hydrogels are also formed in the case of dextran in the continuous phase. Apparently, the amount of PEG in the dextran phase is sufficient to form a crosslinked hydrogel although dextran forms the major part of the continuous phase. After standing overnight, the hydrogels reached a steady

state that does not change anymore, indicating that all PEG/dextran ratios in α -CD-PDP aqueous system had produced compartmentalized hydrogels. In addition, there is no obvious effect of the mixture composition on droplet size (Figure A18d, e, f). As such no significant changes in volume fraction and concentration of the two phases were observed ($28 \pm 1.2 \mu\text{m}$ for PEG_{35k} (3 wt%)/dextran_{40k} (7 wt%), $23 \pm 1.1 \mu\text{m}$ for PEG_{35k} (5 wt%)/dextran_{40k} (5 wt%) and $25 \pm 1.2 \mu\text{m}$ for PEG_{35k} (7 wt%)/dextran_{40k} (3 wt%)).

Stability of Compartmentalized Hydrogels and Targeted Disassembly

Due to the supramolecular nature of the hydrogel, the application of external stimuli can be utilized to modify the structure. Therefore, a number of methods have been applied here. The hydrogel formation was performed at temperatures around 65 °C. The aqueous dispersion of the polymers, α -CD and PDP became cloudy instantaneously after 2 hours of ultrasonication for emulsification, and the hydrogel formed after heating to 65 °C and then cooling down to ambient temperature. Moreover, these compartmentalized hydrogels featured a phase transition from hydrogel to a clear solution after heating to 65 °C, which is a reversible process as hydrogels formed again at ambient temperature. Another option is to increase the temperature during hydrogel formation, i.e. after ultrasonication the samples were heated to 90 °C and then cooled down to ambient temperature. Compartmentalized hydrogels could be formed as well in this way, which can be seen from rheology that G' exceeds G'' and strong hydrogels are obtained regarding to high absolute values of G' (27000 Pa) (Figure 5.5). However, the transition to a solution does not occur again: The compartmentalized hydrogels formed after heat treatment at 90 °C were heated again, but instead of a transparent solution a turbid sol was observed, which is a suspension containing small presumably crystallite particles. Regarding repeated cooling, rheology was measured after repeated heating to 65 °C and G' reached the same level after cooling. In addition, there was no change for repeated heating and cooling

when the hydrogel was prepared after heating to 90 °C. Nevertheless, cooling to ambient temperature resulted in hydrogel formation, which demonstrates that high temperature improves inclusion complex formation as the aggregates do not break completely after heating as observed in the turbid sol character. The increased stability also manifests in the frequency dependency that does not show a crossing of G' and G'' at increased frequencies as it was evident for the hydrogel prepared after heating to 65 °C. However, the compartmentalized hydrogels could not be formed at the heating temperature below 65 °C (Figure A22a). In addition, no significant impact of heating time on the hydrogel formation was found. Emulsions kept at an elevated temperature (65 °C) for different time, 1 min, 5 min, 10 min and 30 min (Figure A22b) turned all into hydrogels.

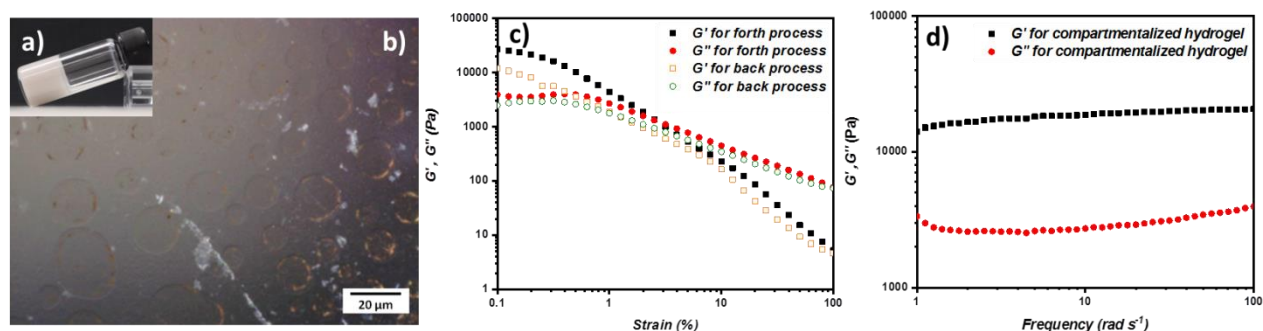


Figure 5.5. Characterizations of the compartmentalized hydrogel via PDP (0.2 g/L) stabilized PEG_{35k} (7 wt%)/dextran_{40k} (3 wt%) w/w system (140 mg/mL of α -CD) after heating to 90 °C and cooling to the ambient temperature: Optical images of (a) compartmentalized hydrogel; optical microscopy images of (b) emulsion droplets within a compartmentalized hydrogel; (c) strain dependency after heating to 90 °C and cooling to the ambient temperature; and (d) G' and G'' values of hydrogel against frequency with constant strain (0.1%).

A disassembly of the compartmentalized hydrogels can be also obtained by addition of competitive guests (Figure 5.6a). Therefore, 10 mM of anthranilic acid was introduced into the

supramolecular compartmentalized hydrogels and the mixture was vortexed for 30 s. The obtained flowing turbid liquid confirms the successful destruction of the hydrogel network structure. The introduction of competitive guest, i.e. anthranilic acid, has a profound competitive effect on the α -CD/PEG PICs. As the addition of additional guests interacts with the present α -CD capacities the equilibrium is shifted, which leads to inclusion complexations between α -CD and anthranilic acid. Thus, the disassembly of the hydrogel is initiated as the PEG is expelled from the α -CD cavities. Hence, it is indicated that disassembly of the hydrogel structure via competitive guest addition is possible. Most importantly, the aqueous two-phase emulsions are still stable after hydrogel disassembly (Figure 5.6b). In order to quantify the required amount of anthranilic acid to break the hydrogels, the concentrations of anthranilic acid were screened between 4 mM and 12 mM (Figure A23). It could be shown that a minimum of 10 mM anthranilic acid is needed to disassemble the hydrogels. However, after addition of competitive guest and dilution by 100%, the emulsion breaks as no droplets can be observed via optical microscopy anymore (Figure 5.6c and d), which is expected due to the shift out of the two phase region in the phase diagram.¹⁸⁶ Moreover, the oscillatory shear rheology indicates hydrogel cleavage as G'' exceeds G' (Figure A24). The confocal images showed disassembly and demulsification after guest addition and dilution as well (Figure A25). No complete droplets could be observed via confocal microscope anymore. However, ill-defined aggregates were visible, which might be corresponding to various α -CD complexes. Therefore, the state of the system can be tailored from compartmentalized hydrogel to emulsion to solution.

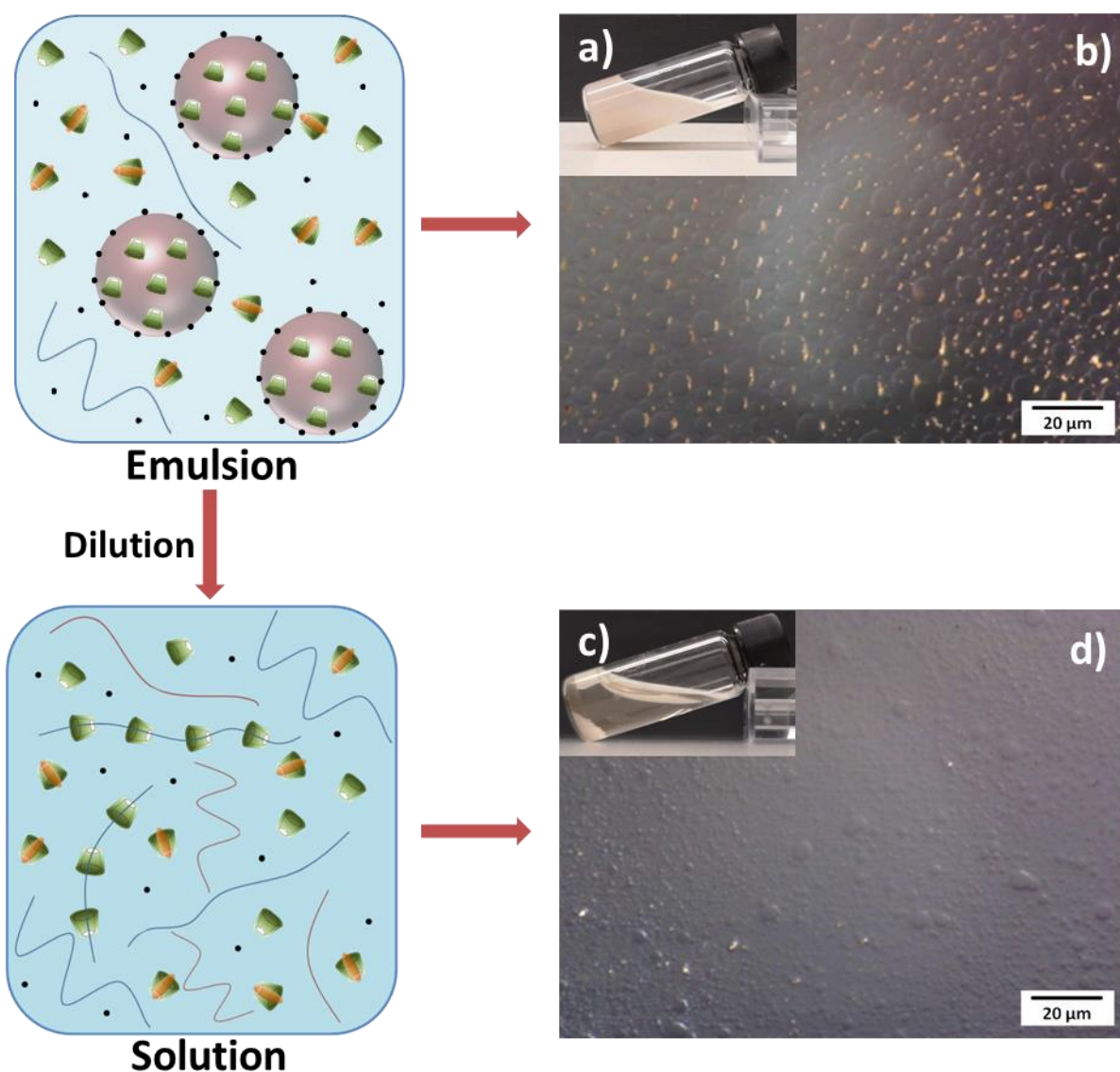


Figure 5.6. Characterizations of the compartmentalized hydrogel via PDP (0.2 g/L) stabilized PEG_{35k} (7 wt%)/dextran_{40k} (3 wt%) water-in-water system (140 mg/mL of α -CD) after heating to 90 °C and cooling to the ambient temperature : Optical images of (a) compartmentalized hydrogel after adding the competitive guest and (c) the following dilution by 50%; optical microscopy images of (b) droplets within an emulsion after adding the competitive guest and (d) the following dilution by 100%.

5.3. Conclusions

In conclusion, a facile, generic approach is presented for fabrication of compartmentalized completely hydrophilic materials by forming a supramolecular hydrogel within mixtures of aqueous phase-separating polymers, in presence of Pickering-type PDP stabilizers, dextran, PEG and α -CD. PEG is found to form inclusion complexes with α -CD molecules, resulting hydrogel formation and in physical compartments from emulsion droplets. The compartmentalized hydrogels were assessed via SEM, OM and CLSM for morphology. The origin of hydrogel formation was confirmed via XRD and the gelation followed by oscillatory shear rheology. By varying the different constituent parts of the hydrogels, e.g. the molar mass of the utilized polymers, the polymer concentration and α -CD concentration as well as the temperature, the properties of the structure could be varied. After addition of a competitive guest, the original network can be disassembled. Notably, after disassembly of the hydrogel via competitive guests, the emulsion stays intact and the emulsion finally breaks after significant dilution. As such, the system can be tuned in a multi-level way from hydrogel to emulsion to solution via external manipulations. Overall, this method can be applied to several all-aqueous emulsions. Such types of compartmentalized hydrogels could potentially provide new opportunities for a wide variety of aqueous multi-phase systems, in the design of novel biomimetic hydrogel catalysts, as the templates of porous soft materials or in fabrication of supramolecular hydrogel scaffolds for tissue engineering.

6. Water-in-Water Pickering Emulsion stabilized by Carbon Nitride

6.1. Overview

As stated in the previous chapters, ATPSs have recently raised big interest recently, like application in Pickering water-in-water emulsions in Chapter 4 and compartmentalized supramolecular hydrogels in Chapter 5. To investigate more about ATPS utilizing in water-in-water emulsion systems stabilized by various kinds of solid particles, carbon nitride stabilized water-in-water Pickering emulsions are formed. PEG/dextran two-phase systems were stabilized into emulsions with five different types of carbon nitride as the Pickering stabilizer. Stable emulsions are obtained from the different carbon nitride that could be broken via dilution or surfactant addition and pH adjustment as shown in Figure 6.1.

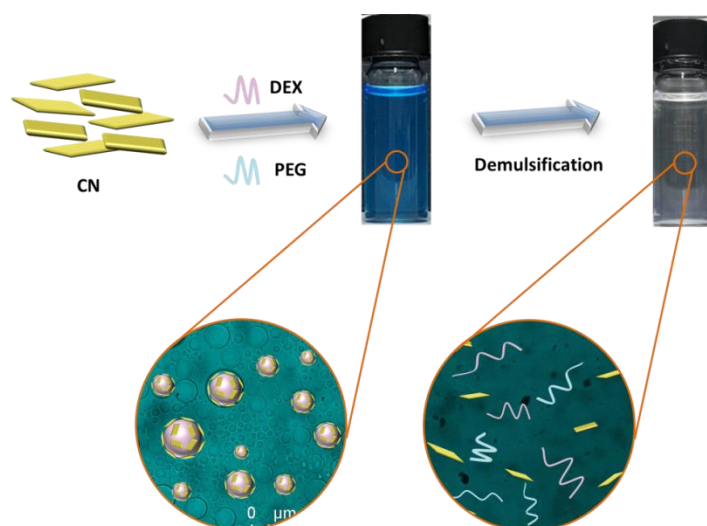


Figure 6.1. Overview of the PEG-dextran water-in-water emulsion formation employing carbon nitride (CN) and utilization in demulsification.

6.2. Results and Discussion

CN stabilized water-in-water Pickering emulsions

Emulsions were successfully produced with the aqueous two-phase systems with a variety of CN variants. Several CN were used with different functionalities, including CN from cyanuric acid-melamine complex (CM),¹⁸⁷ allylamine-grafted CM (CM-AA),¹⁸⁹ AHPA grafted CM (CM-AHPA),¹⁸⁹ decene-grafted CM (CM-Decene),¹⁸⁹ and 4-methyl-5-vinyl thiazole-grafted CMP (CMP-TA).¹⁹⁰ All these CN variants used for emulsion preparation were effective stabilizers, which can be verified via optical microscope showing emulsion droplets (Figure 6.2). CN as Pickering emulsion stabilizers largely benefits from their nanosheet shape (Figure A27), which was reported in organic two-dimensional material structure of CN behaved well in Pickering emulsification.¹⁹¹⁻¹⁹² Benefiting from its unique structure, CN is able to act as a stabilizer in water-in-water emulsions. Besides, CN also showed generality to be used as an emulsifier, which was applied in five different types and the corresponding Pickering emulsions are shown in Figure 6.2. All the emulsions were formed by different types of CN at a quite low CN concentration (0.02 g/L), with the droplets having variable sizes. The stability of the emulsions was examined by monitoring the droplet variation against aging time in an ambient environment. The ability of emulsification for CM-AHPA to emulsify PEG/dextran aqueous two-phase system was higher than other CN, which was assessed according to due to the long-term stability of emulsions (16 weeks compared with 8 weeks of other variants) and high dispersibility in water. Furthermore, DLS of CM-AHPA indicated (Table A5) an average hydrodynamic diameter of 232 nm, allowing for the CM-AHPA as the aspect of size parameter to be a successful Pickering emulsion stabilizer.

These ATPS were generally stable and well defined with PEG and dextran at various weight percentages and PEG: dextran ratios (Table A4). Homogenization provided the most evenly reproducible and long-term stable emulsions and was thus used for further emulsion

preparation. Passive mixing was shown to be incredibly important in the formation of CN stabilized PEG: dextran water-in-water emulsions, as proper settling of both phase in the CN dispersion allows for the proper formation of emulsion droplets. After emulsification it can be observed that two phases form as well as a solid phase, the solid phase is due to an excess of CN that settles from the emulsion. When allowed to mix and homogenize, the resulting emulsion is an even, continuous phase of emulsion which is stable for (at least) 16 weeks.

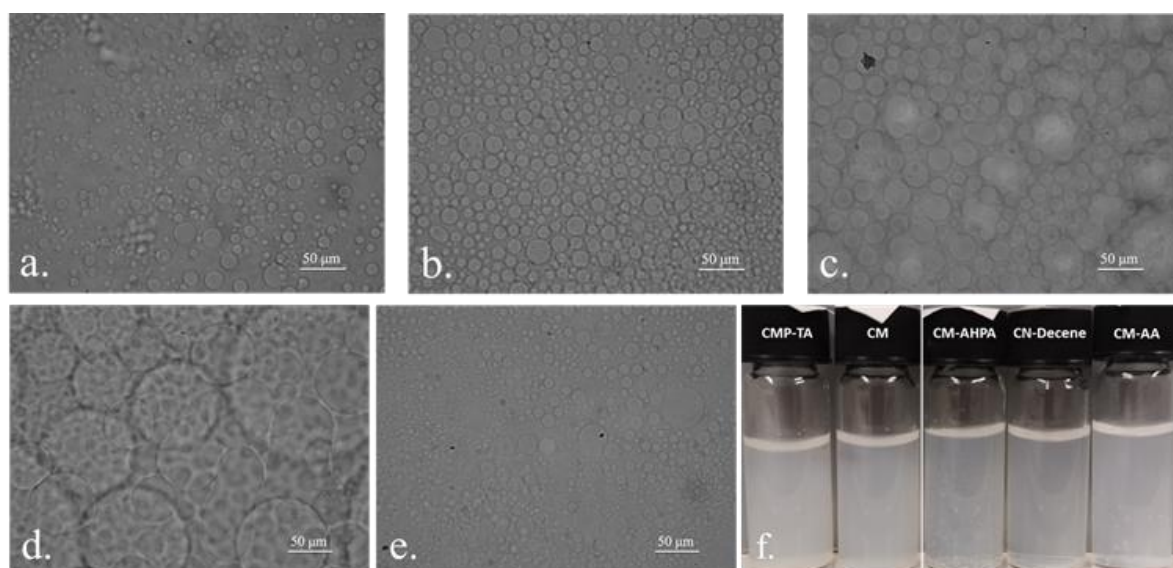


Figure 6.2. Carbon nitride stabilized Pickering emulsions from 3 wt% PEG_{35K}: 7 wt% dextran_{40K} prepared with homogenization, optical microscopy images of 0.1 g/L CMP-TA (a), CM (b), CM-AHPA (c), CN-Decene (d), CM-AA (e) and photographs (f).

For all samples made in this system, regardless of the CN concentration, if two phases appear in the sample, the upper phase contains an emulsion with fewer CN aggregates than the lower phase, which will have almost no droplets and a large amount of CN aggregates and settled CN (Figure 6.3a and b). The concentration of CN inside the overall system has few effects on the

emulsion formation itself. Emulsions can be successfully and stably made for a wide range of CN concentrations (0.1 to 0.02 g/L). Furthermore, CN concentration can be correlated to the distribution of each phase of the ATPS. For samples with a CN concentration decreasing from 0.1g/L to 0.02 g/L, an emulsion can be formed with a decreased volume of non-emulsified phase, where the entire system is a separated emulsion with only emulsified upper part (Figure 6.3b). The well-dispersed diluted CN solution changed the phase system, which makes a water-in-water emulsion approach a one-phase emulsion with decreasing concentration of CN (Figure 6.3c).

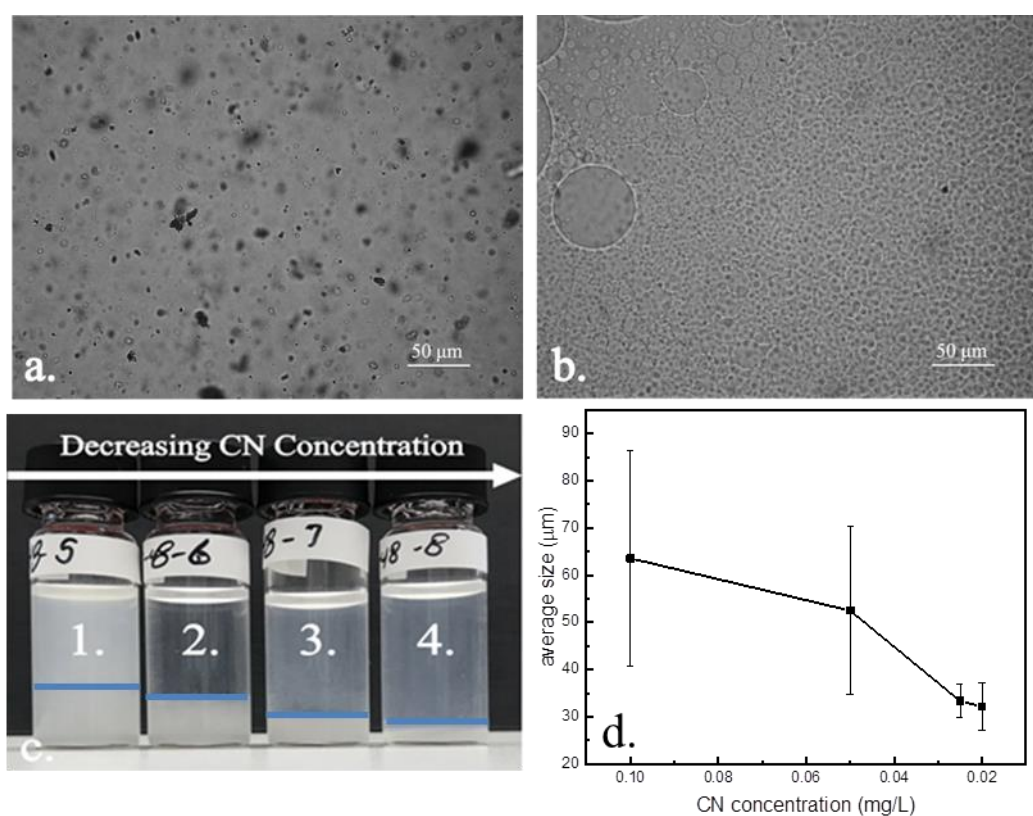


Figure 6.3. CN Concentration effects on CN w/w emulsions. a. lower phase of a CN w/w emulsion (0.02 g/L CM-AHPA in 3 wt% PEG_{35K} : 7 wt% dextran_{40K} emulsion, 30s homogenizer 22,000 RPM). b. the upper (emulsified phase) of the same sample in (a). c. The change in phases as the concentration of CN decreases, (1) 0.1 g/L, (2) 0.05 g/L, (3) 0.025 g/L, (4) 0.02 g/L. d. the size distribution of emulsion droplets for different CN concentrations.

Chapter 6

In addition, the emulsion droplet size with the amount of CN in the dispersion varied as well. For the droplet size of emulsions for different concentrations, there is a correlation between the overall droplet sizes over concentration, where increasing CN concentration decreases the droplet size ranging from 63.6 μm to 32.1 μm (Figure 6.3d, A28). The distribution of droplet sizes is quite large in these types of emulsions, making accurate sampling of the emulsion unreliable (Figure A28). Nevertheless, the general trend of the emulsion droplet size is sustained. The negative correlation between droplet size and CN concentration is mainly due to the aggregation of CN dispersion in water. The higher the concentration of CN dispersion, the more easily CN aggregates are formed in water. The aggregation of CN in increasing concentration of dispersion contributed to increasing emulsion droplet size.

An important question when considering emulsion preparation is the composition of each phase. For emulsion systems, the control of the droplet and continuous phase is necessary. Therefore, CLSM experiments were performed in order to elucidate the polymer partition in the emulsion. Two-phase systems were prepared with a total of 3 wt% PEG_{35K} : 7 wt% dextran_{40K} emulsion as well as 7 wt% PEG_{35K} : 3 wt% dextran_{40K} emulsion, and addition of FITC labelled PEG (20k) and rhodamine labelled dextran (2k). CLSM micrographs offered a dependable trend for the polymer contained within the emulsion droplets and the continuous phase, respectively. For 3 wt% PEG_{35K} : 7 wt% dextran_{40K}, PEG is contained within the emulsion droplets (Figure 6.4, A29). Furthermore, when the emulsion was reversed (7 wt% PEG_{35K} : 3 wt% dextran_{40K}), dextran was located within the emulsion droplet (Figure A30). Given the changing continuous and emulsion phase based on the weight ratio of PEG_{35K} : dextran_{40K} within the ATPS, the emulsion type varied in either dextran-in-PEG emulsion or PEG-in-dextran emulsion. CM-AHPA does not show any preference to either the dextran or the PEG phase, allowing for the phases of the emulsion to switch. As such, the polymer phase inside the droplet can be controlled and changed on purpose (Figure A29, A30).

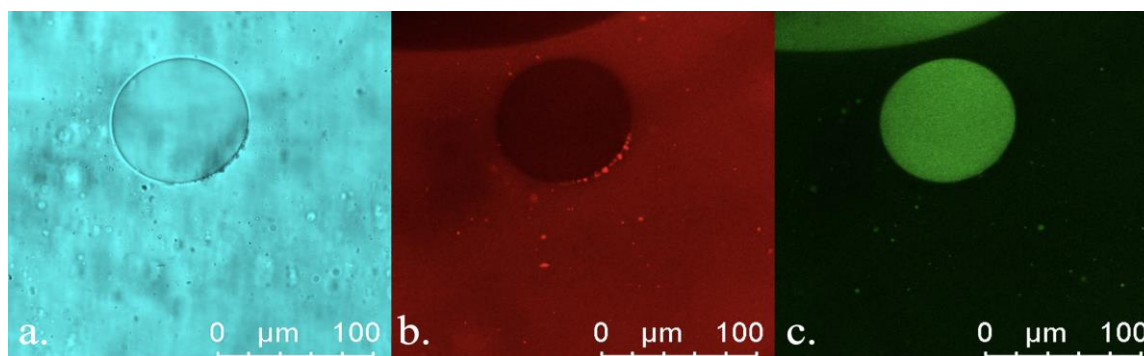


Figure 6.4. Confocal image of CM-AHPA stabilized 3 wt% PEG_{35K} : 7 wt% dextran_{40K} emulsion droplet. a. bright-field image of the emulsion droplet. b. Confocal image displaying rhodamine labelled dextran outside the droplet with CN aggregate at droplet surface. c. confocal image of FITC labelled PEG (20k) within the droplet.

As the particle size for the utilized carbon nitride nanosheets is very small. CN can only be observed at the interface as large aggregates in CLSM. In the case of more concentrated (0.1 g/L) dispersions of CN utilized for emulsions produced via hand mixing, which showed a larger emulsion droplet for better confocal imaging, CN aggregates could be viewed at the edge of the emulsion droplets alluding to the presence of adsorbed CN (Figure 6.4). By contrast, CN stabilized emulsions in a low concentration at 0.02 g/L (Figure A29 and A30) was not observed, which results from low amount of CN aggregates and small emulsion droplet size. Moreover, the CN itself has weak emission. The visible clear bright liquid droplets show the presence of fluorescently labelled PEG dispersed phase inside the emulsion droplets (Figure 6.4c), which indicates the near complete separation of PEG and dextran, as expected. By giving the direct observation fluorescent images, it is known that CN is acting as the Pickering stabilizer for PEG-dextran emulsion system.

Emulsion Stability

CN water-in-water emulsions were monitored over the course of the project, for both high-concentrated CN solutions of 0.1g/L (Figure A31) and lower concentrated solutions 0.02 g/L (Figure A32). Droplet size varies over the entirety of the sample, however, the largest amount of droplets are very small. Samples showed no significant change in emulsion droplet size and were stable over the course of 16 weeks. The stability of the emulsion droplets was not affected by CN concentration, i.e. CM-AHPA-based emulsions were stable for at least 16 weeks at various concentrations.

Demulsification studies were conducted in order to test the stability of Pickering water-in-water emulsions with different CN under several conditions, including dilution of the system, the addition of a surfactant (SDS) and pH dependence. For all cases, the emulsions could be broken on purpose (Figure A33). Demulsification via dilution was tested by addition of water equal to half the system size (50%), equal to the system size (100%), and twice the system size (200%). It could be verified that dilution is effective at breaking these APTS emulsions. In choosing to work near the critical point for phase formation, we were able to use a minimal amount of polymer to achieve two phase systems, and allow more room for viscosity changes. Emulsions with higher water dilution (200%) broke quicker than those with a lower dilution (50%) as expected. Optical microscopy images of separated two phases confirmed the successful demulsification of water-in-water emulsions (Figure 6.5). The emulsion may withstand a certain amount of dilution but as the two phases become miscible the emulsion will eventually break into a continuous solution.

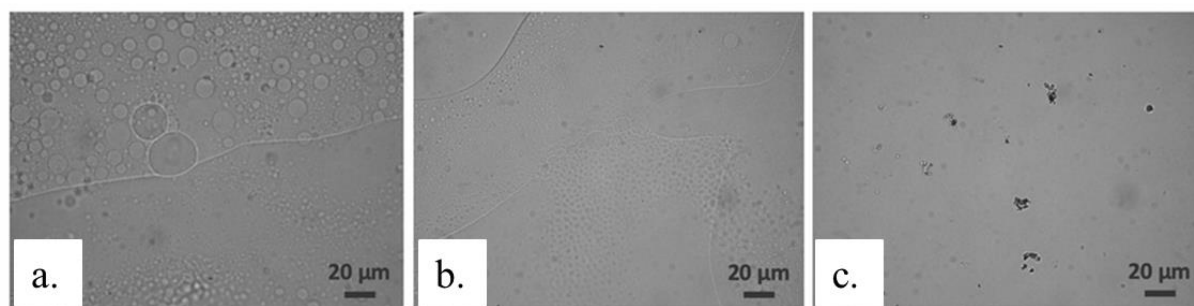


Figure 6.5. Demulsification of CM-AHPA stabilized 3 wt% PEG_{35K} : 7 wt% dextran_{40K} water-in-water Pickering emulsions (0.1 g/L CN). a. 50% dilution. b. 100% diluted emulsion. c. 200% diluted emulsion.

Emulsion stability towards surfactants was tested with the addition of 4 mM SDS. All emulsions were verified with optical microscopy (Figure A33). The introduction of negatively charged SDS has a profound effect on CN. The hydrophobic part of surfactant interacts with the CN surface, which leads to electrostatic repulsion between individual CNs and thus droplet coalescence is initiated as the solid-stabilizer is expelled from the droplet surface. These procedures show the normal causes for breaking of ATPS emulsions, where certain triggered demulsification events can be performed.

pH dependence was tested by adding a small amount of strong acid (HCl) and base (NaOH) to emulsions. For CM-AA stabilized emulsions, ~0.02 mL of HCl (10 mol/L) and ~0.02 mL of NaOH (6 mol/L) were added to 3 mL pre-prepared emulsions, which cannot cause any demulsification by this pretty low dilution, but by pH adjustment (Figure A34). Moreover, the demulsification happened in different pH only for CM-AA (allylamine modified carbon nitride). The amino group is a reactive group that is protonated by HCl and deprotonated in the alkaline condition, which changes the polarity of the stabilizer. For both conditions, the pH sensitive CM-AA played a crucial role in destabilizing emulsions.

Chapter 6

6.3. Conclusions

In conclusion, carbon nitride proved itself as a capable Pickering stabilizer, forming emulsions with lifetimes of at least 16 weeks. Carbon nitride stabilized water-in-water emulsions can be tuned for droplet size via the polymer composition, have the continuous and emulsion phase adjustment, although be demulsified via various methods. Among these, dilution broke emulsions below the level required for phase separation of the APTS. Besides, surfactant addition and pH adjustment (strong acid and base) also demulsify pre-formed emulsions. Carbon nitrides unique properties as a metal-free photocatalyst allow it promising uses for photocatalysis, water splitting and contaminant degradation. With the combination of aqueous two-phase systems, carbon nitride water-in-water Pickering emulsions allow for a unique set of tools for future utilization applications in cosmetics, food, or as waste water treatment with diffusion separation of aqueous phase systems.

7. Conclusion and Outlook

The goal of this thesis focuses on the investigation of aqueous two-phase systems utilizing various solid particles in these dispersed systems and triggering biocompatible polymers in compartmentalized systems.

The first part of this thesis investigated biocompatible PDP and their application in aqueous dextran-PEG systems and enhancement in water-water emulsion preparation. Herein, all aqueous dextran-PEG emulsions were prepared in the presence of PDP (suspension, 0.2 g/L, 3 mL). PDP was synthesized via dopamine hydrochloride under alkaline condition. The stability of the formed emulsions is studied with respect to pH, dilution and addition of surfactants. To inhibit demulsification of the Pickering emulsion, cross-linking of the solid PDP by using poly(acrylic acid) (PAA_{450k}) and water-soluble 1-ethyl-3-(3-dimethylaminopropyl)carbodiimide (EDC) is performed to lock-in the surface structure of emulsion droplets. And the stability of the emulsion was probed again. In contrast to the previous Pickering emulsion, the capsules remained intact after surfactant addition and upon dilution with water although minor swelling of the droplets was observed.

Regarding the well-dispersed solid PDP in aqueous two-phase systems and good performance as stabilizers in water-water emulsions, for the second part of the thesis, a generic method for compartmentalizing aqueous media using aqueous phase separation of incompatible polymers and formation of a supramolecular hydrogel to obtain fixed compartments was presented. Therefore, PEG-dextran w/w emulsions are formed in the presence of PDP and gelation via α -CD was investigated. By forming the supramolecular hydrogel throughout the continuous phase of all-aqueous emulsions stabilized by PDP, distinctly, compartmentalized complexation between PEG and α -CD are formed. The hydrogel formation was performed at temperatures around 65 °C, which led to reversible gelatin as hydrogels formed again at ambient temperature.

Chapter 7

However, there was no change for repeated heating and cooling when the hydrogel was prepared after heating to 90 °C. Moreover, the triggered disassembly of the hydrogels via competitive guest addition was presented, while the emulsion stayed intact keeping a mobile compartmentalization of the solution. The introduction of competitive guest, i.e. anthranilic acid, had a profound competitive effect on the α -CD/PEG PICs. The emulsion was demulsified in a further step leading to a complete loss of structuring. The hydrogels and emulsions were assessed via optical microscopy and confocal laser scanning microscopy showing a supramolecular compartmentalized hydrogel that can be selectively disassembled on various levels of structuring.

The last part of the thesis provides other possible solid particles dispersed in aqueous two-phase systems and utilization as stabilizers in water-in-water emulsions. Here, five types of CN were used, namely, CM, CM-AHPA, CN-Decene, g-CN-AA, and CMP-TA. The majority of the study employed the particular sulfonic acid modified variant CM-AHPA. Carbon nitride will be studied for its viability as Pickering stabilizer, along with its characterization and other properties. To enhance the dispersity of CN, solutions were sonicated and were either allowed to settle or centrifugation to remove excess CN. Emulsions were successfully prepared by using these five types of CN as stabilizers, which kept stable for at least 16 weeks. The variation of droplet sizes is quite large in these types of emulsions, which is related to the different amount of CN and types of CN. The targeted disassembly can be realized by pH adjustment, dilution of the systems and addition of surfactants.

In conclusion, the investigation of solid particles, PDP, various variants of CNs in water-in-water contributed to a high extend to increase understanding of aqueous two-phase systems (ATPS). At the beginning, starting with biocompatible poly (dopamine) particles dispersed in PEG-dextran emulsions as effective stabilizers, the water-in-water emulsions could keep stable and also enhance intact stability by crosslinking in the first chapter. Going on to address

Chapter 7

polydopamine particles in aqueous two-phase systems, the second chapter formed compartmentalized supramolecular hydrogels via addition of α -CD. Finally, the third chapter widens generality of solid particles in aqueous two-phase systems utilizing five types of CN.

A significant number of new aqueous two-phase systems can be easily formed by applying the reported preparation process. Furthermore, novel drug delivery approaches can be developed with the concept of the displayed compartmentalized supramolecular hydrogels addressing to the delivery or providing confinements. Recent advances in ATPSs have addressed controllable generation and stabilization of all-aqueous compartmentalized systems and droplets, and demonstrated diverse applications ranging from manipulating particles, designing artificial cells, preparing biocompatible microparticles, engineering cell micropatterning and 3D bioprinting, to separating cells and biomolecules in microfluidic channels in all-water environments.

In the future, more work still needs to be done to overcome the current challenges and to expand ATPS-based applications towards a much wider range of practical applications. The rapidly emerging understanding of ATPSs brings enormous potential for mimicking liquid – liquid phase separation (LLPS) processes that have important implications in the development of cells, age-related diseases, and neurodegenerative disorders, as well as opportunities for new technologies such as 3D printing of all-aqueous-based highly biocompatible organs with promise for translation into clinical applications.

8. Appendix

8.1. Materials

All materials were used as purchased unless noted otherwise. **Cetyltrimethyl ammonium bromide** (CTAB; analytical grade, Fluka), **dimethylsulfoxide** (DMSO; Acros, extra dry, 99%), **dextran** (40k, analytical grade; 100k, analytical grade, all from Sigma Aldrich), **dopamine hydrochloride** (98%, Sigma Aldrich), **ethylenediamine resin** (polymer-bound, 4.0-5.7 mmol/g, Sigma Aldrich), **1-ethyl-3-(3-dimethylaminopropyl carbodiimide hydrochloride** (EDC; >98%, Sigma Aldrich), **fluorescein isothiocyanate** (FITC; 90%, Sigma Aldrich), **hydrochloric acid** (HCl; fuming, Carl Roth), **poly(acrylic acid)** (PAA; 450k, analytical grade; 1250k, analytical grade, all from Sigma Aldrich), **poly(ethylene glycol)** (PEG; 20k, analytical grade; 35k, analytical grade, all from Sigma Aldrich), **poly(ethylene glycol) diamine** (NH₂-PEG-NH₂; 20k, analytical grade, Sigma Aldrich), **sodium hydroxide** (NaOH; 98%, Sigma-Aldrich) and **sodium dodecyl sulfate** (SDS; analytical grade, Fluka) were used without further purification, **anthranilic acid** (reagent grade, ≥98%, Sigma Aldrich), **α-cyclodextrin** (α-CD; ≥98%, Roth), **dimethylsulfoxide** (DMSO, extra dry, Acros Organics), **N,N dimethylformamide** (DMF, anhydrous 99.8%, Sigma Aldrich), **ethylenediamine resin** (polymer-bound, 4.0-5.7 mmol/g, Sigma Aldrich), **fluorescein isothiocyanate** (FITC; 90%, Sigma Aldrich), **poly(ethylene glycol)** (PEG; 20k, analytical grade; 35k, analytical grade; 40k, analytical grade, all from Sigma Aldrich). **Rhodamine B** (high purity, Sigma), **Methylene Blue** (high purity, biological, Alfa Aesar), **reactive blue 160** (Sigma-Aldrich) were used for the photocatalysis of dyes. **Rhodamine B Isothiocyanate-Dextran** (70k, Sigma) and FITC labelled PEG (2K) were used for confocal experiments. Polydopamine particles (PDP)¹⁹³ and FITC-labeled PEG were obtained according to the literature. Several CN were used with different functionalities, including CN from cyanuric acid-melamine complex (CM),¹⁸⁷ phenyl-

Chapter 8

modified CM (CMP),¹⁸⁸ allylamine-grafted CM (CM-AA),¹⁸⁹ AHPA grafted CM (CM-AHPA),¹⁸⁹ decene-grafted CM (CM-Decene),¹⁸⁹ and 4-methyl-5-vinyl thiazole-grafted CMP (CMP-TA).¹⁹⁰ Milli-Q water was obtained from an Integra UV plus pure water system by SG Water (Germany).

8.2. Synthesis Procedures

8.2.1. Synthesis of materials described in Chapter 4

Preparation of polydopamine particles (PDP)¹⁹⁴: In a typical synthesis of PDP, aqueous ammonia solution (NH₄OH, 0.75 mL, 28-30%) was mixed with ethanol (40 mL) and deionized water (90 mL) under mild stirring at room temperature for 30 min. Dopamine hydrochloride (0.5 g) was dissolved in deionized water (10 mL) and then injected into the mixture. The color of this solution immediately turned to pale brown and gradually changed to dark brown. The reaction was allowed to proceed for 30 h under air. The PDP was obtained by centrifugation and washed with water for three times. The fabricated PDP was dried in the oven at 80 °C for 24 h (yield: 0.38 g PDP). For the use as Pickering stabilizer a stock of PDP suspension was prepared applying ultrasound (Elmasonic S30H).

FITC-labeled PEG: In a dry, argon purged 25 mL round bottom Schlenk flask, NH₂-PEG-NH₂ (20k, 0.5 g, 0.025 mmol, 1 eq.) was dissolved in dry DMSO (6 mL). At first, FITC (9.735 mg, 0.05 mol, 2 eq.) was dissolved in dry DMSO (1.0 mL) in the dark and then added to the reaction mixture. The reaction mixture was stirred at ambient temperature for 24 hours. Ethylenediamine resin (polymer-bound, 100 mg) was added and the reaction mixture was stirred for an additional 24 h. The reaction mixture was filtered off and the solution was dialyzed against deionized water for three days followed by lyophilization to afford FITC labeled PEG (0.189 g, 10.2 μmol, 38% recovery, $M_n = 18\,400\text{ g mol}^{-1}$, PEG standard in THF, $D = 1.3$) as an orange powder.

Exemplary Preparation of Water-in-water Emulsions: Solutions of dextran and PEG were prepared by dissolving the powder in Milli-Q water at neutral pH with stirring. Concentrations of PEG (C_{PEG}) and dextran (C_{Dex}) are indicated as weight percentages. An example emulsion

was formed by mixing PEG_{35k} ($C_{\text{PEG}}=7$ wt%, 0.90 g) and dextran_{40k} ($C_{\text{Dex}}=3$ wt%, 0.40 g) in PDP suspension (0.2 g/L, 3 mL). After mixing, the mixtures were shaken by hand. In this way, a stable dextran-in-PEG emulsion with broad distribution of droplet sizes could be achieved. In order to decrease dispersity of droplet sizes, the procedure was evaluated further. Vortex treatment for 30 s led to emulsion with improved dispersity in droplet size. Other emulsions were formed according to Table A1.

Preparation of Crosslinked Water-in-water Emulsions: A stock solution of PAA_{450k} (100 mM) and freshly-prepared EDC (120 mM) was prepared in Milli-Q water. To obtain crosslinked PDP in water phases, PAA and EDC solution were added into as-formed emulsions stabilized by PDP. First, PEG_{35k} ($C_{\text{PEG}}=7$ wt%, 0.90 g) / dextran_{40k} ($C_{\text{Dex}}=3$ wt%, 0.40 g) emulsions were prepared and then PAA_{450k} solution (0.5 mL) and several droplets of fresh EDC solution (0.4 mL) were added into stable PEG/dextran emulsions, crosslinked PDP surrounding emulsion droplets were fabricated via vortex for 15s.

Demulsification of Various Types of Emulsions: Here, PEG ($C_{\text{PEG}}=7$ wt%, 0.90 g) / dextran ($C_{\text{Dex}}=3$ wt%, 0.40 g) water-in-water solutions were stabilized by PDP as mentioned above. A droplet of the emulsion (~0.2 mL) was placed on a microscopy slide and Milli-Q water (~0.2 mL) was added to dilute the emulsion. In the case of surfactants, SDS or CTAB (4 mM, 0.3 mL) were used for 3 mL of non-crosslinked emulsions as well by directly mixing with original emulsions.

8.2.2. Synthesis of materials described in Chapter 5

Preparation of Compartmentalized Hydrogel: An example compartmentalized hydrogel was formed by mixing PEG_{35k} ($C_{\text{PEG}}=7$ wt%, 0.90 g) and dextran_{40k} ($C_{\text{Dex}}=3$ wt%, 0.40 g) with PDP-

α -CD suspension (0.2 mg/mL of PDP, 140 mg/mL of α -CD, 3 mL). After mixing, the mixture was ultrasonicated for 2 hours for dissolving and emulsification (Elmasonic S30H). Then, the sample was heated to 65 °C and cooled down to ambient temperature for hydrogel formation. To study the temperature sensitivity, the procedure was evaluated further. After ultrasonication for 2 hours, the mixture was directly heated to 90 °C and then cooled down to ambient temperature.

Stability of Emulsions and Compartmentalized Hydrogel:

Dilution Study

Here, PEG ($c_{\text{PEG}}=7$ wt%, 0.90 g) / dextran ($c_{\text{Dex}}=3$ wt%, 0.40 g) w/w α -CD solutions were stabilized by PDP as mentioned above. After ultrasonication, before heating and hydrogel formation a droplet of the emulsion (~0.2 mL) was placed on a microscopy slide and Milli-Q water (~0.2 mL) was added to dilute the emulsion, which breaks the emulsion. However, the dilution by 50% could not demulsify the emulsion.

Competitive Guest Addition

After hydrogel formation a competitive guest was added. Anthranilic acid (10 mM, 0.5 mL) was mixed with compartmentalized hydrogels (3 mL) with vortex for 30 s, which led to a sol. Here, there was no demulsification observed under optical microscope. Finally, the following targeted complete disassembly was performed by diluting ~0.2 mL of the mixture solution by 100% with Milli-Q water (~0.2 mL). When the mixture solution was diluted, a droplet of the solution was directly placed on a microscopy slide and complete demulsification was observed (Figure 5d).

8.2.3. Synthesis of materials described in Chapter 6

Preparation of Carbon Nitride Stabilized Emulsions: Carbon nitride dispersion solutions were prepared first with the addition of CN to deionized water (0.1 g/L). To disperse CN,

Chapter 8

solutions were sonicated via ultrasound (Elmasonic S30H). For more dilute dispersions of CN, the stock solutions were either allowed to settle (7 days) or centrifugation (10K RPM, 10 minutes) to remove excess CN before weighing to find the final concentration of CN in the dispersion. CN begins to settle out of any stock solution within hours of dispersion, and should be fresh dispersed before use or testing to ensure even dispersion concentration. Furthermore, for samples made with similar concentrations, where one was produced by diluting a concentrated CN solution (0.1 g/L to 0.025 g/L) in comparison to a stock solution prepared by allowing the CN to settle naturally (0.02 g/L). Several CN were used with different functionalities, including CM, g-CN-AA, CM-AHPA, CN-Decene, and CMP-TA.

Emulsions were prepared by adding 3 mL of CN dispersion (0.02 to 0.1 g/L) to 3 wt% PEG and 7 wt% DEX, or other weight percentage ratios of PEG/DEX (Table A4). Samples were allowed to mix passively, before emulsification. When two phases can be observed, the samples are then emulsified for observation. Emulsification was performed via hand mixing (10-30s), vortex (10-30s), sonication (5-30 min), or homogenization (30s) (IKA Dispersers T25 digital ULTRA-TURRAX®).

Demulsification of Various Types of Emulsions: Here, 3 wt% PEG_{35K} ($C_{\text{PEG}}=7$ wt%, 0.90 g): 7 wt% DEX_{40K} ($C_{\text{DEX}}=3$ wt%, 0.40 g) water-in-water solutions were stabilized by CN as mentioned above. A droplet of the emulsion (~0.2 mL) was placed on a microscopy slide and Milli-Q water (~0.1 mL) was added to dilute the emulsion to 50%, Milli-Q water (~0.2 mL) to 100% and Milli-Q water (~0.4 mL). In the case of surfactants, SDS (4 mM, final concentration) were used for 3 mL of CN stabilized emulsions as well by directly mixing with original emulsions. For pH adjustment, a small amount of strong acid (HCl, 10 mol/L, ~0.02 mL) and alkaline (NaOH, 6 mol/L, ~0.02 mL) were added to 3 mL of CN stabilized emulsions.

8.3. Characterization

The interfacial tensions between polymer solutions and water were determined by the pendant drop method through droplet shape profile analysis (OCA instrument, Dataphysics ES, Germany). In chapter 4, firstly, the water solution with lower density, dextran solution or PEG solution was poured into a cuvette and a volume of ca. 20 μL aqueous solution containing PDP, and a distinct concentration of the other solution was injected into it by a syringe. Then, the droplet shape profile was analyzed to acquire the value of interfacial tension. At least three independent measurements were performed.

The three-phase contact angle was recorded using the same OCA instrument.¹⁷⁸ To measure the three-phase contact angle of particles (according to different samples) at the air–water interface, a silicon wafer was immersed into particles suspension and left to equilibrate for 24 h. After equilibration, the wafer was washed by distilled water to remove excess particles and dried prior to use. The wafer was placed at the bottom of the stage and ca. 2 μL water droplet was placed gently on the wafer. The contact angle was obtained by measuring three different spots on a wafer.

Fourier transform infrared (FT-IR) spectra were taken on Nicolet iS 5 FT-IR spectrometer. FT-IR is non-destructive and facile method to distinguish functional groups in samples.

Solid state ultraviolet-visible (UV-Vis) spectroscopy was recorded via a Cary 500 Scan spectrophotometer equipped with an integrating sphere. It is predominantly used for determination of photo and electrical properties of materials due to light absorption.

Size exclusion chromatography (SEC) was conducted in *N*-methyl pyrrolidone (NMP, Sigma Aldrich, GC grade) with 0.05 mol·L⁻¹ LiBr and BSME as internal standard using a column system by PSS GRAM 100/1000 column (8 × 300 mm, 7 μm particle size) with a PSS GRAM precolumn (8 × 50 mm) and a Shodex RI-71 detector and a calibration with PS standards from

PSS. The method is utilized to determine molar mass and molecular dispersity of polymer samples.

Nuclear magnetic resonance spectroscopy (NMR) was recorded at ambient temperature at 400 MHz using Bruker Ascend400 for ^1H -NMR. Thus, sample is dissolved in deuterated solvent and immersed in a magnetic field. Depending on the environment of the respective atom, chemical shifts can be measured. In the thesis, resulting spectra were investigated for determination of purity and confirmation of polymer structure.

Freeze drying of cross-linked particles and hydrogel samples are applied for solid state analysis. The samples were transferred into a flask or a metal plate and dried by pump thaw cycles until the moisture droplets were not visible anymore. In this frozen form, they were immediately put into Alpha LSCbasic (Christ, Germany) freeze dryer overnight.

Ultrasonication was performed via an ultrasonicator at 50% amplitude (Branson D450) which facilitates dispersion preparation.

Dynamic light scattering (DLS) measurements were performed on g-CN colloidal suspensions via Malvern Zetasizer Nano ZS90 with $\lambda=633$ nm at $\theta=90^\circ$. DLS provides information about hydrodynamic diameters of particles in solution. As all particles have Brownian motion in solution, random particle motion can be related to particle size using Stokes-Einstein equation. It assumes the particles as spheres and provides hydrodynamic diameter. Number average results were employed for different particle dispersions.

Zeta potential measurements of different colloidal suspensions in chapter 4 and chapter 6 were performed with a Zetasizer Nano ZS90 from Malvern. Zeta potential is an important phenomenon to determine colloidal stability as it is related to electrostatic repulsive forces. The measured value is based on the potential difference of dispersing media and stationary fluid attached to colloidal particle which arises from electric double layer theory. Zeta potential magnitudes more than 30 mV stands for good colloidal stability whereas magnitudes lower than 30 mV generally stand for instability.

Chapter 8

Rheology measurements were performed on Anton Paar MCR 301 rheometer, equipped with a cone plate 12 (CP-12). Measurements were performed at constant angular frequency (10 rad s^{-1}) with strain range from 0.1-100% with 31 measuring points and 0.02 mm gap. Frequency dependent measurements were performed at constant strain (0.1%) with changing frequency in the range of 1-100 rad s^{-1} . Viscosity measurements were performed at ambient temperature with changing shear rate between 1-20 s^{-1} . Rheology stands for the deformation and flow behavior of materials. It can be applied from solids to liquids and provides information about many properties, such as viscosity and viscoelastic behavior. Viscosity explains the resistance of liquids to flow, or a friction between fluid molecules, and one can imagine comparison of materials such as water and honey. Rheology is really helpful to determine viscosity and type of viscosity (shear thinning, shear thickening etc.). Basically, a material is placed between two plates, where bottom plate is stationary and top plate applies shear. Shear stress (τ) is defined as $\tau = F/A$, which F represents shear force (in Newton) and A represents area (m^2). Shear rate ($\dot{\gamma}$) is represented as v/h , which v is velocity (m/s) and h is shear gap (m). Finally, dynamic viscosity (η) can be calculated via $\eta = \tau/\dot{\gamma}$ with resulting $\text{Pa}\cdot\text{s}$ unit. Viscoelastic behavior of materials represents viscous and elastic behavior upon shearing. Rheology is helpful when it comes to investigate such properties of materials. Shear stress is defined in a same manner as shown in viscosity. Shear strain (γ) can be defined as s/h where s shows deflection path (m) and h shows shear gap (m). Therefore, shear modulus (G) is represented as τ/γ with Pa unit. Complex shear modulus (G^*) is derived from oscillatory shear tests which describes viscoelastic behavior of samples. Storage modulus (G') represents elastic character and loss modulus (G'') represents viscous character of sample. In the cases where $G' > G''$, means material has solid-like character and $G' < G''$ shows that material has more liquid character.

X-ray diffraction (XRD) patterns of powders were obtained using Bruker D8 Advance X-ray diffractometer via $\text{Cu-K}\alpha$ radiation and a scintillation counter. XRD provides information about crystallinity and order of the material. Bragg law describes the diffraction of a wavelength

Chapter 8

$$n\lambda = 2d\sin\theta$$

θ is the angle from diffraction, d is distance between planes and n represents the order of diffraction. The resulting pattern is characteristic for a sample which labels the crystalline orientation accordingly.

Scanning electron microscopy (SEM) images were obtained using SM-7500F (JEOL) equipped with an Oxford Instruments X-MAX 80 mm² detector. SEM records scattered electrons from sample after electron beam interaction and SEM images are used to observe the structures of samples.

Cryogenic scanning electron microscopy (Cryo-SEM) was used to visualize the emulsion droplet surface by Jeol JSM 7500F and the cryo-chamber from Gatan (Alto 2500). The prepared fresh dispersion was applied to a copper sample holder, and then the sample holder was put into chamber. In cryo-SEM, the sample is frozen before insertion for measurement to preserve the structure of the sample without drying effects.

Transmission electron microscopy (TEM) images were obtained via Zeiss EM 912 Omega microscope at 120 kV as acceleration voltage. Beam of electrons are transmitted through the sample and resulting image can be utilized to determine the structure (such as crystallinity) of material.

Confocal laser scanning microscopy (CLSM) is a technique for the imaging of thin lateral sections of a sample without the detection of out-of-focus light. The illumination of the sample from a point source such as a laser is focused on a spot inside the sample. In order to improve the acquisition rate, the confocal principle can be extended with a line-scanning microscope. In this case a line is used to illuminate the sample and fluorescence is collected through a slit. As all points in the line are detected at once, acquisition times are greatly improved but this comes at the expense of reduced sectioning strength. CLSM measurements were conducted with a Leica TCS SP5 (Wetzlar, Germany) confocal microscope, using a 63x (1.2 NA) water

Chapter 8

immersion objective. The dye stained samples were excited with a diode pumped solid-state laser at different wavelengths for different samples.

Optical microscopy (OM) images were conducted with a Leica, DM1000 LED optical microscopy (Germany). Optical microscopy is a technique employed to closely view a sample through the magnification of a lens with visible light.

Chapter 8

8.4. Appendix Figures

Table A1. Different concentration of weight ratio in PEG_{35k}/Dex_{40k} mixtures.

	$C_{\text{PEG}} = 8$ wt%	$C_{\text{PEG}} = 7$ wt%	$C_{\text{PEG}} = 6$ wt%	$C_{\text{PEG}} = 5$ wt%	$C_{\text{PEG}} = 4$ wt%	$C_{\text{PEG}} = 3$ wt%	$C_{\text{PEG}} = 2$ wt%
	$C_{\text{Dex}} = 2$ wt%	$C_{\text{Dex}} = 3$ wt%	$C_{\text{Dex}} = 4$ wt%	$C_{\text{Dex}} = 5$ wt%	$C_{\text{Dex}} = 6$ wt%	$C_{\text{Dex}} = 7$ wt%	$C_{\text{Dex}} = 8$ wt%
PEG (g)	1.043	0.903	0.766	0.632	0.532	0.399	0.266
Dex (g)	0.266	0.399	0.532	0.632	0.766	0.903	1.043

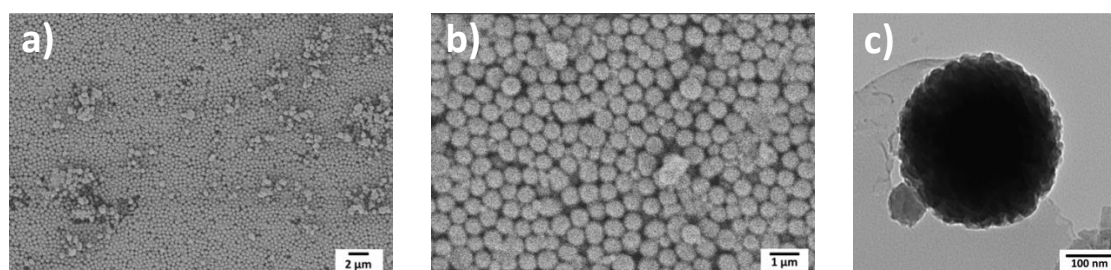


Figure A1. The morphology of polydopamine particles (PDP). a) and b) SEM images of PDP; c) TEM image of PDP.

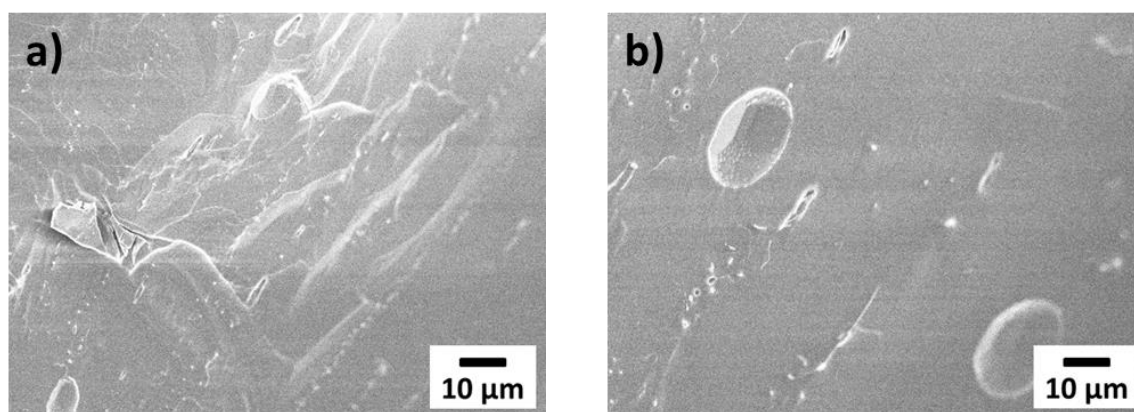


Figure A2. Cryo-SEM images of control sample without PDP stabilizers.

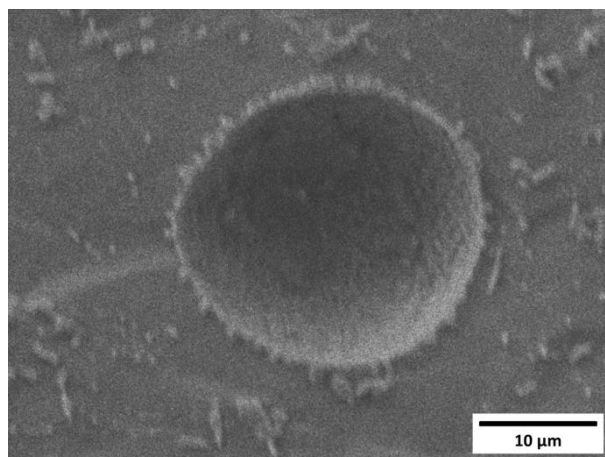


Figure A3. Cryo-SEM images of a single emulsion droplet (PEG_{35k} (7 wt%)/dextran_{40k} (3 wt%)/0.2 g/L PDP water-in-water system).

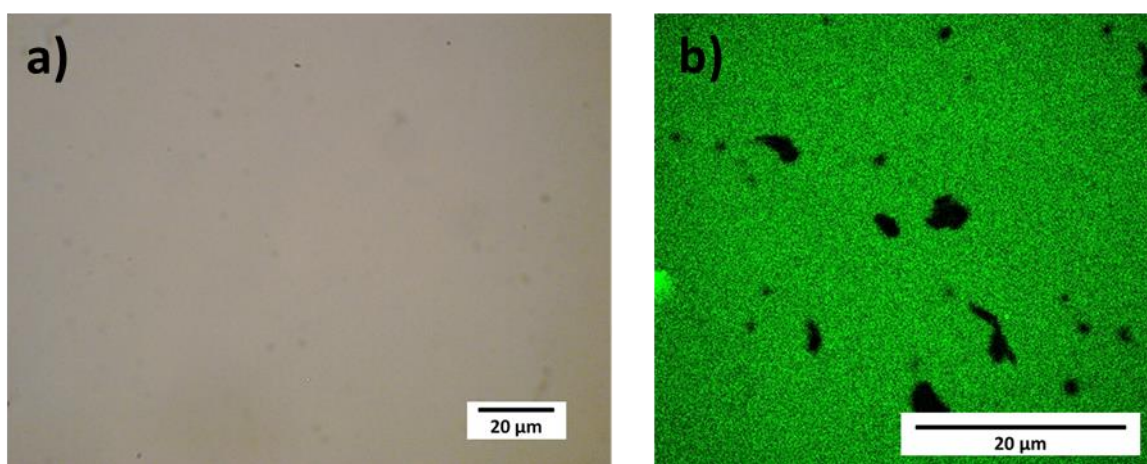


Figure A4. Images for the lower phase of PDP stabilized emulsions via vortex for 30 s. a) optical image of lower phase; b) CLSM image of lower phase.

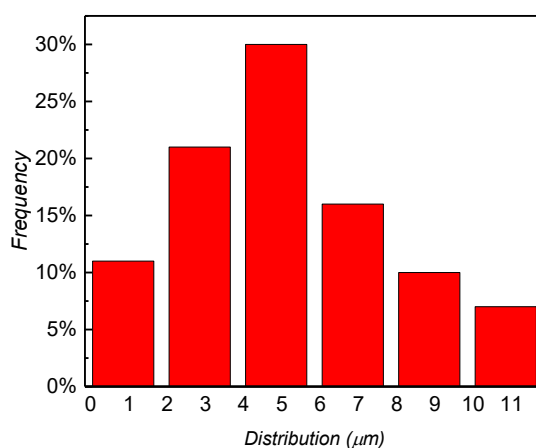


Figure A5. Droplet size distribution for stable emulsion droplets via vortex for 30 s. (The PEG_{35k} (7 wt%)/dextran_{40k} (3 wt%)/0.2 g/L PDP water-in-water system).

Table A2. Dependence of droplet size on PEG/dextran molar mass and concentration for PEG/dextran mixtures via vortex for 30 s (PDP concentration 0.2 g/L).

$C_{\text{PEG}}/C_{\text{Dex}}$ [wt%]	Average droplet diameter [μm] PEG _{20k} ; dextran _{40k}	Average droplet diameter [μm] PEG _{20k} ; dextran _{100k}	Average droplet diameter [μm] PEG _{35k} ; dextran _{40k}
8/2	5.62±0.77 μm	3.57±0.98 μm	3.26±0.92 μm
7/3	5.47±1.23 μm	8.25±0.76 μm	4.62±1.03 μm
6/4	5.55±0.86 μm	9.01±1.21 μm	5.62±1.01 μm
5/5	5.02±1.07 μm	9.68±0.75 μm	10.72±0.91 μm
4/6	No emulsion	11.63±0.96 μm	11.33±0.78 μm
3/7	No emulsion	15.42±1.11 μm	16.01±0.88 μm
2/8	No emulsion	16.39±0.93 μm	17.33±1.03 μm

Chapter 8

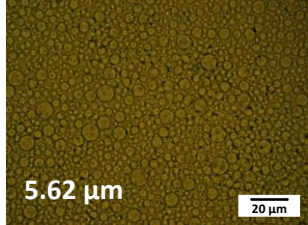
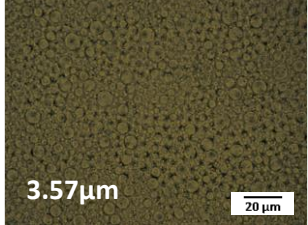
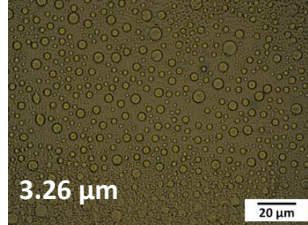
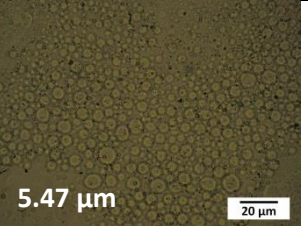
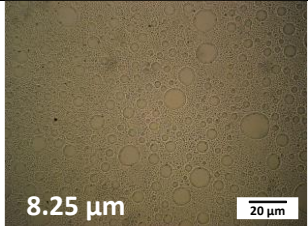
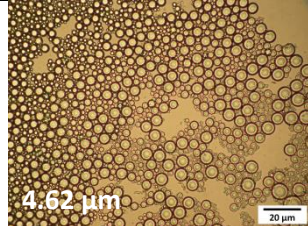
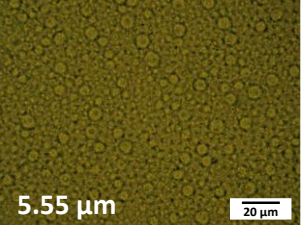
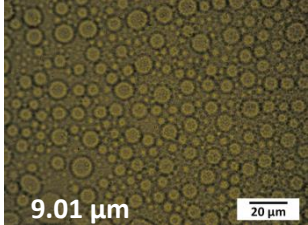
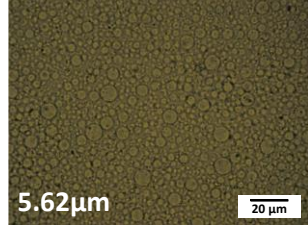
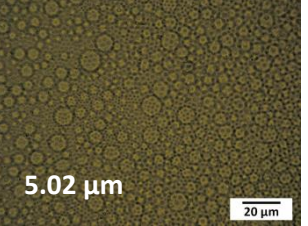
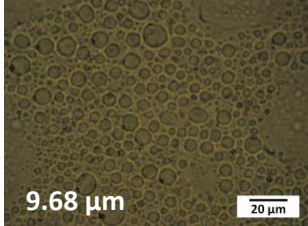
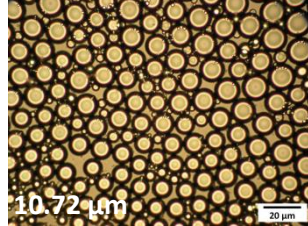
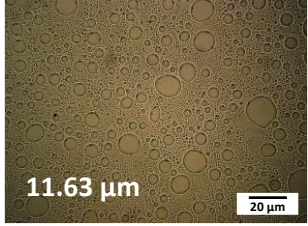
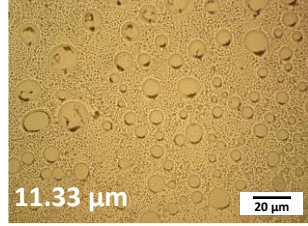
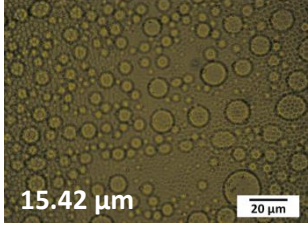
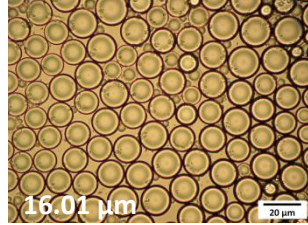
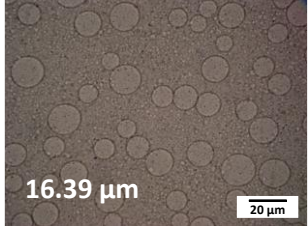
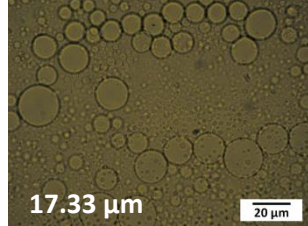
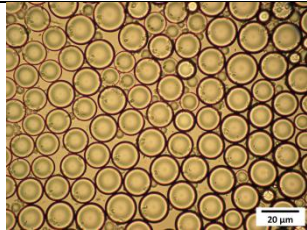
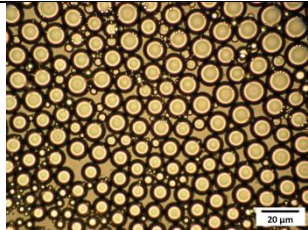
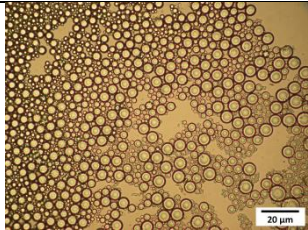
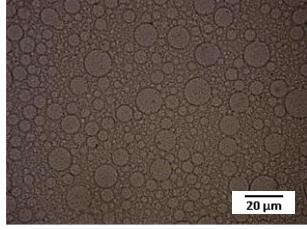
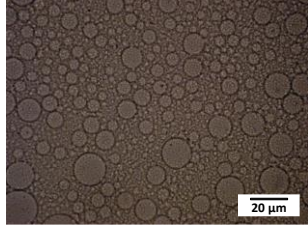
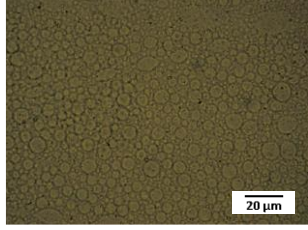
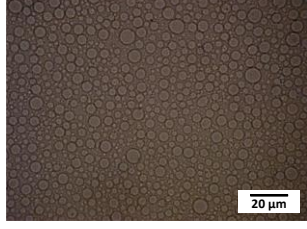
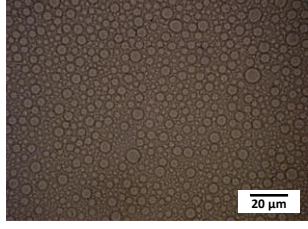
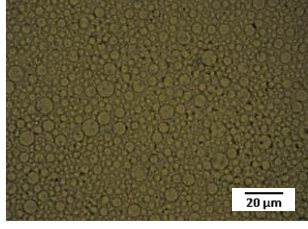
$C_{\text{PEG}}/C_{\text{Dex}}$ [wt%]	Average droplet diameter [μm] PEG _{20k} ; dextran _{40k}	Average droplet diameter [μm] PEG _{20k} ; dextran _{100k}	Average droplet diameter [μm] PEG _{35k} ; dextran _{40k}
8/2	 5.62 μm	 3.57 μm	 3.26 μm
7/3	 5.47 μm	 8.25 μm	 4.62 μm
6/4	 5.55 μm	 9.01 μm	 5.62 μm
5/5	 5.02 μm	 9.68 μm	 10.72 μm
4/6		 11.63 μm	 11.33 μm
3/7		 15.42 μm	 16.01 μm
2/8		 16.39 μm	 17.33 μm

Table A3. Dependence of droplet size on PDP suspension concentration with standard deviation via vortex for 30 s.

PDP concentration (g/L)	$C_{\text{PEG35k}} = 3 \text{ wt\%}$ $C_{\text{Dex40k}} = 7 \text{ wt\%}$	$C_{\text{PEG35k}} = 5 \text{ wt\%}$ $C_{\text{Dex40k}} = 5 \text{ wt\%}$	$C_{\text{PEG35k}} = 7 \text{ wt\%}$ $C_{\text{Dex40k}} = 3 \text{ wt\%}$
0.2			
0.4			
0.6			

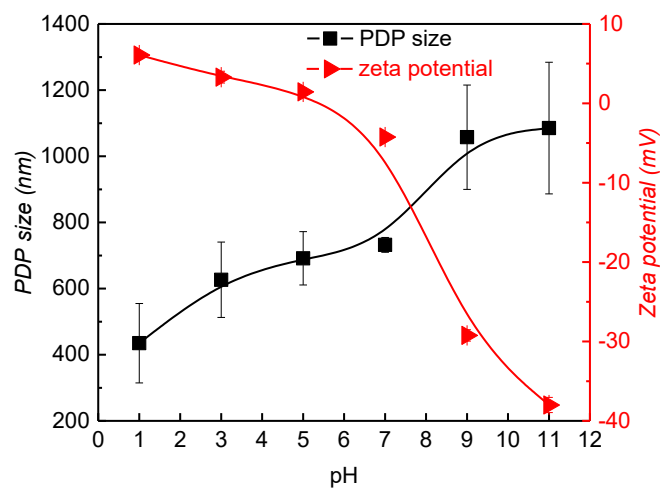


Figure A6. Influence of pH on the average size and zeta potential of PDP.

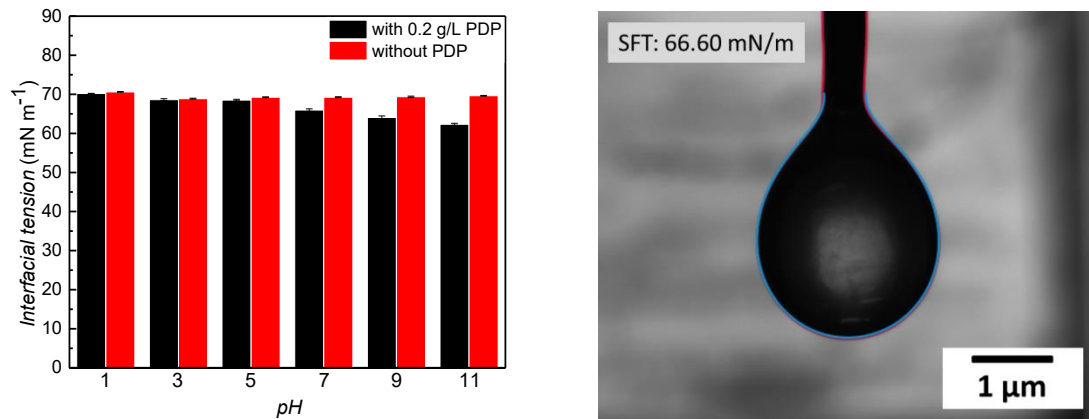


Figure A7. Influence of pH on the interfacial tension of PDP between PEG and dextran solution. The ratio of PEG is 3 wt% and the ratio of dextran is 7 wt%. The profile of pendant drop for interfacial tension. (pH=7, with 0.2 g/L PDP)

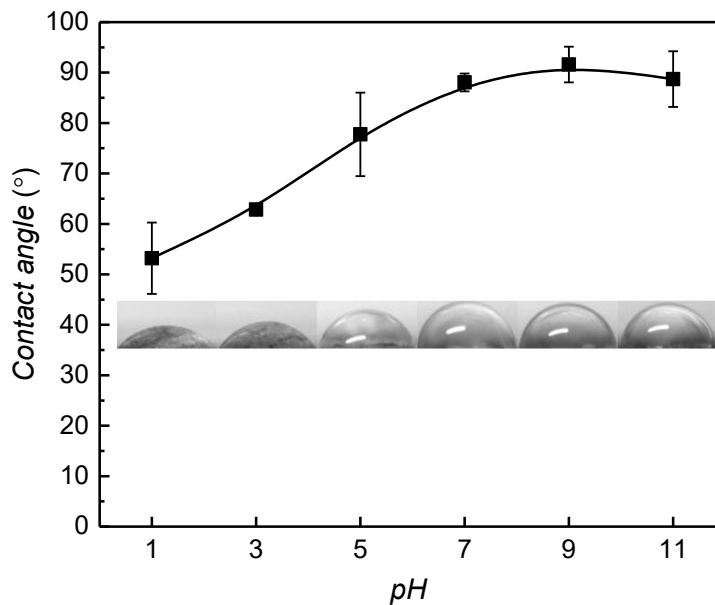


Figure A8. Influence of pH on the contact angle of PDP between PEG and dextran solution. The ratio of PEG is 3 wt% and the ratio of dextran is 7 wt%.

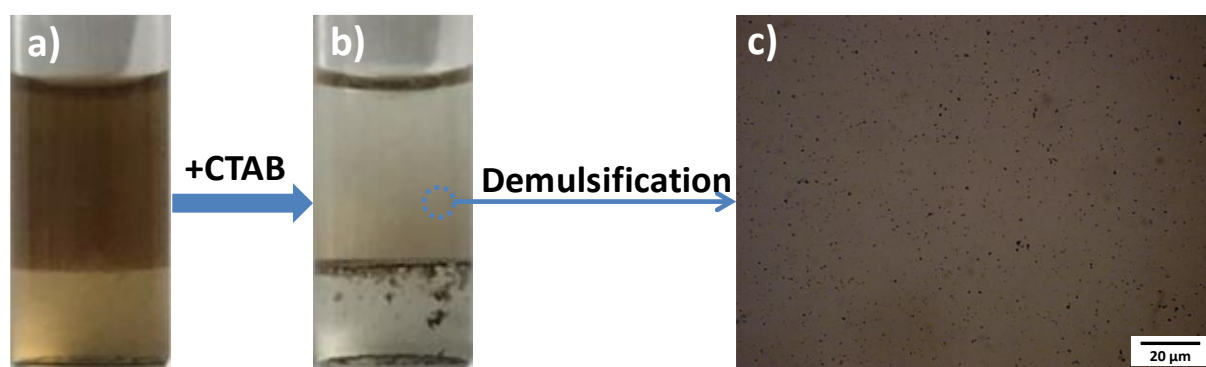


Figure A9. Photographs showing the demulsification of PDP-stabilized emulsions via vortex for 30 s by addition of CTAB. a) PEG-dextran emulsion. b) Phase separation. c) Optical microscope picture of demulsification. Here the emulsion was stabilized by 0.2 g/L PDP suspension. The weight ratio of PEG to dextran is 7 wt% of PEG_{35k}/ 3 wt% of dextran_{40k}.

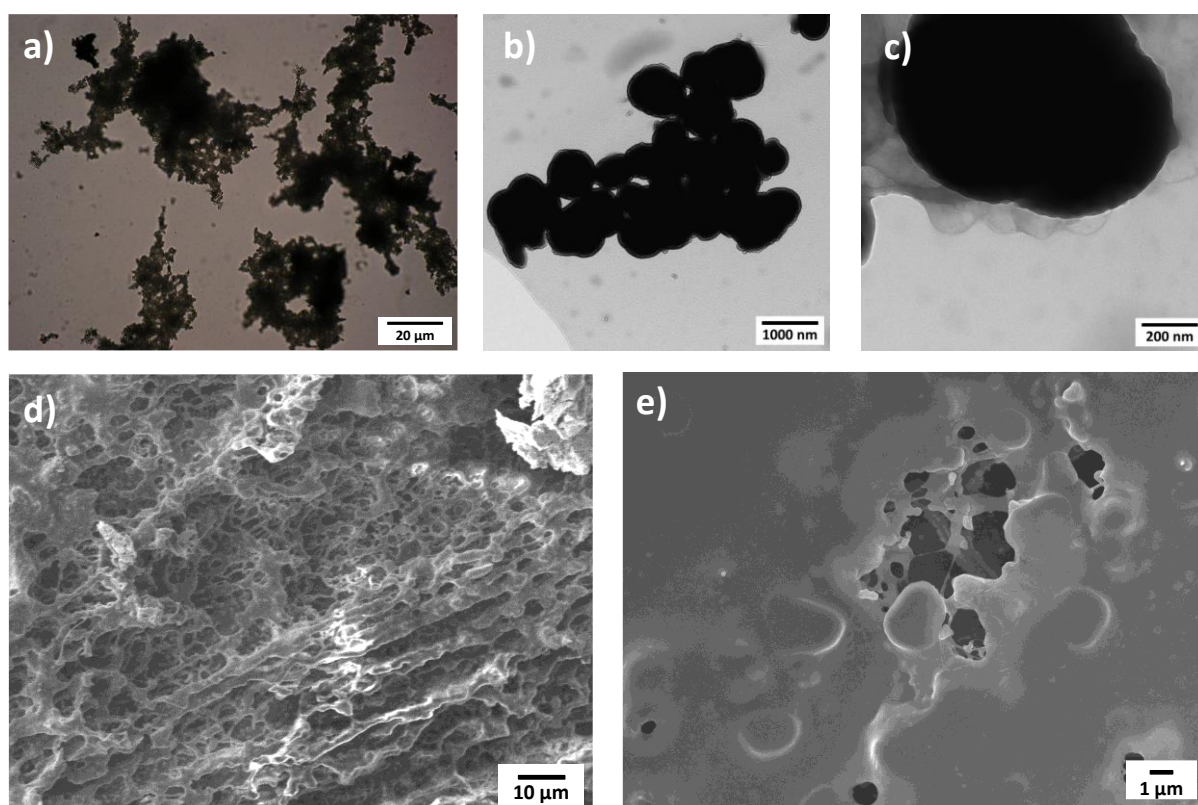


Figure A10. The morphology of crosslinked PDP. a) Optical microscope picture of PDP particles after crosslinking. b) and c) TEM images of crosslinked PDP. d) and e) Cryo-SEM images of crosslinked PDP.

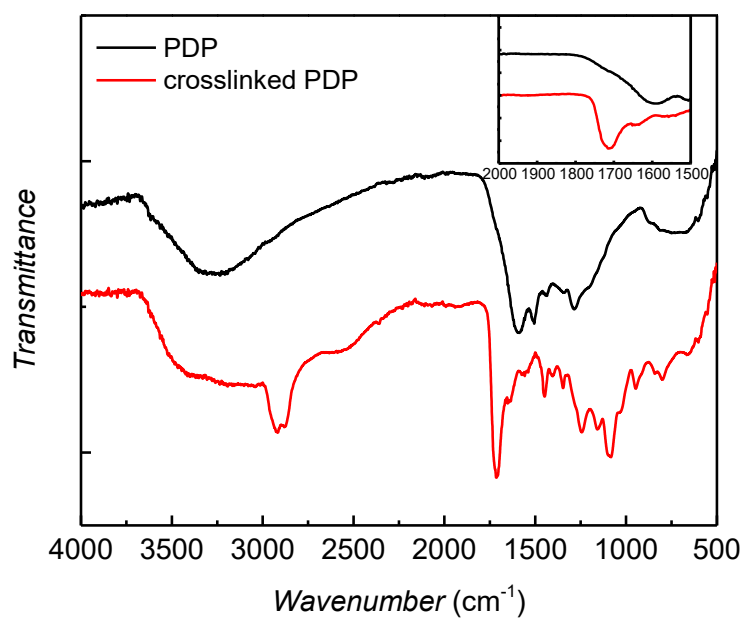


Figure A11. FTIR spectra of PDP particles and crosslinked PDP.

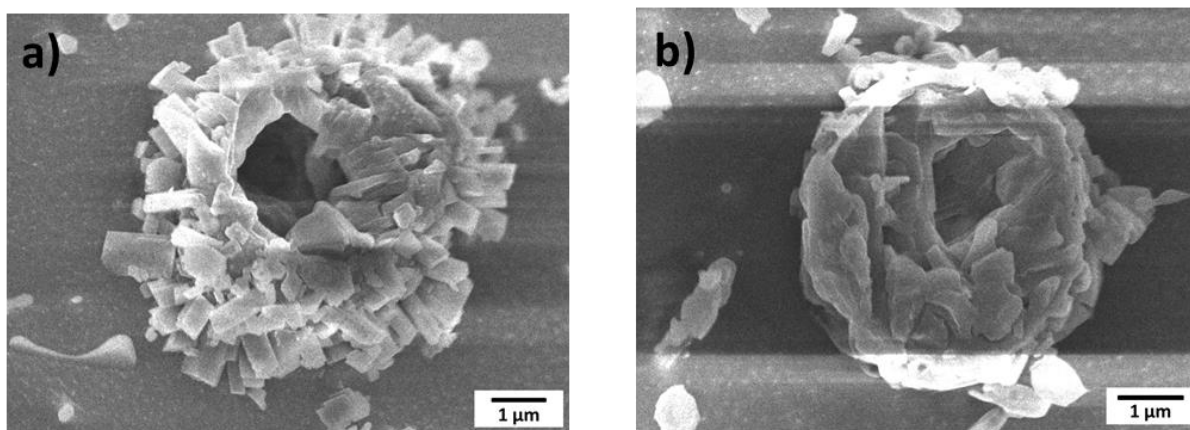


Figure A12. Additional cryo SEM images of emulsions of 7 wt% of PEG_{35k}; 3 wt% of dextran_{40k} system after crosslinking with PAA_{450k}/EDC.

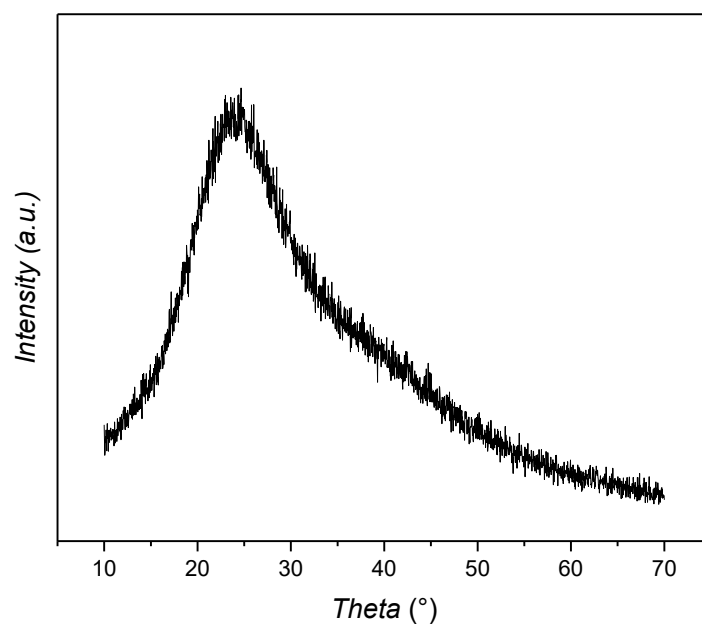


Figure A13. XRD measurement of crosslinked PDP.

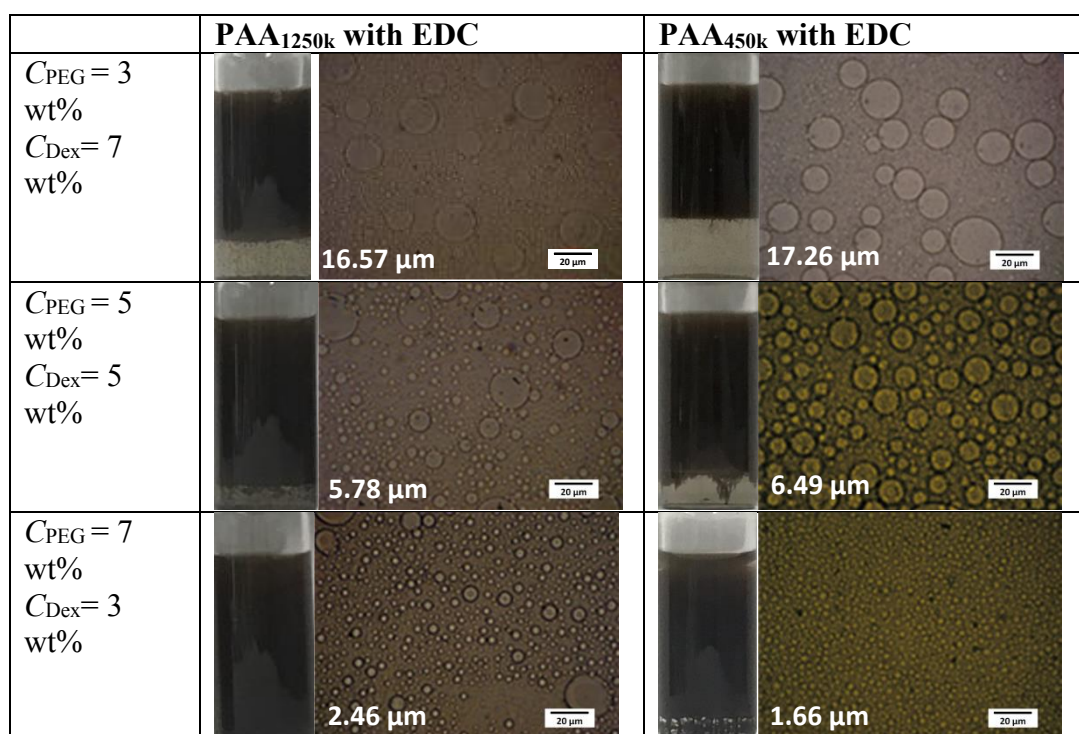


Figure A14. Influence of molar mass of PAA on the droplet size for emulsions for mixtures via vortex for 30 s.

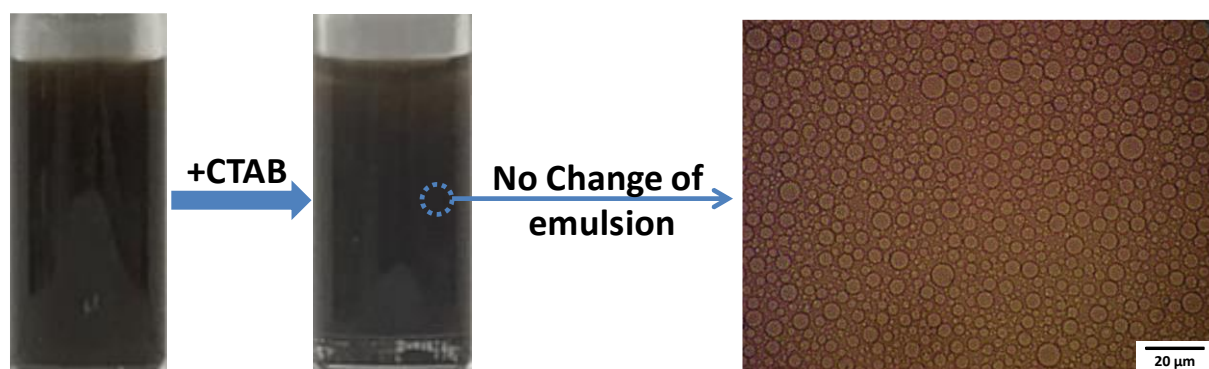


Figure A15. Photographs showing no phase separation of PDP-stabilized emulsions via vortex for 30 s by addition of CTAB. a) PEG-dextran emulsion. b) No phase separation. c) Optical microscope picture of emulsion droplet. Here the emulsion was stabilized by 0.2 g/L PDP suspension. The weight ratio of PEG to dextran is 7 wt% of PEG_{35k}/ 3 wt% of dextran_{40k}.

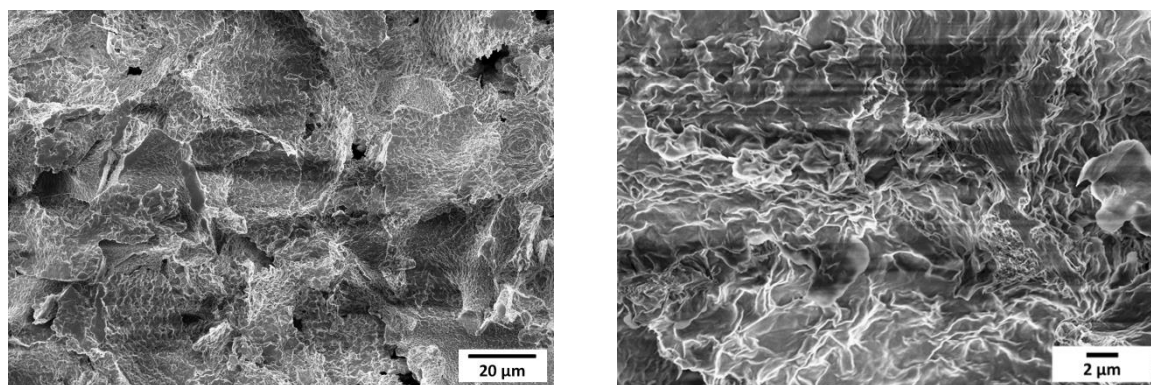


Figure A16. Cryo-SEM images of hydrogel via PEG_{35k} (7 wt%)/dextran_{40k} (3 wt%) water-in-water system (140 mg/mL of α -CD) after heating to 65 °C and cooling to ambient temperature without addition of PDP.

Chapter 8

Eq: calculation pathway for the surface coverage:

The surface area was calculated by the following steps. Firstly, the actual mass of particles utilized for emulsification was calculated by original concentration of PDP and the residual concentration of PDP.

$$6 \times 10^{-3} - 1.14 \times 10^{-3} = 4.86 \times 10^{-3} g \quad (\text{A1})$$

Then the number of emulsion droplets (n):

$$n = (\pi R^2 h) / \left(\frac{4}{3} \pi r^3\right) \quad (\text{A2})$$

R is radius for the glass vial;

r is radius for the emulsion droplet;

h is the height of emulsion;

So the total surface area:

$$n \times (4\pi r^2) = 3\pi R^2 h / r \quad (\text{A3})$$

Finally, the surface coverage:

$$\frac{4.86 \times 10^{-3}}{\frac{3\pi R^2 h}{r}} = 1.168 \times 10^{-6} g \cdot cm^{-2} \quad (\text{A4})$$

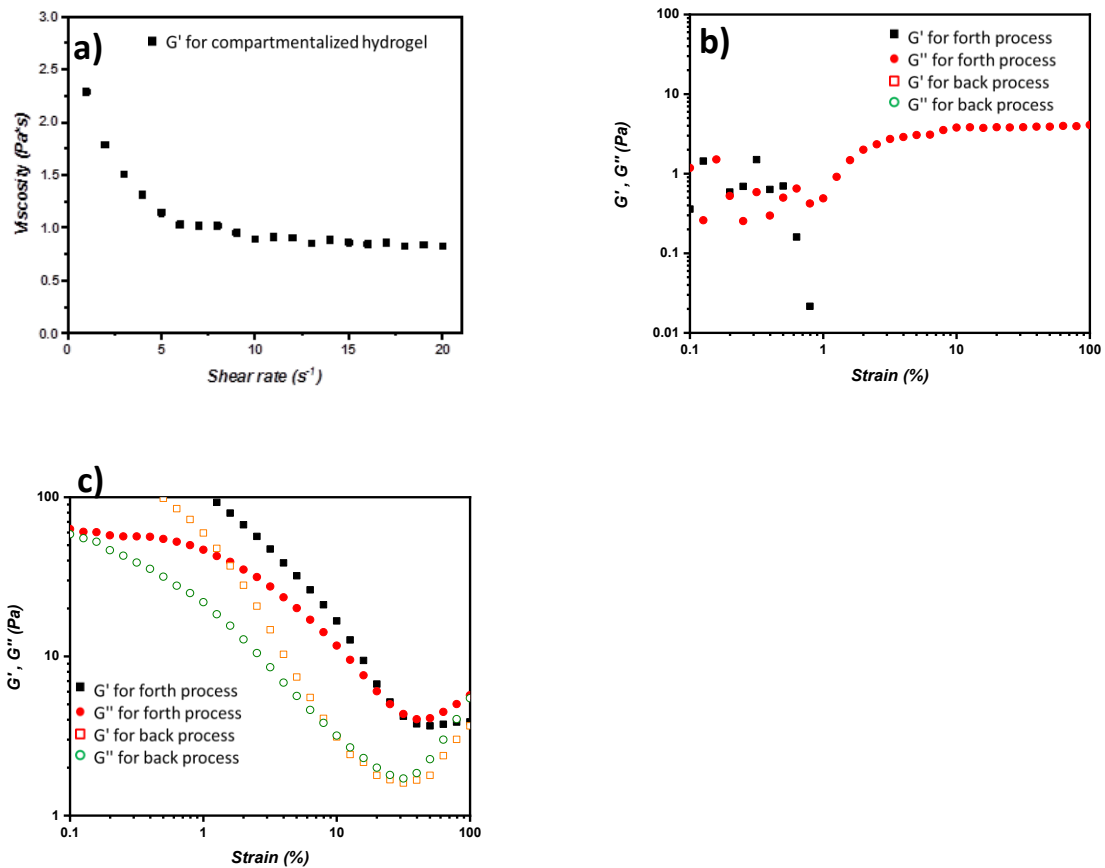


Figure A17. (a) Shear rate dependency of viscosity of compartmentalized hydrogels via PDP (0.2 g/L) stabilized PEG_{35k} (7 wt%)/dextran_{40k} (3 wt%) water-in-water system (140 mg/mL of α -CD); the strain dependency of (b) emulsion via PDP (0.2 g/L) stabilized PEG_{35k} (7 wt%)/dextran_{40k} (3 wt%) w/w system (without α -CD addition) (c) hydrogel via PDP (0.2 g/L) within PEG_{35k} (7 wt%) water system (140 mg/mL of α -CD) after heating to 65 °C and cooling to the ambient temperature.

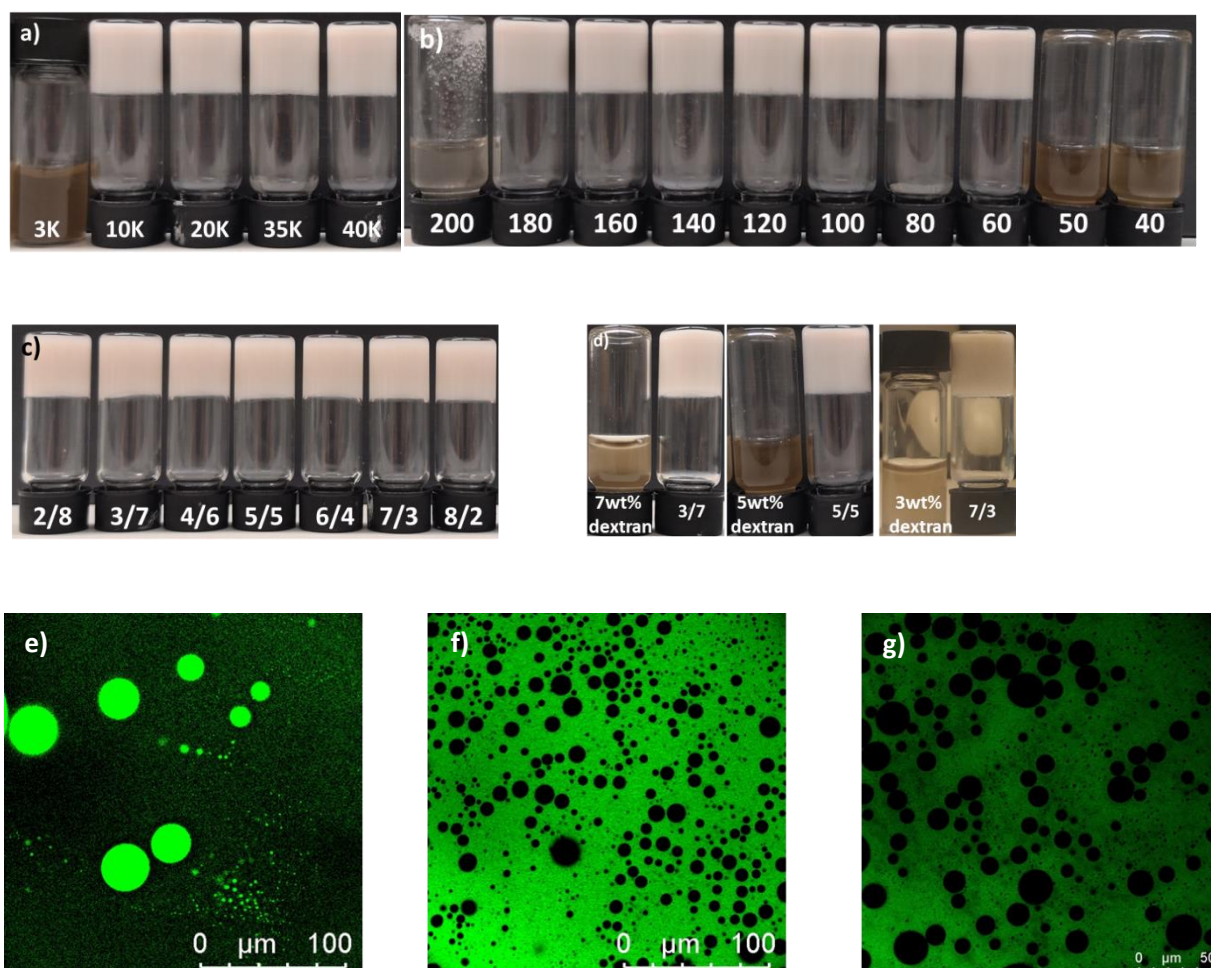


Figure A18. Component dependence of compartmentalized hydrogels via PDP (0.2 g/L) stabilized PEG/dextran w/w system : (a) PEG molar mass dependence for compartmentalized hydrogels via PDP stabilized PEG (7 wt%)/dextran (3 wt%) w/w system (140 mg/mL of α -CD); (b) α -CD concentration dependence for compartmentalized hydrogels via PDP stabilized PEG_{35k} (7 wt%)/dextran_{40k} (3 wt%) w/w system; and (c) PEG/dextran ratio (wt%) dependence for compartmentalized hydrogels via PDP stabilized PEG_{35k} /dextran_{40k} water-in-water system (140 mg/mL of α -CD); (d) hydrogels formed in a dextran phase isolated from a PEG_{35k} /dextran_{40k} water-in-water system (right) after addition of 140 mg/mL of α -CD for the respective PEG/dextran ratio (wt%) and reference of pure PDP/dextran phase (left) after addition of 140 mg/mL of α -CD; CLSM images of emulsion droplets within a compartmentalized hydrogel of the system: (e) PEG_{35k} (3 wt%)/dextran_{40k} (7 wt%); (f) PEG_{35k} (5 wt%)/dextran_{40k} (5 wt%); (f) PEG_{35k} (7 wt%)/dextran_{40k} (3 wt%).

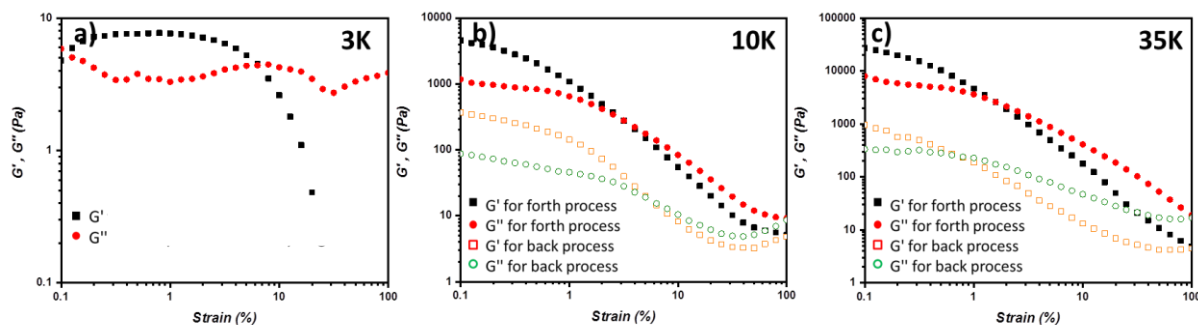


Figure A19. Dependence of PEG molar mass on rheological properties for PDP (0.2 g/L) stabilized PEG (7 wt%)/dextran_{40k} (3 wt%) w/w system (140 mg/mL of α -CD): (a) PEG_{3K}; (b) PEG_{10K}; (c) PEG_{35K}.

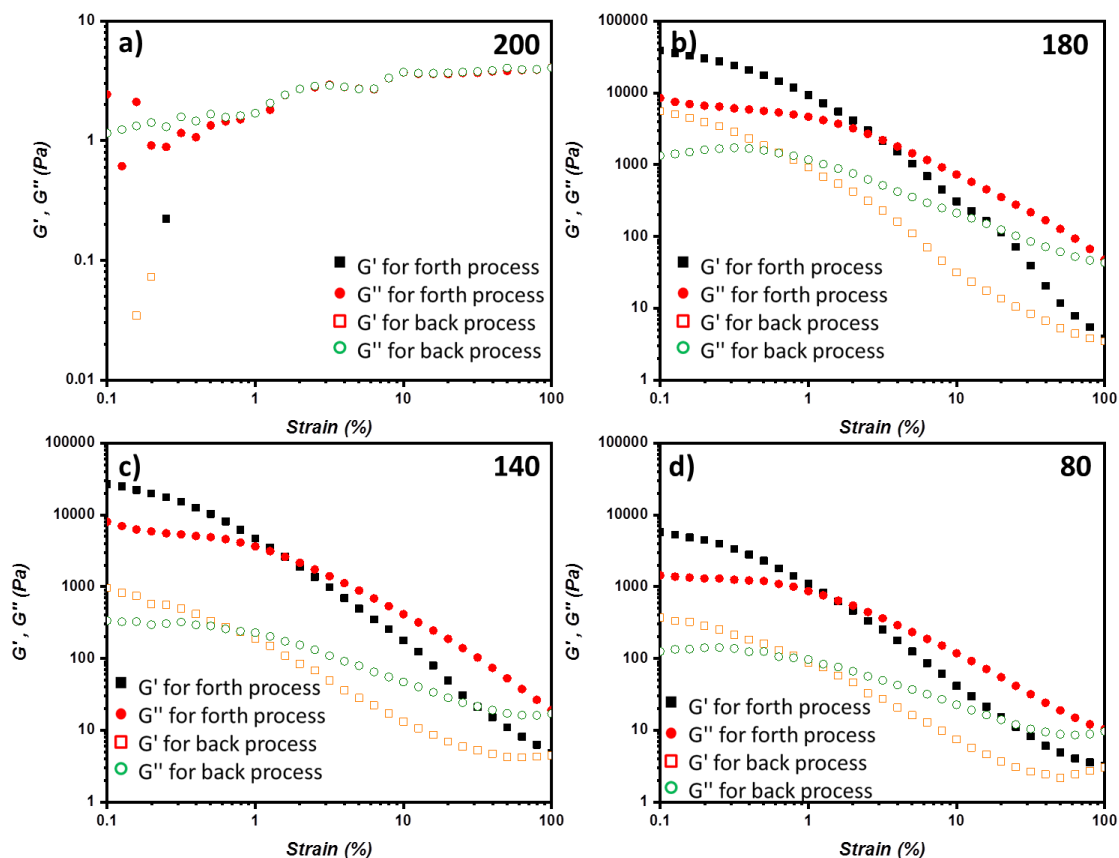


Figure A20. Dependence of α -CD concentration (mg/mL) on rheological properties of for PDP (0.2 g/L) stabilized PEG_{35k} (7 wt%)/dextran_{40k} (3 wt%) w/w system: (a) 200 mg/mL of α -CD; (b) 180 mg/mL of α -CD; (c) 140 mg/mL of α -CD; and (d) 80 mg/mL of α -CD.

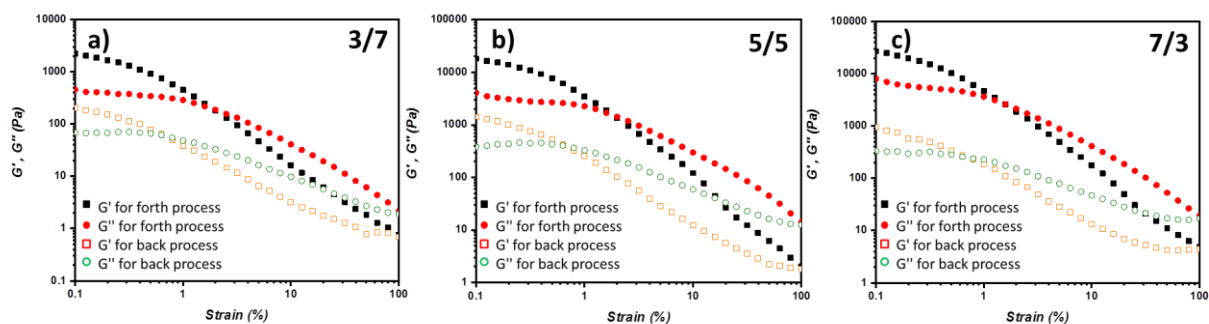


Figure A21. Dependence of PEG/dextran ratio (wt%) on rheological properties for compartmentalized hydrogels via PDP (0.2 g/L) stabilized PEG_{35k} /dextran_{40k} water-in-water system (140 mg/mL of α -CD):(a) PEG (3 wt%)/dextran (7 wt%); (b) PEG (5 wt%)/dextran (5 wt%); and (c) PEG (7 wt%)/dextran (3 wt%).

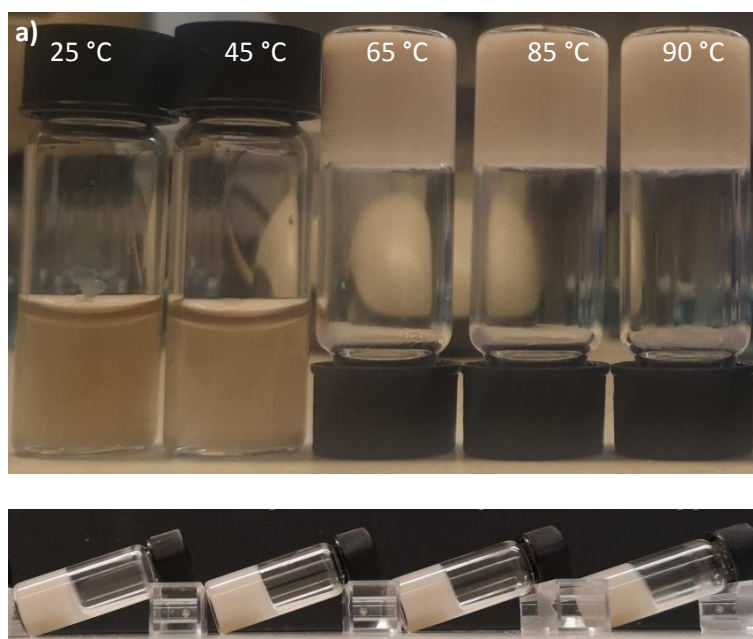


Figure A22. Dependence of preparation conditions on compartmentalized hydrogels via PDP (0.2 g/L) stabilized PEG_{35k} (7 wt%)/dextran_{40k} (3 wt%) w/w system (140 mg/mL of α -CD): (a) heating temperature dependence (b) heating time dependence after heating to 65 °C and cooling to ambient temperature.



Figure A23. Concentration dependence of competitive guest addition for compartmentalized hydrogels via PDP (0.2 g/L) stabilized PEG_{35k} (7 wt%)/dextran_{40k} (3 wt%) w/w system (140 mg/mL of α -CD): (a) 4 mM of anthranilic acid; (b) 6 mM of anthranilic acid; (c) 8 mM of anthranilic acid; (d) 10 mM of anthranilic acid and (e) 12 mM of anthranilic acid.

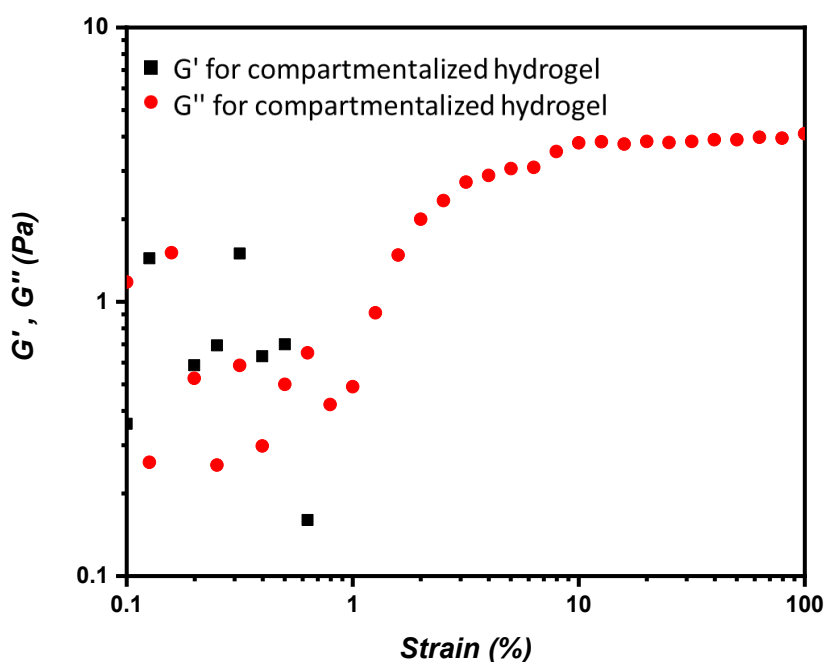


Figure A24. Strain dependency of the compartmentalized hydrogel via PDP (0.2 g/L) stabilized PEG_{35k} (7 wt%)/dextran_{40k} (3 wt%) water-in-water system (140 mg/mL of α -CD) after heating to 90 °C and cooling to the ambient temperature after addition of the competitive guest anthranilic acid.

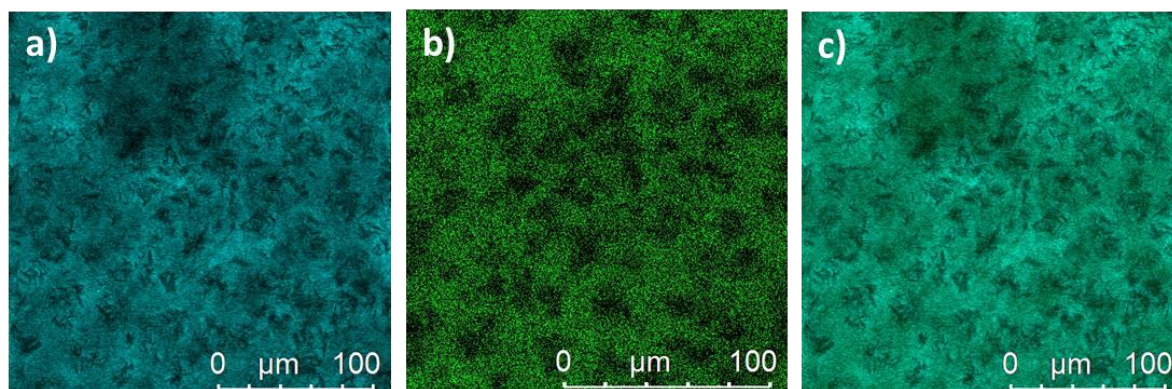


Figure A25. CLSM images of mixture solution via PDP (0.2 g/L) stabilized PEG_{35k} (7 wt%)/dextran_{40k} (3 wt%) water-in-water system (140 mg/mL of α -CD) after heating to 90 °C and cooling to the ambient temperature after adding the competitive guest anthranilic acid and dilution by 100% (a) under bright field; (b) under fluorescent field and (c) under overlay.

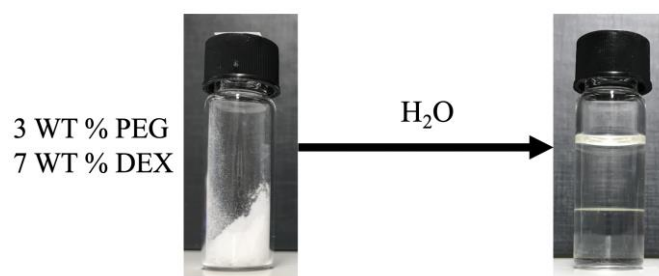


Figure A26. Example of 2-phase formation of 3 wt% poly(ethylene glycol) (PEG) with 7 wt% dextran.

Chapter 8

Table A4. Ratios of PEG:dextran used for the production of ATPS.

PEG:DEX	Peg WT%	Dex WT%	Distilled Water [mL]	PEG (mass added) [mg]	DEX (Mass added) [mg]
1:9	1	9	3	297	33.3
2:8	2	8	3	261	66.6
3:7	3	7	3	226	99.8
4:6	4	6	3	191	133
5:5	5	5	3	158	166
6:4	6	4	3	125	200
7:3	7	3	3	93.8	233
8:2	8	2	3	61.2	266
9:1	9	1	3	30.3	300

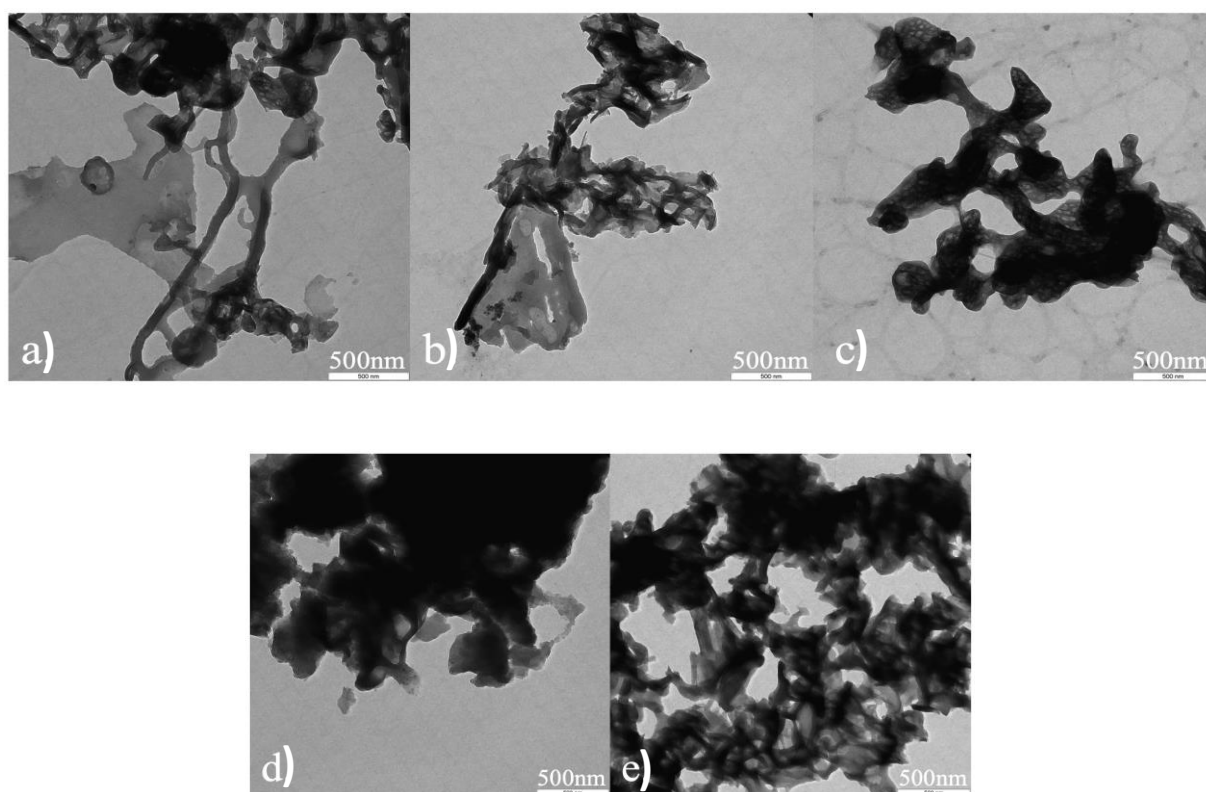


Figure A27. TEM images of various CN variants used in this project. (a) CM; (b) CM-AHPA; (c) CN-Decene; (d) CMP-TA and (e) g-CN-AA.

Table A5. Zeta potential and size distribution of CM-AHPA.

CM-AHPA	
Dextran Phase	0.00134mV
PEG Phase	0.03mV
Size	232nm

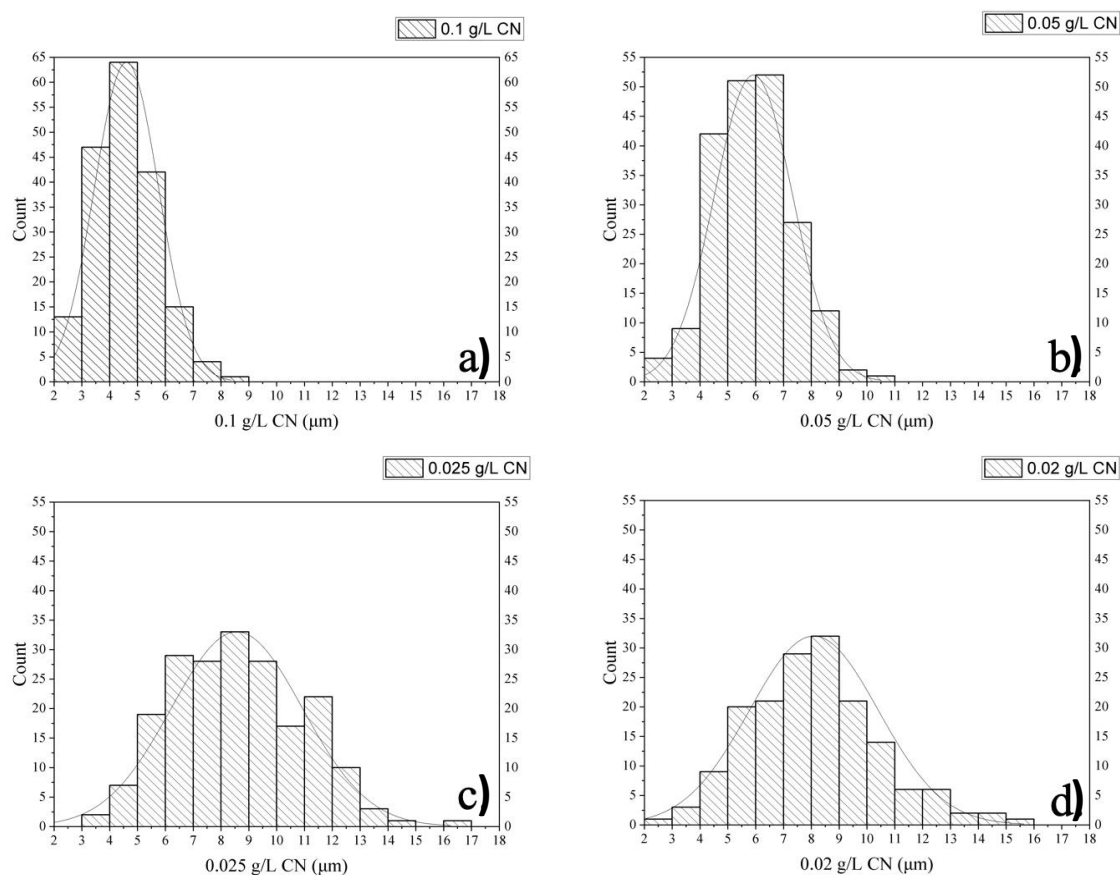


Figure A28. Droplet size of CN water-in-water emulsions with varying CN concentrations. Concentration displayed represents the concentration of CN dispersion added to system. Images taken with bright field microscopy and then processed with Nano Measurer 1.2 (200 sample size). (a) 3:7 wt% PEG:dextran 0.1 g/L CM-AHPA; (b) 3:7 wt% PEG: dextran 0.05 g/L CM-AHPA; (c) 3:7 wt% PEG: dextran 0.025 g/L CM-AHPA; (d) 3:7 wt% PEG: dextran 0.02 g/L CM-AHPA.

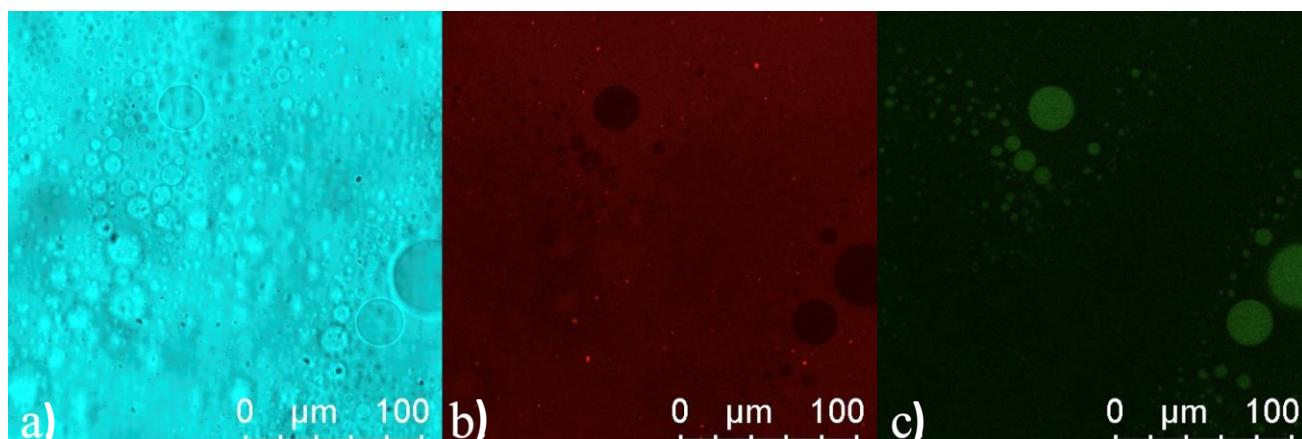


Figure A29. Confocal image of CM-AHPA 3:7 wt% PEG-dextran emulsion droplets, displaying PEG in the emulsion phase and dextran in the continuous phase. a. bright-field image of the emulsion droplets. b. Confocal image displaying rhodamine labelled dextran outside the droplets in the continuous phase. c. confocal image of FITC labelled PEG (20K) within the droplets, exclusive to the emulsion.

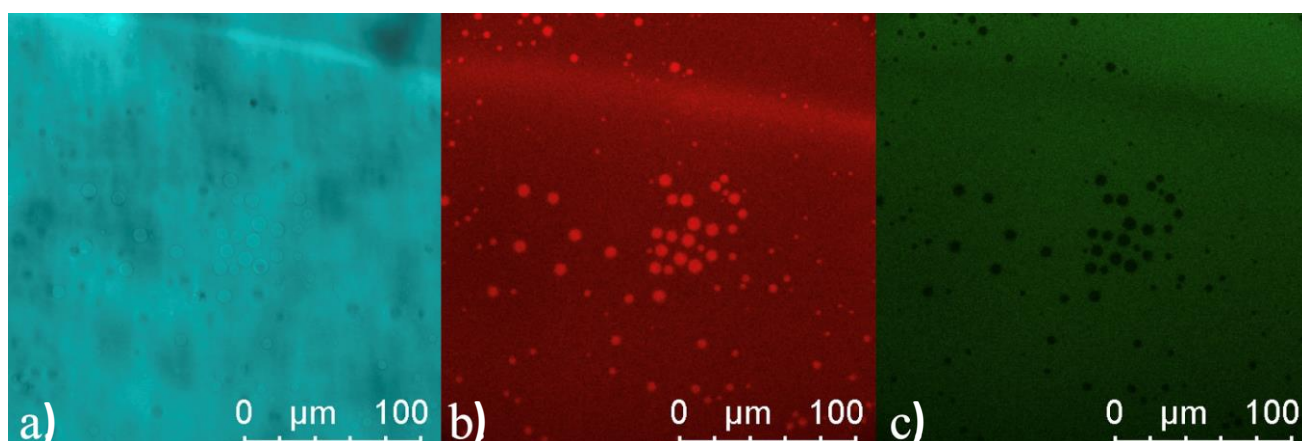


Figure A30. Confocal image of CM-AHPA 7:3 wt% PEG-dextran emulsion droplets, displaying dextran in the droplet phase and PEG in the continuous phase. (a) bright-field image of the emulsion droplets; (b) Confocal image displaying rhodamine labelled dextran outside the droplets in the continuous phase; (c) confocal image of FITC labelled PEG (20k) within the droplets, exclusive to the emulsion.

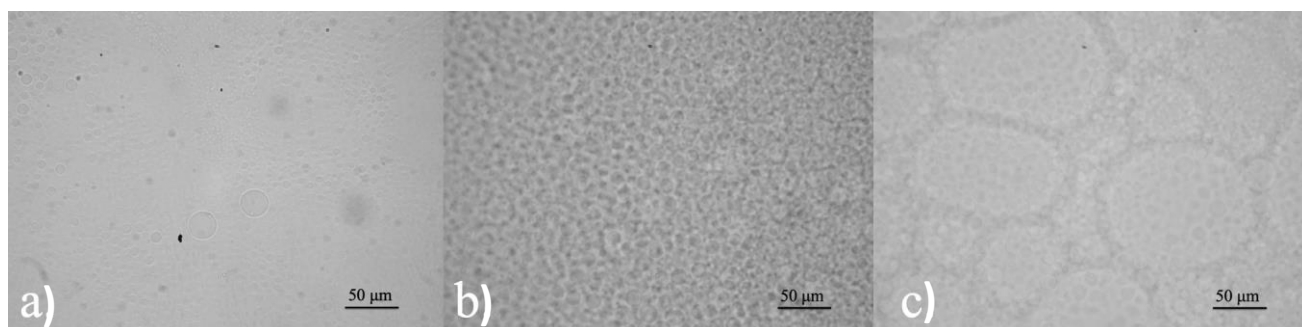


Figure A31. Bright field optical microscopy (50x) of CN water-in-water emulsion with 0.1g/L CM-AHPA in 3:7 wt% PEG: dextran after (a) 1 day; (b) 10 weeks and (c) 16 weeks. Samples were kept under light, at ambient temperature and were undisturbed.

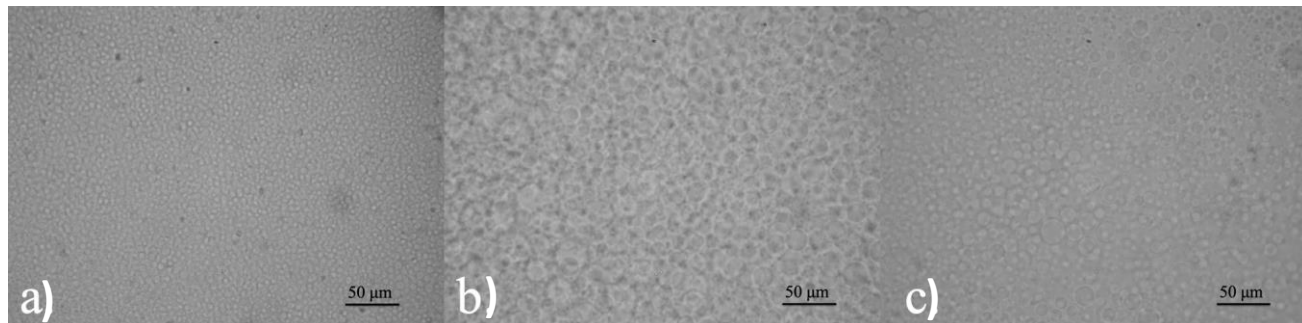


Figure A32. Bright field optical microscopy (50x) of CN water-in-water emulsion with 0.02g/L CM-AHPA in 3:7 wt% PEG: dextran after (a) 1 day; (b) 8 weeks and (c) 14 weeks. Samples were kept under light, at ambient temperature and were undisturbed.

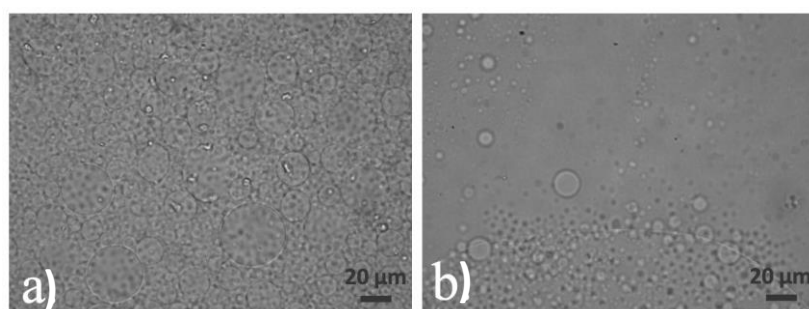


Figure A33. Demulsification of CN stabilized water-in-water Pickering emulsions. (a) control CM-AA 0.1 g/L in 3 wt% PEG_{35K} : 7 wt% Dex_{40K} in deionized water; (b) emulsion with 4 mM SDS added.

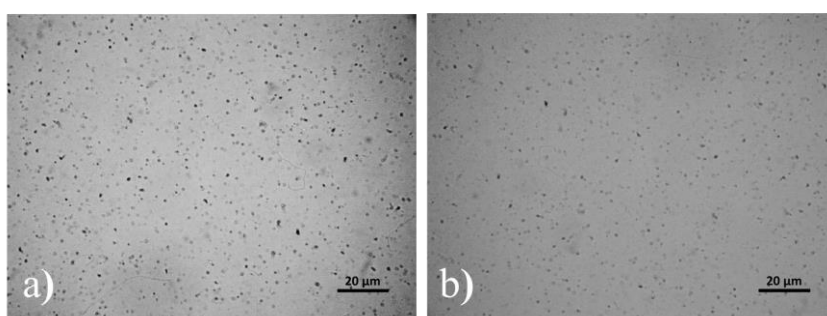


Figure A34. Demulsification of CN stabilized water-in-water Pickering emulsions (CM-AA 0.1 g/L in 3 wt% PEG_{35K} : 7 wt% Dex_{40K}). (a) emulsion with 0.02 mL of 10 mol/L HCl added (b) emulsion with 0.02 mL of 6 mol/L NaOH added.

Chapter 8

8.5. Abbreviations

$^1\text{H-NMR}$	proton nuclear magnetic resonance
$\alpha\text{-CD}$	α -cyclodextrin
AHPA	3-Allyloxy-2-hydroxy-1-propanesulfonic acid sodium salt solution
CLSM	Confocal laser scanning microscopy
CM	Carbon nitride from Cyanuric acid - melamine complex
CM-AHPA	AHPA grafted CM
CMp	Carbon nitride from Cyanuric acid - 2,4-diamino-6-phenyl-1,3,5 triazine complex
CN	Carbon Nitride
CTAB	Cetyltrimethyl ammonium bromide
EDC	1-ethyl-3-(3-dimethylaminopropyl carbodiimide hydrochloride
FITC	fluorescein isothiocyanate
FTIR	fourier transform infrared
DCM	dichloromethane
Dex	dextran
DLS	dynamic light scattering
DMF	N,N-dimethylformamide
DMSO	Dimethyl sulfoxide
GC-MS	gas chromatography-mass spectrometry
g-CN	Graphitic Carbon Nitride
HCl	hydrochloric acid
λ	wavelength
LED	light-emitting diode
MeOH	methanol
M	mol/L
M_n	number-average molar mass
M_w	weight-average molar mass
NaOH	sodium hydroxide
NH ₂ -PEG-NH ₂	poly(ethylene glycol) diamine
OM	optical microscopy
PAA	poly(acrylic acid)
PDP	Poly(dopamine) particles
Đ	Molecular dispersity
PEG	poly(ethylene glycol)
pH	$-\log c(\text{H}^+)$
PSD	pore size distribution
XRD	X-ray diffraction
RT	room temperature
SDS	sodium dodecyl sulfate
SEM	scanning electron microscopy
TEA	triethylamine
TEM	transmission electron microscopy
TGA	thermo gravimetric analysis
THF	tetrahydrofuran
UV	ultra-violet

Chapter 8

UV/Vis

vol %

wt %

ultra-violet/visible

volume %

weight %

8.6. Publication List

1. Supramolecular Compartmentalized Hydrogels via Polydopamine Particle Stabilized Water-in-Water Emulsions

Jianrui Zhang, Baris Kumru, Bernhard V.K.J. Schmidt, *Langmuir* 2019, 35, 34, 11141-11149.

2. Water-in-water Pickering emulsion stabilized by polydopamine particles and crosslinking

Jianrui Zhang, Jongkook Hwang, Markus Antonietti, Bernhard V.K.J. Schmidt, *Biomacromolecules*, 2019, 20(1), 204-211.

3. Facile Fabrication of Cyclodextrin-Modified Magnetic Particles for Effective Demulsification from Various Types of Emulsions

Jianrui Zhang, Yiming Li, Mutai Bao, Xiaolong Yang, Zhining Wang, *Environ. Sci. Technol.* 2016, 50(16), 8809-8816.

4. Cascade Kinetics in an Enzyme-Loaded Aqueous Two-Phase System

Marko Pavlovic, Alexander Plucinski, Jianrui Zhang, Markus Antonietti, Lukas Zeininger, Bernhard V.K.J. Schmidt, *Langmuir* 2020, 36, 6, 1401-1408.

5. Robust Carbon Nitride-Based Thermoset Coatings for Surface Modification and Photochemistry

Baris Kumru, Jesus Barrio, Jianrui Zhang, Markus Antonietti, Menny Shalom, Bernhard V.K.J. Schmidt, *ACS Appl. Mater. Interfaces*, 2019, 11(9), 9462-9469.

6. Highly permeable and stable forward osmosis (FO) membrane based on the incorporation of Al₂O₃ nanoparticles into both substrate and polyamide active layer

Chapter 8

Wande Ding, Yiming Li, Mutai Bao, Jianrui Zhang, Jinren Lu, *RSC Adv*, 2017, 7(64), 40311-40320.

7. The formation process and responsive impacts of single oil droplet in submerged process

Haoshuai Li, Long Meng, Tiantian Shen, Jianrui Zhang, Peiyan Sun, *Mar. Pollut. Bull.*, 2017, 124(1), 139-146.

8. Preparation of Oil-in-Seawater Emulsions Based on Environmentally Benign Nanoparticles and Biosurfactant for Oil Spill Remediation

Guilu Pi, Yiming Li, Mutai Bao, Haiyue Gong, Jianrui Zhang, *ACS Sustainable Chem. Eng.* 2015, 3(11), 2686-2693.

Chapter 8

8.7. Declaration

Die vorliegende Dissertation entstand im Zeitraum zwischen September 2017 und Mai 2020 unter der Betreuung von Prof. Dr. Dr. h.c. Markus Antonietti am Max Planck Institut für Kolloid und Grenzflächenforschung.

Hiermit erkläre ich, dass die vorliegende Arbeit selbständig angefertigt wurde und nur keine anderen als die angegebenen Hilfsmittel und Quellen verwendet wurden.

The present work was carried out and written during September 2017 and May 2020 at the Max Planck Institute of Colloids and Interfaces under the supervision of Prof. Dr. Dr. h.c. Markus Antonietti.

I declare that I have produced all the work using only literature and other aids as described here.

JIANRUI ZHANG,

POTSDAM, MAI 2020

9. References

1. Rosen, M. J.; Kunjappu, J. T., *Surfactants and interfacial phenomena*. John Wiley & Sons: **2012**.
2. Kim, H.-C.; Park, S.-M.; Hinsberg, W. D., Block Copolymer Based Nanostructures: Materials, Processes, and Applications to Electronics. *Chem. Rev.* **2010**, *110* (1), 146-177.
3. Galatsis, K.; Wang, K. L.; Ozkan, M.; Ozkan, C. S.; Huang, Y.; Chang, J. P.; Monbouquette, H. G.; Chen, Y.; Nealey, P.; Botros, Y., Patterning and Templating for Nanoelectronics. *Adv. Mater.* **2010**, *22* (6), 769-778.
4. Bang, J.; Jeong, U.; Ryu, D. Y.; Russell, T. P.; Hawker, C. J., Block Copolymer Nanolithography: Translation of Molecular Level Control to Nanoscale Patterns. *Adv. Mater.* **2009**, *21* (47), 4769-4792.
5. Black, C. T., Polymer Self-Assembly as a Novel Extension to Optical Lithography. *ACS Nano* **2007**, *1* (3), 147-150.
6. Ge, Z.; Xie, D.; Chen, D.; Jiang, X.; Zhang, Y.; Liu, H.; Liu, S., Stimuli-Responsive Double Hydrophilic Block Copolymer Micelles with Switchable Catalytic Activity. *Macromolecules* **2007**, *40* (10), 3538-3546.
7. Gall, B.; Bortenschlager, M.; Nuyken, O.; Weberskirch, R., Cascade Reactions in Polymeric Nanoreactors: Mono (Rh)- and Bimetallic (Rh/Ir) Micellar Catalysis in the Hydroaminomethylation of 1-Octene. *Macromol Chem Phys* **2008**, *209* (11), 1152-1159.
8. Frith, W. J., Mixed biopolymer aqueous solutions – phase behaviour and rheology. *Adv Colloid Interfac* **2010**, *161* (1), 48-60.
9. Nguyen, B. T.; Nicolai, T.; Benyahia, L., Stabilization of Water-in-Water Emulsions by Addition of Protein Particles. *Langmuir* **2013**, *29* (34), 10658-10664.
10. Tromp, R. H.; Vis, M.; Ern , B. H.; Blokhuis, E. M., Composition, concentration and charge profiles of water–water interfaces. *J. Phys.: Condens. Matter* **2014**, *26* (46), 464101.
11. Balakrishnan, G.; Nicolai, T.; Benyahia, L.; Durand, D., Particles Trapped at the Droplet Interface in Water-in-Water Emulsions. *Langmuir* **2012**, *28* (14), 5921-5926.
12. Dewey, D. C.; Strulson, C. A.; Cacace, D. N.; Bevilacqua, P. C.; Keating, C. D., Bioreactor droplets from liposome-stabilized all-aqueous emulsions. *Nat. Commun.* **2014**, *5*, 4670.
13. Firoozmand, H.; Rousseau, D., Tailoring the morphology and rheology of phase-separated biopolymer gels using microbial cells as structure modifiers. *Food Hydrocoll.* **2014**, *42*, 204-214.
14. Hanazawa, T.; Murray, B. S., The influence of oil droplets on the phase separation of protein–polysaccharide mixtures. *Food Hydrocoll.* **2014**, *34*, 128-137.
15. Murray, B. S.; Phisarnchananan, N., The effect of nanoparticles on the phase separation of waxy corn starch+locust bean gum or guar gum. *Food Hydrocoll.* **2014**, *42*, 92-99.
16. Poortinga, A. T., Microcapsules from Self-Assembled Colloidal Particles Using Aqueous Phase-Separated Polymer Solutions. *Langmuir* **2008**, *24* (5), 1644-1647.
17. Buzza, D. M. A.; Fletcher, P. D. I.; Georgiou, T. K.; Ghasdian, N., Water-in-Water Emulsions Based on Incompatible Polymers and Stabilized by Triblock Copolymers–Templated Polymersomes. *Langmuir* **2013**, *29* (48), 14804-14814.
18. Ramsden, W., Separation of solids in the surface-layers of solutions and ‘suspensions’(observations on surface-membranes, bubbles, emulsions, and mechanical coagulation).—Preliminary account. *Proc. R. Soc. London* **1904**, *72* (477-486), 156-164.
19. Pickering, S. U., CXCVI.-Emulsions. *J. Chem. Soc., Dalton Trans.* **1907**, *91* (0), 2001-2021.
20. Ding, P.; Wolf, B.; Frith, W. J.; Clark, A. H.; Norton, I. T.; Patek, A. W., Interfacial Tension in Phase-Separated Gelatin/Dextran Aqueous Mixtures. *J. Colloid Interface Sci.* **2002**, *253* (2), 367-376.
21. Wang, C.; Zhang, G.; Liu, G.; Hu, J.; Liu, S., Photo- and thermo-responsive multicompartment hydrogels for synergistic delivery of gemcitabine and doxorubicin. *J Control Release* **2017**, *259*, 149-159.
22. Shum, H. C.; Weitz, D. A., Multicompartment polymersome gel for encapsulation. *Soft Matter* **2011**, *7* (19), 8762-8765.

Chapter 9

23. Velev, O. D.; Furusawa, K.; Nagayama, K., Assembly of Latex Particles by Using Emulsion Droplets as Templates. 1. Microstructured Hollow Spheres. *Langmuir* **1996**, *12* (10), 2374-2384.
24. Dinsmore, A.; Hsu, M. F.; Nikolaidis, M.; Marquez, M.; Bausch, A.; Weitz, D., Colloidosomes: selectively permeable capsules composed of colloidal particles. *Science* **2002**, *298* (5595), 1006-1009.
25. Croll, L. M.; Stöver, H. D., Formation of Tectocapsules by Assembly and Cross-linking of Poly (divinylbenzene-*a* It-maleic anhydride) Spheres at the Oil– Water Interface. *Langmuir* **2003**, *19* (14), 5918-5922.
26. He, X. D.; Ge, X. W.; Wang, M. Z.; Zhang, Z. C., The preparation of composite microsphere with hollow core/porous shell structure by self-assembling of latex particles at emulsion droplet interface. *J. Colloid Interface Sci.* **2006**, *299* (2), 791-796.
27. Mytnyk, S.; Olive, A. G. L.; Versluis, F.; Poolman, J. M.; Mendes, E.; Eelkema, R.; van Esch, J. H., Compartmentalizing Supramolecular Hydrogels Using Aqueous Multi-phase Systems. *Angew. Chem. Int. Ed.* **2017**, *129* (47), 15119-15123.
28. Hatti-Kaul, R., Aqueous two-phase systems. *Mol. Biotechnol.* **2001**, *19* (3), 269-277.
29. Chao, Y.; Shum, H. C., Emerging aqueous two-phase systems: from fundamentals of interfaces to biomedical applications. *Chem. Soc. Rev.* **2020**, *49* (1), 114-142.
30. Walter, H., *Partitioning in aqueous two-phase system: theory, methods, uses, and applications to biotechnology*. Elsevier: **2012**.
31. Albertsson, P.-Å., Partition of proteins in liquid polymer–polymer two-phase systems. *Nature* **1958**, *182* (4637), 709-711.
32. Hatti-Kaul, R., *Aqueous two-phase systems: methods and protocols*. Springer Science & Business Media: **2000**; Vol. 11.
33. Schmidt, B. V. K. J., Double Hydrophilic Block Copolymer Self-Assembly in Aqueous Solution. *Macromol Chem Phys* **2018**, *219* (7), 1700494.
34. Grilo, A. L.; Raquel Aires-Barros, M.; Azevedo, A. M., Partitioning in Aqueous Two-Phase Systems: Fundamentals, Applications and Trends. *Sep Purif Rev* **2016**, *45* (1), 68-80.
35. Yau, Y. K.; Ooi, C. W.; Ng, E.-P.; Lan, J. C.-W.; Ling, T. C.; Show, P. L., Current applications of different type of aqueous two-phase systems. *Bioresour. Bioprocess.* **2015**, *2* (1), 49.
36. Soares, R. R. G.; Azevedo, A. M.; Van Alstine, J. M.; Aires-Barros, M. R., Partitioning in aqueous two-phase systems: Analysis of strengths, weaknesses, opportunities and threats. *Biotechnol. J.* **2015**, *10* (8), 1158-1169.
37. van Berlo, M.; Luyben, K. C. A. M.; van der Wielen, L. A. M., Poly(ethylene glycol)–salt aqueous two-phase systems with easily recyclable volatile salts. *J. chromatogr., B, Biomed. sci. appl.* **1998**, *711* (1), 61-68.
38. Zafarani-Moattar, M. T.; Hamzehzadeh, S.; Nasiri, S., A new aqueous biphasic system containing polypropylene glycol and a water-miscible ionic liquid. *Biotechnol. Prog.* **2012**, *28* (1), 146-156.
39. Mazzola, P. G.; Lopes, A. M.; Hasmann, F. A.; Jozala, A. F.; Penna, T. C.; Magalhaes, P. O.; Rangel-Yagui, C. O.; Pessoa Jr, A., Liquid–liquid extraction of biomolecules: an overview and update of the main techniques. *J. Chem. Technol. Biotechnol.* **2008**, *83* (2), 143-157.
40. Hernández, L. E.; Rojas-Ojeda, P.; Cooke, D. T.; Carpena-Ruiz, R., Purification of pea nodule symbiosomes using an aqueous polymer two-phase system. *J. chromatogr., B, Biomed. sci. appl.* **1996**, *680* (1), 171-181.
41. Chethana, S.; Nayak, C. A.; Raghavarao, K. S. M. S., Aqueous two phase extraction for purification and concentration of betalains. *J. Food Eng.* **2007**, *81* (4), 679-687.
42. Zettl, R.; Feldwisch, J.; Boland, W.; Schell, J.; Palme, K., 5'-Azido-[3,6-3H₂]-1-naphthylphthalamic acid, a photoactivatable probe for naphthylphthalamic acid receptor proteins from higher plants: identification of a 23-kDa protein from maize coleoptile plasma membranes. *PNAS* **1992**, *89* (2), 480-484.
43. Edahiro, J.-i.; Yamada, M.; Seike, S.; Kakigi, Y.; Miyanaga, K.; Nakamura, M.; Kanamori, T.; Seki, M., Separation of cultured strawberry cells producing anthocyanins in aqueous two-phase system. *J. Biosci. Bioeng.* **2005**, *100* (4), 449-454.

44. Raja, S.; Murty, V. R.; Thivaharan, V.; Rajasekar, V.; Ramesh, V., Aqueous two phase systems for the recovery of biomolecules—a review. *Sci Technol* **2011**, *1* (1), 7-16.
45. Mashayekhi, F.; Meyer, A. S.; Shiigi, S. A.; Nguyen, V.; Kamei, D. T., Concentration of mammalian genomic DNA using two-phase aqueous micellar systems. *Biotechnol Bioeng* **2009**, *102* (6), 1613-1623.
46. Pavlovic, M.; Plucinski, A.; Zhang, J.; Antonietti, M.; Zeininger, L.; Schmidt, B. V. K. J., Cascade Kinetics in an Enzyme-Loaded Aqueous Two-Phase System. *Langmuir* **2020**, *36* (6), 1401-1408.
47. Ao, G.; Streit, J. K.; Fagan, J. A.; Zheng, M., Differentiating Left- and Right-Handed Carbon Nanotubes by DNA. *J. Am. Chem. Soc.* **2016**, *138* (51), 16677-16685.
48. Ao, G.; Khripin, C. Y.; Zheng, M., DNA-Controlled Partition of Carbon Nanotubes in Polymer Aqueous Two-Phase Systems. *J. Am. Chem. Soc.* **2014**, *136* (29), 10383-10392.
49. Hamta, A.; Dehghani, M. R., Application of polyethylene glycol based aqueous two-phase systems for extraction of heavy metals. *J. Mol. Liq.* **2017**, *231*, 20-24.
50. Ruiz-Ruiz, F.; Benavides, J.; Aguilar, O.; Rito-Palomares, M., Aqueous two-phase affinity partitioning systems: Current applications and trends. *J. Chromatogr. A* **2012**, *1244*, 1-13.
51. Molino, J. V. D.; Viana Marques, D. d. A.; Júnior, A. P.; Mazzola, P. G.; Gatti, M. S. V., Different types of aqueous two-phase systems for biomolecule and bioparticle extraction and purification. *Biotechnol. Prog.* **2013**, *29* (6), 1343-1353.
52. Xiao, J.-X.; Sivars, U.; Tjerneld, F., Phase behavior and protein partitioning in aqueous two-phase systems of cationic–anionic surfactant mixtures. *J. chromatogr., B, Biomed. sci. appl.* **2000**, *743* (1), 327-338.
53. Albertsson, P. Å., Fractionation of particles and macromolecules in aqueous two-phase systems. *Biochem. Pharmacol.* **1961**, *5* (4), 351-358.
54. Louwrier, A., Model Phase Separations of Proteins Using Aqueous/Ethanol Components. *Biotechnol. Tech.* **1998**, *12* (5), 363-365.
55. Jiang, B.; Li, Z.-G.; Dai, J.-Y.; Zhang, D.-J.; Xiu, Z.-L., Aqueous two-phase extraction of 2,3-butanediol from fermentation broths using an ethanol/phosphate system. *Process Biochem.* **2009**, *44* (1), 112-117.
56. Bordier, C., Phase separation of integral membrane proteins in Triton X-114 solution. *J Biol Chem* **1981**, *256* (4), 1604-1607.
57. Lye, G. J.; Asenjo, J. A.; Pyle, D. L., Extraction of lysozyme and ribonuclease-a using reverse micelles: Limits to protein solubilization. *Biotechnology and Bioengineering* **1995**, *47* (5), 509-519.
58. Berthod, A.; Ruiz-Ángel, M. J.; Carda-Broch, S., Ionic liquids in separation techniques. *J. Chromatogr. A* **2008**, *1184* (1), 6-18.
59. Johansson, H.-O.; Persson, J.; Tjerneld, F., Thermoseparating water/polymer system: A novel one-polymer aqueous two-phase system for protein purification. *Biotechnol Bioeng* **1999**, *66* (4), 247-257.
60. Chen, J.-P.; Lee, M.-S., Enhanced production of *Serratia marcescens* chitinase in PEG/dextran aqueous two-phase systems. *Enzyme Microb Tech* **1995**, *17* (11), 1021-1027.
61. Benavides, J.; Rito-Palomares, M., Simplified two-stage method to B-phycoerythrin recovery from *Porphyridium cruentum*. *J. Chromatogr. B* **2006**, *844* (1), 39-44.
62. Liu, C.-I.; Kamei, D. T.; King, J. A.; Wang, D. I. C.; Blankschtein, D., Separation of proteins and viruses using two-phase aqueous micellar systems. *J. chromatogr., B, Biomed. sci. appl.* **1998**, *711* (1), 127-138.
63. Shu, Y.; Gao, M.; Wang, X.; Song, R.; Lu, J.; Chen, X., Separation of curcuminoids using ionic liquid based aqueous two-phase system coupled with in situ dispersive liquid–liquid microextraction. *Talanta* **2016**, *149*, 6-12.
64. Tomotika, S.; Taylor, G. I., On the instability of a cylindrical thread of a viscous liquid surrounded by another viscous fluid. *Proceedings of the Royal Society of London. Series A - Mathematical and Physical Sciences* **1935**, *150* (870), 322-337.
65. Guillot, P.; Colin, A.; Utada, A. S.; Ajdari, A., Stability of a Jet in Confined Pressure-Driven Biphasic Flows at Low Reynolds Numbers. *Phys. Rev. Lett.* **2007**, *99* (10), 104502.

Chapter 9

66. Fragkopoulos, A. A.; Ellis, P. W.; Fernandez-Nieves, A., Teaching Rayleigh–Plateau instabilities in the laboratory. *Eur. J. Phys.* **2015**, *36* (5), 055023.
67. Shum, H. C.; Varnell, J.; Weitz, D. A., Microfluidic fabrication of water-in-water (w/w) jets and emulsions. *Biomicrofluidics* **2012**, *6* (1), 012808.
68. Geschiere, S. D.; Ziemecka, I.; Steijn, V. v.; Koper, G. J. M.; Esch, J. H. v.; Kreutzer, M. T., Slow growth of the Rayleigh-Plateau instability in aqueous two phase systems. *Biomicrofluidics* **2012**, *6* (2), 022007.
69. Shang, L.; Cheng, Y.; Zhao, Y., Emerging Droplet Microfluidics. *Chem. Rev.* **2017**, *117* (12), 7964-8040.
70. Perazzo, A.; Nunes, J. K.; Guido, S.; Stone, H. A., Flow-induced gelation of microfiber suspensions. *PNAS* **2017**, *114* (41), E8557-E8564.
71. Yu, Y.; Shang, L.; Guo, J.; Wang, J.; Zhao, Y., Design of capillary microfluidics for spinning cell-laden microfibers. *Nat. Protoc.* **2018**, *1*.
72. Mak, S. Y.; Chao, Y.; Shum, H. C., The dripping-to-jetting transition in a co-axial flow of aqueous two-phase systems with low interfacial tension. *RSC Adv.* **2017**, *7* (6), 3287-3292.
73. Asenjo, J. A.; Andrews, B. A., Aqueous two-phase systems for protein separation: A perspective. *J. Chromatogr. A* **2011**, *1218* (49), 8826-8835.
74. Andrews, B. A.; Schmidt, A. S.; Asenjo, J. A., Correlation for the partition behavior of proteins in aqueous two-phase systems: Effect of surface hydrophobicity and charge. *Biotechnol Bioeng* **2005**, *90* (3), 380-390.
75. Andrews, B. A.; Asenjo, J. A., Theoretical and Experimental Evaluation of Hydrophobicity of Proteins to Predict their Partitioning Behavior in Aqueous Two Phase Systems: A Review. *Sep Sci Technol* **2010**, *45* (15), 2165-2170.
76. Cote, J.; Sson, O., Effects of salts on the partition of proteins in aqueous polymeric biphasic systems. *Acta Chem. Scand. B* **1974**, *28* (873), 82.
77. Raja, S.; Murty, V. R.; Thivaharan, V.; Rajasekar, V.; Ramesh, V., Aqueous two phase systems for the recovery of biomolecules-a review. *Science and Technology* **2011**, *1* (1), 7-16.
78. Olivera-Nappa, A.; Lagomarsino, G.; Andrews, B. A.; Asenjo, J. A., Effect of electrostatic energy on partitioning of proteins in aqueous two-phase systems. *J. Chromatogr. B* **2004**, *807* (1), 81-86.
79. Pavlovic, M.; Antonietti, M.; Schmidt, B. V. K. J.; Zeininger, L., Responsive Janus and Cerberus emulsions via temperature-induced phase separation in aqueous polymer mixtures. *Colloid Interface Sci.* **2020**, *575*, 88-95.
80. Abelson, J. N.; Simon, M. I., *Aqueous two-phase systems*. Elsevier: **1994**; Vol. 228.
81. Emi, S.; Yasuhiko, I.; Kazunari, A.; Shohei, K., Platelet Separation From Whole Blood in an Aqueous Two-Phase System With Water-Soluble Polymers. *J. Pharmacol. Sci.* **2006**, *101* (1), 91-97.
82. Aguilar, O.; Rito-Palomares, M., Aqueous two-phase systems strategies for the recovery and characterization of biological products from plants. *J. Sci. Food Agric.* **2010**, *90* (9), 1385-1392.
83. Toner, M.; Irimia, D., Blood-on-a-Chip. *Annu. Rev. Biomed. Eng.* **2005**, *7* (1), 77-103.
84. SooHoo, J. R.; Walker, G. M., Microfluidic aqueous two phase system for leukocyte concentration from whole blood. *Biomed. Microdevices* **2009**, *11* (2), 323-329.
85. Shin, H.; Han, C.; Labuz, J. M.; Kim, J.; Kim, J.; Cho, S.; Gho, Y. S.; Takayama, S.; Park, J., High-yield isolation of extracellular vesicles using aqueous two-phase system. *Sci. Rep.* **2015**, *5* (1), 13103.
86. Zhang, D.-Y.; Zu, Y.-G.; Fu, Y.-J.; Wang, W.; Zhang, L.; Luo, M.; Mu, F.-S.; Yao, X.-H.; Duan, M.-H., Aqueous two-phase extraction and enrichment of two main flavonoids from pigeon pea roots and the antioxidant activity. *Sep. Purif. Technol.* **2013**, *102*, 26-33.
87. Wu, X.; Liang, L.; Zou, Y.; Zhao, T.; Zhao, J.; Li, F.; Yang, L., Aqueous two-phase extraction, identification and antioxidant activity of anthocyanins from mulberry (*Morus atropurpurea* Roxb.). *Food Chem.* **2011**, *129* (2), 443-453.
88. Montalvo-Hernández, B.; Rito-Palomares, M.; Benavides, J., Recovery of crocins from saffron stigmas (*Crocus sativus*) in aqueous two-phase systems. *J. Chromatogr. A* **2012**, *1236*, 7-15.
89. Chandrasekhar, J.; Madhusudhan, M. C.; Raghavarao, K. S. M. S., Extraction of anthocyanins from red cabbage and purification using adsorption. *Food Bioprod Process* **2012**, *90* (4), 615-623.

90. Li, C.-X.; Han, J.; Wang, Y.; Yan, Y.-S.; Xu, X.-H.; Pan, J.-M., Extraction and mechanism investigation of trace roxithromycin in real water samples by use of ionic liquid–salt aqueous two-phase system. *Anal. Chim. Acta* **2009**, *653* (2), 178-183.
91. Han, J.; Wang, Y.; Yu, C.-l.; Yan, Y.-s.; Xie, X.-q., Extraction and determination of chloramphenicol in feed water, milk, and honey samples using an ionic liquid/sodium citrate aqueous two-phase system coupled with high-performance liquid chromatography. *Anal. Bioanal. Chem.* **2011**, *399* (3), 1295-1304.
92. Cha, K.-M.; Lee, E.-S.; Kim, I.-W.; Cho, H.-K.; Ryu, J.-H.; Kim, S.-K., Canola oil is an excellent vehicle for eliminating pesticide residues in aqueous ginseng extract. *Journal of Ginseng Research* **2016**, *40* (3), 292-299.
93. Yang, X.; Yu, R.; Zhang, S.; Cao, B.; Liu, Z.; Lei, L.; Li, N.; Wang, Z.; Zhang, L.; Zhang, H.; Chen, Y., Aqueous two-phase extraction for determination of triazine herbicides in milk by high-performance liquid chromatography. *J. Chromatogr. B* **2014**, *972*, 111-116.
94. Ferreira, A. M.; Coutinho, J. A. P.; Fernandes, A. M.; Freire, M. G., Complete removal of textile dyes from aqueous media using ionic-liquid-based aqueous two-phase systems. *Sep. Purif. Technol.* **2014**, *128*, 58-66.
95. Robinson, T.; McMullan, G.; Marchant, R.; Nigam, P., Remediation of dyes in textile effluent: a critical review on current treatment technologies with a proposed alternative. *Bioresour. Technol.* **2001**, *77* (3), 247-255.
96. Mageste, A. B.; de Lemos, L. R.; Ferreira, G. M. D.; da Silva, M. d. C. H.; da Silva, L. H. M.; Bonomo, R. C. F.; Minim, L. A., Aqueous two-phase systems: An efficient, environmentally safe and economically viable method for purification of natural dye carmine. *J. Chromatogr. A* **2009**, *1216* (45), 7623-7629.
97. Ivetic, D. Z.; Sciban, M. B.; Vasic, V. M.; Kukic, D. V.; Prodanovic, J. M.; Antov, M. G., Evaluation of possibility of textile dye removal from wastewater by aqueous two-phase extraction. *Desalin Water Treat* **2013**, *51* (7-9), 1603-1608.
98. Rogers, R. D.; Griffin, S. T., Partitioning of mercury in aqueous biphasic systems and on ABEC™ resins. *J. chromatogr., B, Biomed. sci. appl.* **1998**, *711* (1), 277-283.
99. Raghavarao, K.; Ranganathan, T.; Srinivas, N.; Barhate, R., Aqueous two phase extraction-an environmentally benign technique. *Clean technologies and environmental policy* **2003**, *5* (2), 136-141.
100. Kang, C. H.; Sandler, S. I., Phase behavior of aqueous two-polymer systems. *Fluid Phase Equilib.* **1987**, *38* (3), 245-272.
101. Grinberg, V. Y.; Tolstoguzov, V. B., Thermodynamic incompatibility of proteins and polysaccharides in solutions. *Food Hydrocoll.* **1997**, *11* (2), 145-158.
102. Norton, I. T.; Frith, W. J., Microstructure design in mixed biopolymer composites. *Food Hydrocoll.* **2001**, *15* (4), 543-553.
103. Atefi, E.; Fyffe, D.; Kaylan, K. B.; Tavana, H., Characterization of Aqueous Two-Phase Systems from Volume and Density Measurements. *J. Chem. Eng. Data* **2016**, *61* (4), 1531-1539.
104. Scholten, E.; Visser, J. E.; Sagis, L. M. C.; Van Der Linden, E., Ultralow Interfacial Tensions in an Aqueous Phase-Separated Gelatin/Dextran and Gelatin/Gum Arabic System: A Comparison. *Langmuir* **2004**, *20* (6), 2292-2297.
105. Antonov, Y. A.; Van Puyvelde, P.; Moldenaers, P., Interfacial tension of aqueous biopolymer mixtures close to the critical point. *Int. J. Biol. Macromol.* **2004**, *34* (1), 29-35.
106. Ryden, J.; Albertsson, P.-a., Interfacial tension of dextran—polyethylene glycol—water two—phase systems. *J. Colloid Interface Sci.* **1971**, *37* (1), 219-222.
107. Forciniti, D.; Hall, C. K.; Kula, M. R., Interfacial tension of polyethyleneglycol-dextran-water systems: influence of temperature and polymer molecular weight. *J. Biotechnol.* **1990**, *16* (3), 279-296.
108. Vis, M.; Peters, V. F. D.; Blokhuis, E. M.; Lekkerkerker, H. N. W.; Ern , B. H.; Tromp, R. H., Decreased Interfacial Tension of Demixed Aqueous Polymer Solutions due to Charge. *Phys. Rev. Lett.* **2015**, *115* (7), 078303.

109. Vis, M.; Peters, V. F. D.; Blokhuis, E. M.; Lekkerkerker, H. N. W.; Ern , B. H.; Tromp, R. H., Effects of Electric Charge on the Interfacial Tension between Coexisting Aqueous Mixtures of Polyelectrolyte and Neutral Polymer. *Macromolecules* **2015**, *48* (19), 7335-7345.
110. Nguyen, B. T.; Wang, W.; Saunders, B. R.; Benyahia, L.; Nicolai, T., pH-Responsive Water-in-Water Pickering Emulsions. *Langmuir* **2015**, *31* (12), 3605-3611.
111. Firoozmand, H.; Murray, B. S.; Dickinson, E., Interfacial Structuring in a Phase-Separating Mixed Biopolymer Solution Containing Colloidal Particles. *Langmuir* **2009**, *25* (3), 1300-1305.
112. Aveyard, R.; Binks, B. P.; Clint, J. H., Emulsions stabilised solely by colloidal particles. *Adv. Colloid Interface Sci.* **2003**, *100-102*, 503-546.
113. de Freitas, R. A.; Nicolai, T.; Chassenieux, C.; Benyahia, L., Stabilization of Water-in-Water Emulsions by Polysaccharide-Coated Protein Particles. *Langmuir* **2016**, *32* (5), 1227-1232.
114. Nicolai, T.; Murray, B., Particle stabilized water in water emulsions. *Food Hydrocoll.* **2017**, *68*, 157-163.
115. Stokes, J. R.; Wolf, B.; Frith, W. J., Phase-separated biopolymer mixture rheology: Prediction using a viscoelastic emulsion model. *J. Rheol.* **2001**, *45* (5), 1173-1191.
116. Spyropoulos, F.; Frith, W. J.; Norton, I. T.; Wolf, B.; Pacek, A. W., Sheared aqueous two-phase biopolymer–surfactant mixtures. *Food Hydrocoll.* **2008**, *22* (1), 121-129.
117. Wolf, B.; Frith, W. J.; Norton, I. T., Influence of gelation on particle shape in sheared biopolymer blends. *J. Rheol.* **2001**, *45* (5), 1141-1158.
118. Shewan, H. M.; Stokes, J. R., Review of techniques to manufacture micro-hydrogel particles for the food industry and their applications. *J. Food Eng.* **2013**, *119* (4), 781-792.
119. Butler, M. F.; Heppenstall-Butler, M., Phase separation in gelatin/dextran and gelatin/maltodextrin mixtures. *Food Hydrocoll.* **2003**, *17* (6), 815-830.
120. Wolf, B.; Scirocco, R.; Frith, W. J.; Norton, I. T., Shear-induced anisotropic microstructure in phase-separated biopolymer mixtures. *Food Hydrocoll.* **2000**, *14* (3), 217-225.
121. Turgeon, S. L.; Schmitt, C.; Sanchez, C., Protein–polysaccharide complexes and coacervates. *Curr. Opin. Colloid Interface Sci.* **2007**, *12* (4), 166-178.
122. Oh, J. K.; Drumright, R.; Siegwart, D. J.; Matyjaszewski, K., The development of microgels/nanogels for drug delivery applications. *Prog. Polym. Sci.* **2008**, *33* (4), 448-477.
123. Song, Y. P., Laguerre isoparametric hypersurfaces in R^n with two distinct non-zero principal curvatures. *Acta Math. Sin., Engl. Series* **2013**, *29* (1), 1-12.
124. Moon, B.-U.; Abbasi, N.; Jones, S. G.; Hwang, D. K.; Tsai, S. S. H., Water-in-Water Droplets by Passive Microfluidic Flow Focusing. *Anal. Chem.* **2016**, *88* (7), 3982-3989.
125. Binks, B. P., Particles as surfactants—similarities and differences. *Curr. Opin. Colloid Interface Sci.* **2002**, *7* (1), 21-41.
126. Binks, B. P.; Horozov, T. S., *Colloidal particles at liquid interfaces*. Cambridge University Press: **2006**.
127. Ku, K. H.; Lee, Y. J.; Yi, G.-R.; Jang, S. G.; Schmidt, B. V. K. J.; Liao, K.; Klinger, D.; Hawker, C. J.; Kim, B. J., Shape-Tunable Biphasic Janus Particles as pH-Responsive Switchable Surfactants. *Macromolecules* **2017**, *50* (23), 9276-9285.
128. Pickering, S. U., Cxcvii.—emulsions. *Journal of the Chemical Society, Transactions* **1907**, *91*, 2001-2021.
129. Adams, F.; Walstra, P.; Brooks, B.; Richmond, H.; Zerfa, M.; Bibette, J.; Hibberd, D.; Robins, M.; Weers, J.; Kabalnov, A., *Modern aspects of emulsion science*. Royal Society of Chemistry: **2007**.
130. Levine, S.; Bowen, B. D.; Partridge, S. J., Stabilization of emulsions by fine particles I. Partitioning of particles between continuous phase and oil/water interface. *Colloids Surf.* **1989**, *38* (2), 325-343.
131. Becher, P., *Encyclopedia of emulsion technology*. Marcel Dekker New York: **1983**; Vol. 1.
132. Binks, B. P.; Lumsdon, S. O., Influence of Particle Wettability on the Type and Stability of Surfactant-Free Emulsions. *Langmuir* **2000**, *16* (23), 8622-8631.
133. Levine, S.; Sanford, E., Stabilisation of emulsion droplets by fine powders. *The Canadian Journal of Chemical Engineering* **1985**, *63* (2), 258-268.

134. Abend, S.; Lagaly, G., Bentonite and double hydroxides as emulsifying agents. *Clay Miner.* **2001**, *36* (4), 557-570.
135. Ashby, N. P.; Binks, B. P., Pickering emulsions stabilised by Laponite clay particles. *Phys. Chem. Chem. Phys.* **2000**, *2* (24), 5640-5646.
136. Schlaepfer, A. U. M., XLIII. Water-in-oil emulsions. *Journal of the Chemical Society, Transactions* **1918**, *113*, 522-526.
137. Moore, W. C., Emulsification Of Water And Of Ammonium Chloride Solutions By Means Of Lamp Black. *J. Am. Chem. Soc.* **1919**, *41* (6), 940-946.
138. Gelot, A.; Friesen, W.; Hamza, H. A., Emulsification of oil and water in the presence of finely divided solids and surface-active agents. *Colloids Surf.* **1984**, *12*, 271-303.
139. Binks, B. P.; Lumsdon, S. O., Pickering Emulsions Stabilized by Monodisperse Latex Particles: Effects of Particle Size. *Langmuir* **2001**, *17* (15), 4540-4547.
140. Dinsmore, A. D.; Hsu, M. F.; Nikolaidis, M. G.; Marquez, M.; Bausch, A. R.; Weitz, D. A., Colloidosomes: Selectively Permeable Capsules Composed of Colloidal Particles. *Science* **2002**, *298* (5595), 1006-1009.
141. Amalvy, J. I.; Armes, S. P.; Binks, B. P.; Rodrigues, J. A.; Unali, G. F., Use of sterically-stabilised polystyrene latex particles as a pH-responsive particulate emulsifier to prepare surfactant-free oil-in-water emulsions. *Chem. Commun. (Cambridge, U. K.)* **2003**, (15), 1826-1827.
142. Amalvy, J. I.; Unali, G. F.; Li, Y.; Granger-Bevan, S.; Armes, S. P.; Binks, B. P.; Rodrigues, J. A.; Whitby, C. P., Synthesis of Sterically Stabilized Polystyrene Latex Particles Using Cationic Block Copolymers and Macromonomers and Their Application as Stimulus-Responsive Particulate Emulsifiers for Oil-in-Water Emulsions. *Langmuir* **2004**, *20* (11), 4345-4354.
143. Melle, S.; Lask, M.; Fuller, G. G., Pickering Emulsions with Controllable Stability. *Langmuir* **2005**, *21* (6), 2158-2162.
144. Zhou, J.; Qiao, X.; Binks, B. P.; Sun, K.; Bai, M.; Li, Y.; Liu, Y., Magnetic Pickering Emulsions Stabilized by Fe₃O₄ Nanoparticles. *Langmuir* **2011**, *27* (7), 3308-3316.
145. Wang, H.; Hobbie, E. K., Amphiphobic Carbon Nanotubes as Macroemulsion Surfactants. *Langmuir* **2003**, *19* (8), 3091-3093.
146. Laredj-Bourezg, F.; Chevalier, Y.; Boyron, O.; Bolzinger, M.-A., Emulsions stabilized with organic solid particles. *Colloid Surface A* **2012**, *413*, 252-259.
147. Schelero, N.; Lichtenfeld, H.; Zastrow, H.; Möhwald, H.; Dubois, M.; Zemb, T., Single particle light scattering method for studying aging properties of Pickering emulsions stabilized by catanionic crystals. *Colloid Surface A* **2009**, *337* (1), 146-153.
148. Binks, B. P.; Clint, J. H.; Mackenzie, G.; Simcock, C.; Whitby, C. P., Naturally Occurring Spore Particles at Planar Fluid Interfaces and in Emulsions. *Langmuir* **2005**, *21* (18), 8161-8167.
149. Dorobantu, L. S.; Yeung, A. K. C.; Foght, J. M.; Gray, M. R., Stabilization of Oil-Water Emulsions by Hydrophobic Bacteria. *Appl. Environ. Microbiol.* **2004**, *70* (10), 6333-6336.
150. Wongkongkatep, P.; Manopwisedjaroen, K.; Tiposoth, P.; Archakunakorn, S.; Pongtharangkul, T.; Suphantharika, M.; Honda, K.; Hamachi, I.; Wongkongkatep, J., Bacteria Interface Pickering Emulsions Stabilized by Self-assembled Bacteria-Chitosan Network. *Langmuir* **2012**, *28* (13), 5729-5736.
151. Ngai, T.; Behrens, S. H.; Auweter, H., Novel emulsions stabilized by pH and temperature sensitive microgels. *Chem. Commun. (Cambridge, U. K.)* **2005**, (3), 331-333.
152. Brugger, B.; Richtering, W., Magnetic, Thermosensitive Microgels as Stimuli-Responsive Emulsifiers Allowing for Remote Control of Separability and Stability of Oil in Water-Emulsions. *Adv. Mater.* **2007**, *19* (19), 2973-2978.
153. Tsuji, S.; Kawaguchi, H., Thermosensitive Pickering Emulsion Stabilized by Poly(N-isopropylacrylamide)-Carrying Particles. *Langmuir* **2008**, *24* (7), 3300-3305.
154. Destribats, M.; Lapeyre, V.; Sellier, E.; Leal-Calderon, F.; Ravaine, V.; Schmitt, V., Origin and Control of Adhesion between Emulsion Drops Stabilized by Thermally Sensitive Soft Colloidal Particles. *Langmuir* **2012**, *28* (8), 3744-3755.

155. Fujii, S.; Read, E. S.; Binks, B. P.; Armes, S. P., Stimulus-Responsive Emulsifiers Based on Nanocomposite Microgel Particles. *Adv. Mater.* **2005**, *17* (8), 1014-1018.
156. Gautier, F.; Destribats, M.; Perrier-Cornet, R.; Dechézelles, J.-F.; Giermanska, J.; Héroguez, V.; Ravaine, S.; Leal-Calderon, F.; Schmitt, V., Pickering emulsions with stimuable particles: from highly- to weakly-covered interfaces. *Phys. Chem. Chem. Phys.* **2007**, *9* (48), 6455-6462.
157. Fujii, S.; Aichi, A.; Muraoka, M.; Kishimoto, N.; Iwahori, K.; Nakamura, Y.; Yamashita, I., Ferritin as a bionano-particulate emulsifier. *J. Colloid Interface Sci.* **2009**, *338* (1), 222-228.
158. van Rijn, P.; Mougin, N. C.; Franke, D.; Park, H.; Böker, A., Pickering emulsion templated soft capsules by self-assembling cross-linkable ferritin–polymer conjugates. *Chem. Commun. (Cambridge, U. K.)* **2011**, *47* (29), 8376-8378.
159. Leunissen, M. E.; van Blaaderen, A.; Hollingsworth, A. D.; Sullivan, M. T.; Chaikin, P. M., Electrostatics at the oil–water interface, stability, and order in emulsions and colloids. *PNAS* **2007**, *104* (8), 2585-2590.
160. Wang, H.; Singh, V.; Behrens, S. H., Image Charge Effects on the Formation of Pickering Emulsions. *J. Phys. Chem. Lett.* **2012**, *3* (20), 2986-2990.
161. Wiley, R. M., Limited coalescence of oil droplets in coarse oil-in-water emulsions. *J. Colloid Sci.* **1954**, *9* (5), 427-437.
162. Arditty, S.; Whitby, C. P.; Binks, B. P.; Schmitt, V.; Leal-Calderon, F., Some general features of limited coalescence in solid-stabilized emulsions. *Eur. Phys. J. E* **2003**, *12* (2), 355.
163. Frelichowska, J.; Bolzinger, M.-A.; Chevalier, Y., Effects of solid particle content on properties of o/w Pickering emulsions. *J. Colloid Interface Sci.* **2010**, *351* (2), 348-356.
164. Arditty, S.; Schmitt, V.; Giermanska-Kahn, J.; Leal-Calderon, F., Materials based on solid-stabilized emulsions. *J. Colloid Interface Sci.* **2004**, *275* (2), 659-664.
165. Arditty, S.; Schmitt, V.; Lequeux, F.; Leal-Calderon, F., Interfacial properties in solid-stabilized emulsions. *Eur. Phys. J. B* **2005**, *44* (3), 381-393.
166. Horozov, T. S.; Binks, B. P., Particle-Stabilized Emulsions: A Bilayer or a Bridging Monolayer? *Angew. Chem. Int. Ed.* **2006**, *45* (5), 773-776.
167. Destribats, M.; Ravaine, S.; Heroguez, V.; Leal-Calderon, F.; Schmitt, V. In *Outstanding Stability of Poorly-protected Pickering Emulsions*, Berlin, Heidelberg, Springer Berlin Heidelberg: Berlin, Heidelberg, **2010**; 13-18.
168. Qiao, X.; Zhou, J.; Binks, B. P.; Gong, X.; Sun, K., Magnetorheological behavior of Pickering emulsions stabilized by surface-modified Fe₃O₄ nanoparticles. *Colloid Surface A* **2012**, *412*, 20-28.
169. Binks, B. P.; Whitby, C. P., Silica Particle-Stabilized Emulsions of Silicone Oil and Water: Aspects of Emulsification. *Langmuir* **2004**, *20* (4), 1130-1137.
170. Kruglyakov, P. M., *Hydrophile-lipophile balance of surfactants and solid particles: physicochemical aspects and applications*. Elsevier: **2000**; Vol. 9.
171. Kruglyakov, P. M.; Nushtayeva, A. V., Phase inversion in emulsions stabilised by solid particles. *Adv. Colloid Interface Sci.* **2004**, *108-109*, 151-158.
172. Binks, B. P.; Lumsdon, S. O., Catastrophic Phase Inversion of Water-in-Oil Emulsions Stabilized by Hydrophobic Silica. *Langmuir* **2000**, *16* (6), 2539-2547.
173. Binks, B. P.; Rodrigues, J. A., Types of Phase Inversion of Silica Particle Stabilized Emulsions Containing Triglyceride Oil. *Langmuir* **2003**, *19* (12), 4905-4912.
174. Binks, B. P.; Lumsdon, S. O., Effects of oil type and aqueous phase composition on oil–water mixtures containing particles of intermediate hydrophobicity. *Phys. Chem. Chem. Phys.* **2000**, *2* (13), 2959-2967.
175. Vis, M.; Opdam, J.; van 't Oor, I. S. J.; Soligno, G.; van Roij, R.; Tromp, R. H.; Ern , B. H., Water-in-Water Emulsions Stabilized by Nanoplates. *ACS Macro Lett.* **2015**, *4* (9), 965-968.
176. Midmore, B., Effect of aqueous phase composition on the properties of a silica-stabilized W/O emulsion. *J. Colloid Interface Sci.* **1999**, *213* (2), 352-359.
177. Binks, B.; Lumsdon, S., Catastrophic phase inversion of water-in-oil emulsions stabilized by hydrophobic silica. *Langmuir* **2000**, *16* (6), 2539-2547.

178. Zhang, J.; Li, Y.; Bao, M.; Yang, X.; Wang, Z., Facile fabrication of cyclodextrin-modified magnetic particles for effective demulsification from various types of emulsions. *Environ. Sci. Technol.* **2016**, *50* (16), 8809-8816.
179. Elanchezhiyan, S. S. D.; Meenakshi, S., Facile Fabrication of Metal Ions - Incorporated Chitosan/ β -Cyclodextrin Composites for Effective Removal of Oil from Oily Wastewater. *ChemistrySelect* **2017**, *2* (35), 11393-11401.
180. Al Nakeeb, N.; Kochovski, Z.; Li, T.; Zhang, Y.; Lu, Y.; Schmidt, B. V. K. J., Poly(ethylene glycol) brush-b-poly(N-vinylpyrrolidone)-based double hydrophilic block copolymer particles crosslinked via crystalline α -cyclodextrin domains. *RSC Adv.* **2019**, *9* (9), 4993-5001.
181. Huh, K. M.; Ooya, T.; Lee, W. K.; Sasaki, S.; Kwon, I. C.; Jeong, S. Y.; Yui, N. J. M., Supramolecular-structured hydrogels showing a reversible phase transition by inclusion complexation between poly(ethylene glycol) grafted dextran and α -cyclodextrin. *Macromolecules* **2001**, *34* (25), 8657-8662.
182. Li, T.; Kumru, B.; Al Nakeeb, N.; Willersinn, J.; Schmidt, B. J. P., Thermoadaptive Supramolecular α -Cyclodextrin Crystallization-Based Hydrogels via Double Hydrophilic Block Copolymer Templating. *Polymers* **2018**, *10* (6), 576.
183. Harada, A.; Li, J.; Kamachi, M., Preparation and properties of inclusion complexes of polyethylene glycol with α -cyclodextrin. *Macromolecules* **1993**, *26* (21), 5698-5703.
184. Mace, C. R.; Akbulut, O.; Kumar, A. A.; Shapiro, N. D.; Derda, R.; Patton, M. R.; Whitesides, G. M., Aqueous Multiphase Systems of Polymers and Surfactants Provide Self-Assembling Step-Gradients in Density. *J. Am. Chem. Soc.* **2012**, *134* (22), 9094-9097.
185. Dimova, R.; Lipowsky, R., Lipid membranes in contact with aqueous phases of polymer solutions. *Soft Matter* **2012**, *8* (24), 6409-6415.
186. Zhang, J.; Hwang, J.; Antonietti, M.; Schmidt, B. V. K. J., Water-in-Water Pickering Emulsion Stabilized by Polydopamine Particles and Cross-Linking. *Biomacromolecules* **2019**, *20* (1), 204-211.
187. Shalom, M.; Inal, S.; Fetteshauer, C.; Neher, D.; Antonietti, M., Improving Carbon Nitride Photocatalysis by Supramolecular Preorganization of Monomers. *J. Am. Chem. Soc.* **2013**, *135* (19), 7118-7121.
188. Cui, Q.; Xu, J.; Wang, X.; Li, L.; Antonietti, M.; Shalom, M., Phenyl-Modified Carbon Nitride Quantum Dots with Distinct Photoluminescence Behavior. *Angew. Chem. Int. Ed.* **2016**, *55* (11), 3672-3676.
189. Kumru, B.; Antonietti, M.; Schmidt, B. V. K. J., Enhanced Dispersibility of Graphitic Carbon Nitride Particles in Aqueous and Organic Media via a One-Pot Grafting Approach. *Langmuir* **2017**, *33* (38), 9897-9906.
190. Kumru, B.; Cruz, D.; Heil, T.; Schmidt, B. V. K. J.; Antonietti, M., Electrostatic Stabilization of Carbon Nitride Colloids in Organic Solvents Enables Stable Dispersions and Transparent Homogeneous CN Films for Optoelectronics. *J. Am. Chem. Soc.* **2018**, *140* (50), 17532-17537.
191. Xu, J.; Antonietti, M., The Performance of Nanoparticulate Graphitic Carbon Nitride as an Amphiphile. *J. Am. Chem. Soc.* **2017**, *139* (17), 6026-6029.
192. Cao, Q.; Heil, T.; Kumru, B.; Antonietti, M.; Schmidt, B. V. K. J., Visible-light induced emulsion photopolymerization with carbon nitride as a stabilizer and photoinitiator. *Polym. Chem.* **2019**, *10* (39), 5315-5323.
193. Lee, H.; Dellatore, S. M.; Miller, W. M.; Messersmith, P. B. J. s., Mussel-inspired surface chemistry for multifunctional coatings. *Science* **2007**, *318* (5849), 426-430.
194. Ai, K.; Liu, Y.; Ruan, C.; Lu, L.; Lu, G. M., Sp²C-Dominant N-Doped Carbon Sub-micrometer Spheres with a Tunable Size: A Versatile Platform for Highly Efficient Oxygen-Reduction Catalysts. *Adv. Mater.* **2013**, *25* (7), 998-1003.

10. Acknowledgements

Firstly, I would like to acknowledge my senior supervisor, Prof. Dr. Markus Antonietti, giving me the opportunity to study in the Max Planck Institute of Colloids and Interfaces. I really appreciate his guidance and support not only for the research work, but also for my career.

I express my deep acknowledgement to my supervisor to Dr. Bernhard. He was always patient to me and guided me in science. He was quite knowledgeable in polymer science and tolerant to my stupid mistakes in lab. His fruitful discussions, constructive suggestions, ideas and support in the over two more years paved my way of PhD study. Without his splendid guidance and teaching, I would never finish my study here.

I show special thanks to Baris, a good team worker and a super nice group leader, letting me work in his group and leading me to the new projects. He cared about me not only in science but also in life. It was a very pleasant experience to work with him.

Thanks to Prof. Helmut Schlaad for being my second supervisor, providing me the opportunity to do teaching assistant in the lab.

Moreover, I would like to thank Lukas. His passion for science inspired me a lot and was kind to me, making me have the access to his Drop-Lab.

I feel quite grateful to my lunch friends, we shared the very happy moments together. Thank Guigang and his family, the whole family treated me delicious food and his lovely baby healed each sorrow from life. In addition, I want to show thanks to Kai and Lu. We had lots of good time together, celebrating important festivals, cooking, hiking and watching movies.

Many thanks to Runyu, a true friend. His kindness and company always made me feel warm. He taught me many skills that were helpful with job applications.

Chapter 10

Special thanks to Qian, the best sis here. We hung out, travelled, and did interesting sports together. I appreciate it that she accompanied me around when I was depressed.

Thank Qing, a good friend. I could share my happiness and sadness with her and she brought me lots of fun.

Many thanks to Bradley Frank, the best and first intern ever, helped me a lot with my project and English. Moreover, he inspired me with my projects.

Thank Bowen and Yuan, my best drinking friends in Germany. The hotpot parties we had here were the best part with you two.

I am very grateful to Marlies, the Queen of the lab, in charge of everything. She helped me with everything in the lab work, also did countless GPC for me. I would like to show thanks to Heike, Bogi, Tobias and Rona for SEM and TEM training and measurements.

Many thanks to my group members, Kook, Noah, Alex, Huichun, for the very nice atmosphere in the group.

Thank my officemates, Chris often shared sweets with me, Alex shared the morning coffee. Special thanks to Huichun, took care of me as elder sister. As well as Marko, not only nice to me, but also had a very pleasant cooperation in project.

I am very grateful to my friends, Lijia and Yiqing, even supporting me overseas. I treasure the friendship between us for more than ten years. Special thanks to my parents for supporting me all the time, no matter what difficulties I met, they trust me and become my back. They support me to do whatever I like and all they hope is that I could live a happy life.

I thank my committee members and reviewers for their valuable suggestions and time. Finally yet importantly, I acknowledge the final support from China Scholarship Council.